SYNTHESIS OF BIODIESEL AND GLYCEROL

CARBONATE USING HETEROGENEOUS CATALYSTS

Wuttichai Roschat

A Thesis Submitted in Partial Fulfillment of the Requirements for the

Degree of Doctor of Philosophy in Chemistry

Suranaree University of Technology

Academic Year 2015

การสังเคราะห์ไบโอดีเซลและกลีเซอรอลคาร์บอเนต

โดยใช้ตัวเร่งปฏิกิริยาวิวิธพันธุ์

นายวุฒิชัย รสชาติ

วิทยานิพนธ์นี้เป็นส่วนหนึ่งของการศึกษาตามหลักสูตรปริญญาวิทยาศาสตรดุษฎีบัณฑิต
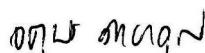สาขาวิชาเคมี
มหาวิทยาลัยเทคโนโลยีสุรนารี
ปีการศึกษา 2558

SYNTHESIS OF BIODIESEL AND GLYCEROL CARBONATE

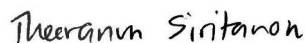# USING HETEROGENEOUS CATALYSTS

Suranaree University of Technology has approved this thesis submitted in partial fulfillment of the requirements for the Degree of Doctor of Philosophy.

Thesis Examining Committee

_____

(Assoc. Prof. Dr. Jatuporn Wittayakun)

Chairperson

_____

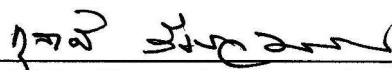(Asst. Prof. Dr. Theeranun Siritanon)

Member (Thesis Advisor)

_____

(Prof. Dr. Vinich Promarak)

Member

_____

(Asst. Prof. Dr. Rapee Utke)

Member

_____

(Asst. Prof. Dr. Kunwadee Rangsriwatananon)

Member

_____

(Asst. Prof. Dr. Taweesak Sudyoadsuk)

Member

_____

(Prof. Dr. Sukit Limpijumnong)   (Prof. Dr. Santi Maensiri)

Vice Rector for Academic Affairs   Dean of Institute of Science

and Innovation

วุฒิชัย รสชาติ : การสังเคราะห์ไบโอดีเซลและกลีเซอรอลคาร์บอเนตโดยใช้ตัวเร่งปฏิกิริยา
วิวิธพันธุ์ (SYNTHESIS OF BIODIESEL AND GLYCEROL CARBONATE USING
HETEROGENEOUS CATALYSTS) อาจารย์ที่ปรึกษา :
ผู้ช่วยศาสตราจารย์ ดร.ธีรนันท์ ศิริตานนท์, 215 หน้า

จุดมุ่งหมายของวิทยานิพนธ์นี้คือการค้นคว้าวิธีการที่เรียบง่ายและเป็นมิตรกับสิ่งแวดล้อม
เพื่อเป็นทางเลือกสำหรับกระบวนการผลิตไบโอดีเซล สามารถแบ่งเนื้อหางานวิจัยออกเป็น
สามส่วน ประกอบด้วยส่วนที่หนึ่งเกี่ยวข้องกับวัตถุดิบสารตั้งต้นที่ใช้สำหรับการผลิตไบโอดีเซล
และการใช้เทคนิคโครมาโทกราฟีแบบผิวบาง (TLC) และแสงยูวี (UV) ซึ่งเป็นวิธีการวิเคราะห์ที่
มีศักยภาพสำหรับการคัดกรองและการตรวจสอบเบื้องต้นของกระบวนการผลิตไบโอดีเซล ส่วนที่
สองซึ่งเป็นส่วนหลักของงานวิจัยนี้ มุ่งเน้นตัวเร่งปฏิกิริยาวิวิธพันธุ์ที่ได้จากวัสดุธรรมชาติสำหรับ
การเร่งปฏิกิริยาทรานส์เอสเทอริฟิเคชัน ส่วนสุดท้ายของการศึกษานี้คือการผลิตกลีเซอรอล
คาร์บอเนตที่เป็นผลิตภัณฑ์มูลค่าสูงโดยใช้ตัวเร่งปฏิกิริยาที่เป็นมิตรกับสิ่งแวดล้อมและสารตั้งต้น
กลีเซอรอลที่เป็นผลผลิตพลอยได้จากการสังเคราะห์ไบโอดีเซล

ในส่วนของน้ำมันจากเมล็ดยางพาราจากการศึกษาพบว่าเป็นวัตถุดิบที่ได้จากพืชที่ไม่ใช่พืช
อาหารและมีศักยภาพสูงสำหรับใช้ในการผลิตไบโอดีเซล โดยผลิตภัณฑ์ไบโอดีเซลที่ได้จากน้ำมัน
เมล็ดยางพาราดังกล่าวที่ทำปฏิกิริยาทรานส์เอสเทอร์ริฟิเคชันกับเมทานอลในงานวิจัยนี้ พบว่า
น้ำมันไบโอดีเซลที่ได้มีคุณภาพเหมือนการใช้น้ำมันชนิดอื่น ๆ ในการผลิตไบโอดีเซล

ในขณะที่การใช้เทคนิคโครมาโทกราฟีแบบผิวบาง และแสงยูวี สำหรับการตรวจสอบและ
ติดตามความก้าวหน้าของปฏิกิริยาทรานส์เอสเทอร์ริฟิเคชันในกระบวนการผลิตไบโอดีเซล พบว่า
มีความค่าคลาดเคลื่อนเล็กน้อยคือ ±2-4% เมื่อเปรียบเทียบกับการวิเคราะห์ด้วยเทคนิค ^{1}H NMR
และเทคนิค GC และพบว่าชนิดของตัวเร่งปฏิกิริยาที่ใช้ในกระบวนการผลิตไบโอดีเซลไม่มีผลต่อ
การวิเคราะห์ผลิตภัณฑ์ไบโอดีเซลที่ได้ด้วยเทคนิคโครมาโทกราฟีแบบผิวบาง ดังกล่าว

นอกจากนี้ สาร CaO ที่เตรียมได้จากปูนขาวและเปลือกหอยขมถูกใช้เป็นตัวเร่งปฏิกิริยา
ทรานส์เอสเทอริฟิเคชันของน้ำมันปาล์มในการสังเคราะห์ไบโอดีเซล ภายใต้สภาวะที่ดีที่สุดพบว่า
ตัวเร่งปฏิกิริยา CaO ที่ได้จากวัตถุดิบทั้งสองสามารถเร่งปฏิกิริยาการได้ผลิตภัณฑ์ไบโอดีเซล
มากกว่า 97% ภายในระยะเวลาการทำปฏิกิริยา 2 ชั่วโมง ในส่วนของ CaO ที่เตรียมได้จาก
เปลือกหอยขมถูกใช้เป็นตัวเร่งปฏิกิริยารวมกับวิธีการเติมตัวทำละลายร่วม 10% v/v THF ใน
ปฏิกิริยาการสังเคราะห์ไบโอดีเซลได้ผลผลิต 98.5% ภายในระยะเวลาการทำปฏิกิริยา 1.5 ชั่วโมง
นอกจากตัวเร่งปฏิกิริยา CaO ดังกล่าวแล้ว ในงานวิจัยนี้ยังได้ทำการศึกษาการเตรียมตัวเร่ง

ปฏิกิริยาโซเดียมซิลิเกตจากแกลบ โดยผลการศึกษาพบว่าโซเดียมซิลิเกตที่เตรียมได้สามารถเร่ง
ปฏิกิริยาได้ผลิตภัณฑ์ไบโอดีเซล 97%   ภายในระยะเวลาการทำปฏิกิริยา 30 นาที ที่สภาวะ
อุณหภูมิในการทำปฏิกิริยา 65   องศาเซลเซียส   และได้ผลิตภัณฑ์ไบโอดีเซล 94%   ในการทำ
ปฏิกิริยาที่อุณหภูมิห้อง

สำหรับการสังเคราะห์กลีเซอรอลคาร์บอเนตด้วยปฏิกิริยาทรานส์เอสเทอริฟิเคชันของสาร
ไดเมทิลคาร์บอเนตและสารกลีเซอรอลโดยมี CaO   ที่ได้จากแหล่งวัสดุธรรมชาติเป็นตัวเร่ง
ปฏิกิริยา ภายใต้สภาวะในการทำปฏิกิริยาที่ดีที่สุด ผลิตภัณฑ์กลีเซอรอลคาร์บอเนตที่ได้มากกว่า
97%   ในระยะเวลาในการทำปฏิกิริยา 1.5   ชั่วโมง โดยสามารถแยกตัวเร่งปฏิกิริยาออกจาก
ปฏิกิริยาได้อย่างง่ายและนำกลับมาใช้ซ้ำได้อย่างน้อย 4 ครั้ง โดยที่ตัวเร่งปฏิกิริยาดังกล่าวยังคงมี
ประสิทธิภาพเช่นเดิม

สาขาวิชาเคมี   ลายมือชื่อนักศึกษา_____
ปีการศึกษา 2558   ลายมือชื่ออาจารย์ที่ปรึกษา_____

WUTTICHAI ROSCHAT : SYNTHESIS OF BIODIESEL AND GLYCEROL
CARBONATE USING HETEROGENEOUS CATALYSTS.

THESIS ADVISOR : ASST. PROF. THEERANUN SIRITANON, Ph.D. 215 PP.

BIODIESEL/ GLYCEROL CARBONATE/ CALCIUM OXIDE/ CaO/ SODIUM
SILICATE/ Na_2SiO_3/ TRANSESTERIFICATION/ HETREOGENEOUS BASIC
CATALYSTS

The aim of this thesis is to search for an alternative green and simple way to
improve biodiesel production. The thesis are divided into three major parts. The first
part deals with the starting reactant for biodiesel preparation and the use of thin layer
chromatography (TLC) visualized UV light as a potential analysis method for cursory
screening and monitoring the biodiesel production process. The second part, the
majority of the thesis, focuses on green heterogeneous catalysts obtained from natural
sources for transesterification. The last part, studies the production of higher valued
glycerol carbonate from glycerol, the by-product from biodiesel synthesis utilizing a
green catalyst.

Rubber seed oil was evaluated as a high potential non-edible feedstock for
biodiesel production. It was demonstrated in this work that using rubber seed oil in
transesterification with methanol did give biodiesel of similar quality as a commercial
oil.

TLC visualized UV light can be utilized as a potential screening and monitoring
technique in biodiesel production by transesterification process. This method has a
small error of %FAME within ±2-4% compared with ^{1}H NMR and GC

chromatograph. The types of catalysts have no effects on the results obtained from the TLC analysis.

In addition, the hydrated lime-derived CaO and river snail shells-derived CaO were used as a catalyst for the transesterification of palm oil to biodiesel. Under the optimized conditions, both catalysts gave over 97% yield of biodiesel in only 2 h. In the case of river snail shells-derived CaO, with co-solvent method where 10% v/v of THF in methanol was used, %FAME yield of 98.5% was achieved in only 1.5 h. Besides CaO, sodium silicate (Na_2SiO_3) prepared from rice husk was investigated as a catalyst for biodiesel synthesis. The results showed that FAME yield reached 97% in only 30 min at 65 °C, and reached 94% in 2.5 h at room temperature.

Preparation of glycerol carbonate via transesterification of dimethyl carbonate with glycerol in the presence of CaO catalysts derived from natural sources was investigated. Under the optimal reaction conditions, over 97% yield of glycerol carbonate product could be achieved within 1.5 h. It is also noted that the CaO catalysts could be easily recovered after the reaction and reused for at least four times without a serious catalyst deactivation.

School of Chemistry   Student's Signature _Wutthichai Roschat_

Academic Year 2015   Advisor's Signature _Theeranun Siritanon_

ACKNOWLEDGEMENTS

Thank to all of my good friends in the Organic Materials and Alternative Energy Research Laboratory Group and School of Chemistry, Institute of Science, Suranaree University of Technology for help and the impressive atmosphere.

Finally, I would like to thank very much my family for their under standings, encouragements, motivations and building up inspirations.

Wuttichai Roschat

CONTENTS

CONTENTS (Continued)

CONTENTS (Continued)

CONTENTS (Continued)

CONTENTS (Continued)

CONTENTS (Continued)

CONTENTS (Continued)

CONTENTS (Continued)

CONTENTS (Continued)

CONTENTS (Continued)

LIST OF TABLES

LIST OF TABLES (Continued)

LIST OF FIGURES

LIST OF FIGURES (Continued)

LIST OF FIGURES (Continued)

LIST OF FIGURES (Continued)

LIST OF FIGURES (Continued)

LIST OF FIGURES (Continued)

LIST OF FIGURES (Continued)

LIST OF FIGURES (Continued)

LIST OF FIGURES (Continued)

LIST OF FIGURES (Continued)

LIST OF FIGURES (Continued)

LIST OF FIGURES (Continued)

LIST OF ABBREVIATIONS

XRD	=	X-ray Diffraction
DTA	=	Differential Thermal Analysis
TGA	=	Thermogravimetric Analysis
FT-IR	=	Fourier Transforms Infrared
XRF	=	X-ray Fluorescence
GC	=	Gas Chromatography
GC-MS	=	Gas Chromatography–Mass Spectrometry
BET	=	Brunauer Emmett Teller
TPD	=	Temperature Programmed Desorption
SEM	=	Scanning Electron Microscopy
^{1}H NMR	=	Proton Nuclear Magnetic Resonance
^{13}C NMR	=	Carbon Nuclear Magnetic Resonance
AAS	=	Atomic Absorption Spectrophotometry
FAME	=	Fatty Acid Methyl Ester
FFAs	=	Free Fatty Acids
IUPAC	=	International Union of Pure and Applied Chemistry

CHAPTER I

INTRODUCTION

1.1 World energy consumption

The world energy consumption increases significantly with the economic development and incremental population of the world. Primary energy sources take many forms including nuclear energy, fossil energy and renewable sources. These primary sources are converted to electricity, a secondary energy, which flows through power lines and other transmission infrastructures to homes, businesses and industries. According to the world total primary energy supply in 2013 as shown in Figure 1.1, the main power sources are fossil fuels namely petroleum oil, coal and natural gas respectively (International Energy Agency, 2015).
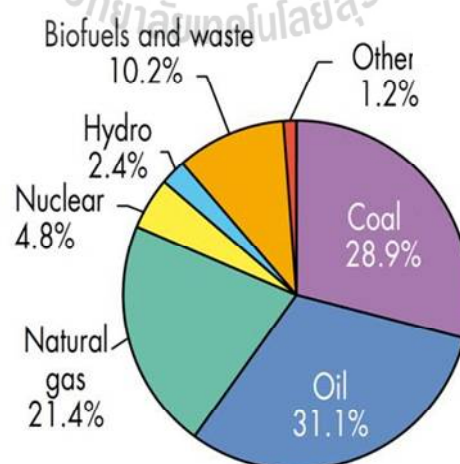
Figure 1.1 The world total primary energy supply in 2013 (International Energy Agency, 2015).

The global demand for fossil fuels especially petroleum oil, which is the most important energy source, has increased over the years as a result of industrialization and motorization (Salaheldeen et al., 2015; Onoji et al., 2016). However, the high rates of crude oil depletion, price instability and global warming crisis are the global significant issues. The serious problem associated with the use of petroleum fuel is the pollutants emissions especially carbon dioxide (CO_2) which is the primary greenhouse gas. Emission of CO_2 from fuel combustion has continuously increased as shown in Figure 1.2 (International Energy Agency, 2015; Onoji et al., 2016). As a result, alternative energy such as sunlight, wind, biomass, hydropower, tidal waves and geothermal have gained much interest as they are renewable and environmental friendly.
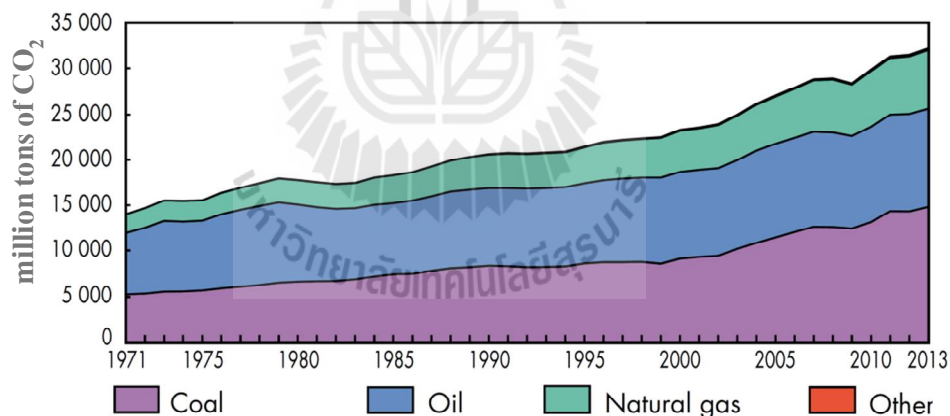
Figure 1.2 The world CO_2 emissions from fuel combustion from 1971 to 2013 by fuel (International Energy Agency, 2015).

Biomass is one of the mentioned alternative energy. It is a term for all organic materials obtained from plants (including algae, trees and crops) or animal tissues which is not only renewable, but also clean and cheap. The energy from biomass has

been used around the world such wood, animal fats, vegetable oils and waste cooking oil. In addition, biomass emits less CO_2, hydro carbon (HC), NO_x, and SO_x when used in the combustion thus it appears to also reduce global warming (McKendry, 2002; Zeng et al., 2015; Myint, 2007).

1.2 Background of biodiesel

Biomass sources, particularly vegetable oils and animal fats, have attracted much attention as an alternative energy source. In 1900, Rudolf Diesel, a German inventor of the diesel engine, presented the use of pure peanut oil for compression ignition engine at the World Exhibition in Paris. However, because cheap petroleum fuels were easily available, few people were interested in the alternatives (Pahl, 2005; Ahmad et al., 2012; Borgman, 2007).

As early as the 1930s, there was interest in splitting the fatty acids from glycerin in vegetable oils in order to create a thinner product similar to petroleum diesel. In 1937, Chavanne was granted a Belgian patent for an ethyl ester of palm oil which would be called biodiesel today. In 1938, a passenger bus fueled with palm oil ethyl ester plied the route between Brussels and Louvain. During World War II (1939 to 1945), when petroleum fuel supplies were interrupted, vegetable oil was used as fuel by several countries including Brazil, Argentina, China, India, and Japan. However, when the war ended and petroleum supplies were again cheap and plentiful, vegetable oil fuel was forgotten (Knothe et al., 2005).

In the 1970s, the petroleum oil embargo caused many countries to look at vegetable oil as a possible fuel. Scientists discovered that straight vegetable oil could be used to run diesel engines, however, the poor quality of the fuel spray caused by

the high viscosity of the vegetable oil would eventually cause damages to the engines. Therefore, scientists have presented the conversion of sunflower oil to methyl esters and then conducted experiments to convert the other vegetable oils into biodiesel. Thus, the word "biodiesel" was probably first used in about 1984 (Gerpen et al., 2007).

Nowadays, biodiesel has become an established product traded daily and globally. It is promoted in many countries especially in European countries, the United States, Brazil, Argentina, Indonesia and Thailand where biodiesel is encouraged to be used in automobiles (Speranza et al., 2015). Furthermore, production of the vegetable oils and animal fats, sources of biodiesel, has increased in the last decade. By 2012, global biodiesel production reached 22.5 billion litres as listed in Table 1.1 (World Bioenergy Association, 2014).

Table 1.1 Global production of biodiesel (billion liters) (World Bioenergy Association, 2014).

Year	World	USA	Brazil	Argentina	Thailand	Indonesia	EU
2005	3.8	0.3	-	1.0	1.0	-	3.6
2009	17.8	2.1	1.6	1.4	0.6	1.0	8.9
2010	18.5	1.2	2.3	2.1	0.6	0.7	10.0
2011	22.4	3.2	2.7	2.8	0.6	1.4	9.2
2012	22.5	3.4	2.7	2.8	0.9	1.5	9.1

1.3 Biodiesel in Thailand

As a majority of Thai are in farming households, there can be a variety of used materials which could turn in to a commercial fuel. Several vegetable oils or animal fats are produced in Thailand such as palm oil, soybean oil, jatropha oil, coconut oil and lard. Additionally, waste cooking oil from hotels, restaurants, and other food industries can be used as raw material for biodiesel production (Department of Alternative Energy Development and Efficiency-Thailand, 2011). Using such materials to produce biomass fuels would reduce the dependence on imported fossil fuel.
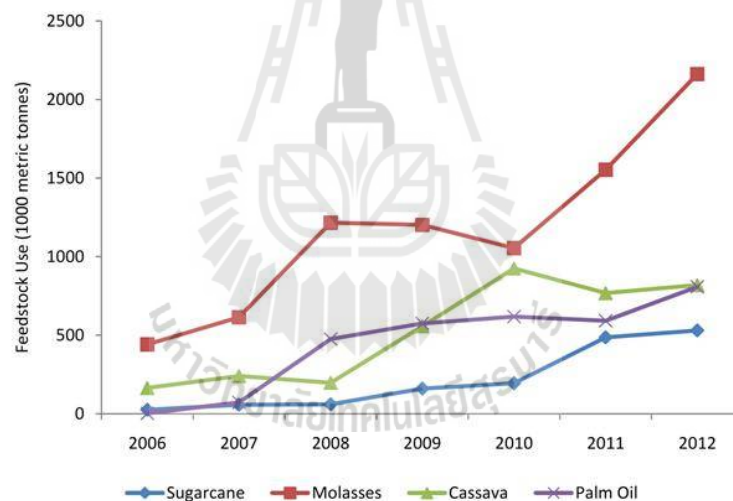
Figure 1.3 Feedstock use for ethanol and biodiesel production in Thailand (Kumar et al., 2013).

The history of biodiesel in Thailand starts in 1985 when the Royal initiative project related to biodiesel was first established. Then, in 2005, biodiesel has been officially implemented across the country. In 2008, Thai Government has established renewable energy development plan to promote the use of alternative energy. Since

2012, biodiesel has been used to blend with petro-diesel in the ratio of 5% (B5 fuel) and the Royal Thai Government has determined that this ratio must reach 10% (B10) for marketing approximately 5.97×10^6 L/day in 2021 (Department of Alternative Energy Development and Efficiency-Thailand, 2012; Chen et al., 2014; Wattana, 2014).
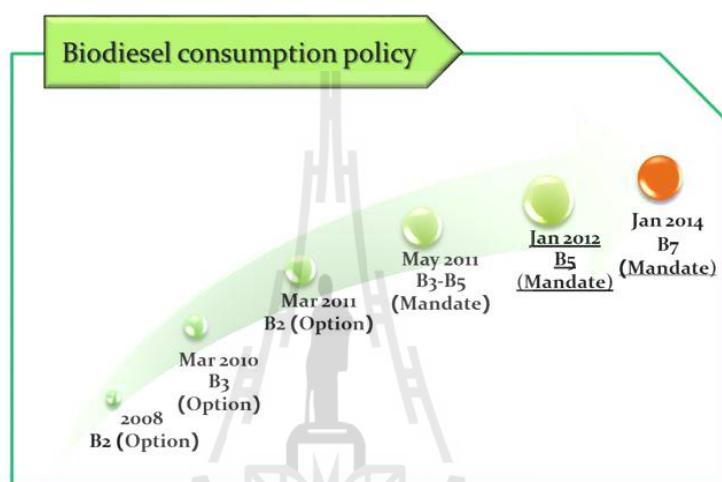
Figure 1.4 The announcement of Department of Energy Business about the policy of biodiesel B7 (Department of Alternative Energy Development and Efficiency-Thailand, 2014).

The plan focuses on both supply and demand. On the supply side, the government will promote the expansion of oil palm acreage to a targeted 5.5 million rai (880,000 hectares) with a total oil palm harvested area of 5.3 million rai (848,000 hectares) by 2021. Average yields are expected to reach 3.2 ton/rai (30 ton/hectare) in 2021 while crude palm oil crushing rates should be above 18 percent. On the demand side, the government anticipates balancing its compulsory production of biodiesel with domestic palm oil supplies. The plan also introduces pilot projects for B10 or

B20 blend to be used in fleet trucks and fishery boats (Wattana, 2014; Department of Alternative Energy Development and Efficiency-Thailand, 2014).

1.4 Biodiesel production

1.4.1 Transesterification reaction

Biodiesel is generally known as mono-alkyl esters of fatty acids derived from sources such as vegetable oils and animal fats where the corresponding triglycerides react with short chain alcohols (e.g. methanol or ethanol) in the presence of a catalyst (Alhassan et al., 2014; Zabeti et al., 2009). In general, 1 mol of triglyceride and 3 mol of alcohol generate 3 mol of biodiesel and 1 mol of glycerol by-product in a transesterification reaction as shown in Figure 1.5 (Birla et al., 2012; Mahesh et al., 2015). When methanol is used, the biodiesel product will be fatty acid methyl ester (FAME). On the other hand, fatty acid ethyl ester (FAEE) is obtained when ethanol is used.
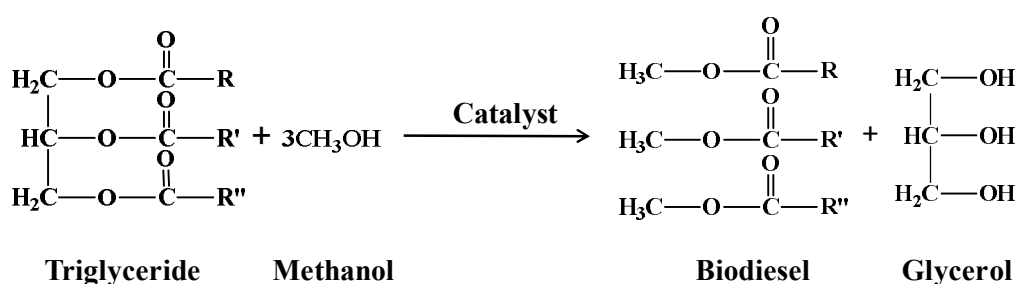
Figure 1.5 The overall transesterification reaction of triglyceride and methanol (Mahesh et al., 2015).

1.4.2 Feedstock for biodiesel production

The raw materials for transesterification to produce biodiesel can be divided into different categories including edible oil such as palm oil, soybean oil, sunflower oil and rice bran oil and non-edible oil such as jatropha oil, cotton seed oil, waste cooking oil, animal fats and algal lipids (Marchetti et al., 2012; Avhad and Marchetti, 2015). There are two kinds of fatty acids composition in the oils: saturated fatty acids containing only carbon-carbon single bonds, and unsaturated fatty acids which contain one or more carbon-carbon double bonds. The most common fatty acids found in the oils feedstock are palmitic acid (16:0), stearic acid (18:0), oleic acid (18:1), linoleic acid (18:2), and linolenic acid (18:3). The other fatty acids which are also present in several plant oils include myristic acid (14:0), palmitoleic acid (16:1), arachidic acid (20:0), and erucic acid (22:1). Besides the presence of fatty acids, additional components such as phospho- lipids, carotenes, tocopherols, sulphur compounds, and water might also be present in plant oils (Marchetti et al., 2012; Avhad and Marchetti, 2015).

1.4.3 Catalysts for transesterification

Generally, there are three types of catalysts for biodiesel production via transesterification process including biological (enzymes), homogeneous, and heterogeneous catalysts. The utilization of enzymes as an effective biocatalyst has been an emerging contribution for biodiesel production because they are tolerance to free fatty acid (FFAs) and water and their reaction requires low energy (Avhad and Marchetti, 2015). Transesterification reaction can be catalyzed with enzymes such as *Candida antarctica lipase* and *Candida sp. 99–125* (Tan et al., 2010), *Pseudomonas*

cepacia and *Pseudomonas fluorescens* (Salis et al., 2008), *Rhizomucor miehei* and *Chromobacterium viscosum* (Shieh et al., 2003) and *Rhizopus oryzae lipase* (Pizarro and Park, 2003). However, when enzymes are used, the reaction rate is very slow and the reaction temperature must be low (Shah et al., 2004; Leung et al., 2010). In addition, the presence of alcohol also inhibits enzymes activity.

Transesterification with homogeneous catalysts (acid or base) such as NaOH, KOH, NaOCH$_3$, H$_2$SO$_4$, and HCl results in high yield of biodiesel (over 90%) in relatively short reaction time (1-3 h) under mild condition (40-65 °C atmospheric pressure) (Chen et al., 2012; Farag et al., 2011; Su, 2013). Nevertheless, using homogenous catalyst has several drawbacks including problems related to corrosion, catalyst recovery and quality of the glycerol by-product. In addition, large amount of water is required to eliminate the catalyst which will otherwise contaminate the biodiesel product. These will increase both the overall cost of production and the environmental issues (Farooq et al., 2013; Suryaputra et al., 2013).

In this regard, heterogeneous catalysts are promoted as an economic and green process because they are non-corrosive, easy to be separated from the reaction mixture and reusable for several times. Using heterogeneous catalysts would also produce glycerol by-product with more purity (Mahesh et al., 2015; Roschat et al., 2016. A large variety of different heterogeneous catalysts for biodiesel production have been reported. Some of these catalysts include alkaline-earth metal oxides such as CaO, MgO and SrO (Birla et al., 2012), hydrotalcides (Liu et al., 2008), zeolites (Brito et al., 2007), alkali or oxides of alkaline earth metals supported over large surface area such ZnO–La$_2$O$_3$, Mg–Al hydrotalcite, K$_2$CO$_3$/γ-Al$_2$O$_3$, Na$_2$CO$_3$/γ-Al$_2$O$_3$ and KNO$_3$/KL zeolite (Atadashi et al., 2013), anion exchanged resins (Long et al.,

2011), etc. However, some of these materials still have to be improved as they show low catalytic activity and high amount of catalyst loading constitutes a three-phase system in the reaction mixture which inhibits the reaction. Moreover, they are highly sensitive to moisture, soluble in methanol and some are complicated to regenerate (Roschat et al., 2016; Atadashi et al., 2013; Leung et al., 2010).

1.4.4 Glycerol by-product obtained from biodiesel production

Nowadays, the costs of triglyceride starting material and production process contribute the most to biodiesel price. The high triglyceride quality is also always in demand with food producers. Therefore, the utilization of the glycerol by-product from biodiesel production would significantly improve the economic aspect of overall biodiesel production (Roschat et al., 2012). For every 1000 kg of biodiesel production by transesterification of oils with methanol, around 100 kg of glycerol is produced (Malyaadri et al., 2011).

According to Oil World's estimate, the world market for biodiesel is expected to reach 37 billion gallons per year by 2016. As a result, around 4 billion gallons of crude glycerol will be produced in the same year (Rastegari et al., 2015). Glycerol is one of the most versatile and valuable known chemicals and has a wide variety of uses and applications such as food, pharmaceutical, cosmetic, coating and other industries. Additionally, it can be converted into several important chemicals such as propane diols, glycerol carbonate, acrolein, esters of glycerol and glyceric acid, etc (Roschat et al., 2012; Malyaadri et al., 2011).

1.5 Conversion of glycerol to glycerol carbonate product

Among different chemicals related to glycerol, glycerol carbonate is one of the important derivatives because it has been widely used as a polar high boiling solvent, a surfactant component, a membrane component for gas separation and a component for industrial of coating, detergent, polymers, ink, paint, lubricant and electrolyte (Malyaadri et al., 2011; Jagadeeswaraiah et al., 2014; Teng et al., 2014). Furthermore, glycerol carbonate can also be used as chemical intermediates to synthesize other chemical compounds such as glycidol which is employed in textile, plastics, pharmaceutical and cosmetics industries as demonstrated in Figure 1.6 (Malyaadri et al., 2011; Gade and Munshi, 2012).
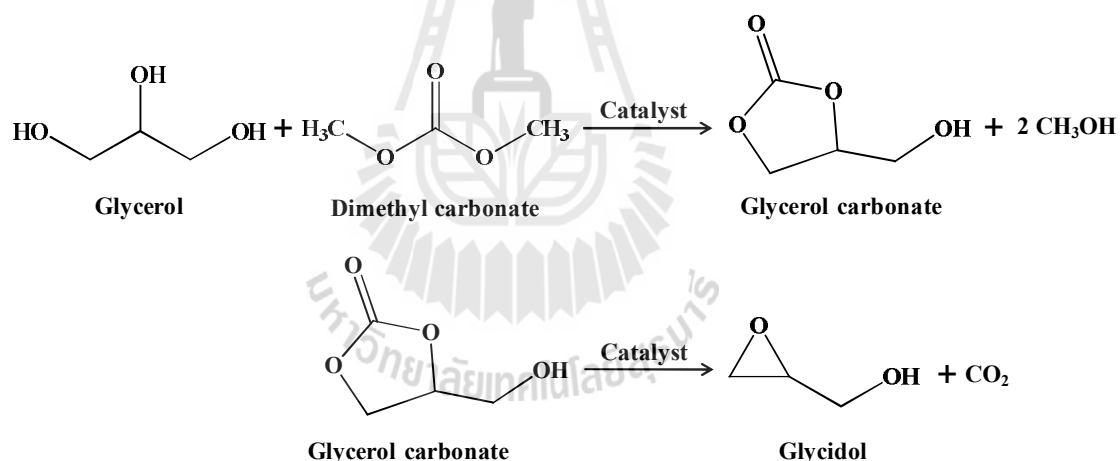
Figure 1.6 Synthesis of glycerol carbonate from glycerol with dimethyl carbonate and synthesis of glycidol from glycerol carbonate (Gade and Munshi, 2012).

Glycerol carbonate can be synthesized from glycerol by different pathways involving chemicals such as CO/H_2, organic carbonate (such as dimethyl carbonate, diethyl carbonate, and ethylene carbonate), urea and carbon dioxide (Teng et al., 2014; Gade and Munshi, 2012; Saiyong et al., 2012). Among these pathways, the

transesterification between glycerol and dimethyl carbonate is one convenient method which could be performed under mild conditions (at 50-100 °C under atmospheric pressure) in the presence of a catalyst as shown in Figure 1.6 (Gade and Munshi, 2012; Saiyong et al., 2012; Bai et al., 2013). The catalysts used to convert glycerol to glycerol carbonate can be homogeneous catalysts such as K_2CO_3, NaOH and H_2SO_4 (Bai et al., 2013; Arzamendi et al., 2007), enzymatic catalyst (Bai et al., 2013) and heterogeneous catalysts such as CaO, NaOH/γ-Al_2O_3 and Mg/Al/Zr mixed oxide (Malyaadri et al., 2011; Jagadeeswaraiah et al., 2014; Arzamendi et al., 2007).

1.6 Research objective

The objectives of this thesis are:

1. To study the extraction, properties and transesterification reaction of rubber seed oil as a potential non-edible feedstock for biodiesel production in Thailand.

2. To develop the TLC method visualized by UV light as an easy, convenient, and very low-cost technique for cursory screening and monitoring the reaction progress of biodiesel production.

3. To synthesize biodiesel product from palm oil using hydrated lime-derived CaO as a low-cost basic heterogeneous catalyst.

4. To study the use of river snail shells-derived heterogeneous catalyst and co-solvent method as an economical and green biodiesel production process.

5. To synthesize and characterize sodium silicate from rice husk as a high efficient and low-cost basic heterogeneous catalyst for biodiesel production.

6. To synthesize and characterize of glycerol carbonate obtained from transesterification of dimethyl carbonate and glycerol using natural source material-derived CaO catalyst.

1.7 References

Ahmad, M., Khan, M. A., Zafar, M. and Sultana, S. (2012). Practical handbook on biodiesel production and properties, Chemical industries. USA: **Taylor & Francis.**

Alhassan, Y., Kumar, N., Bugaje, I. M., Pali, H. S. and Kathkar, P. (2014). Co-solvent transesterification of cotton seed oil into biodiesel: effects of reaction condition on quality of fatty acids methyl esters. **Energy Conversion and Management**. 84: 640-648.

Arzamendi, G., Campo, I., Arguiñarena, E., Sánchez, M., Montes, M. and Gandía, L. M. (2007). Synthesis of biodiesel with heterogeneous NaOH/alumina catalysts: comparison with homogeneous NaOH. **Chemical Engineering Journal**. 134: 123-130.

Atadashi, I. M., Aroua, M. K., Abdul, A. A. R. and Sulaiman, N. M. N. (2013). The effects of catalysts in biodiesel production: A review. **Journal of Industrial and Engineering Chemistry**. 19: 14-26.

Avhad, M. R. and Marchetti, J. M. (2015). A review on recent advancement in catalytic materials for biodiesel production. **Renewable & Sustainable Energy Reviews**. 50: 696-718.

Bai, R., Wang, Y., Wang, S., Mei, F., Li, T. and Li, G. (2013). Synthesis of glycerol carbonate from glycerol and dimethyl carbonate catalyzed by NaOH/γ-Al$_2$O$_3$. **Fuel Processing Technology**. 106: 209-214.

Birla, A., Singh, B., Upadhyay, S. N. and Sharma, Y. C. (2012). Kinatics studies of synthesis of biodiesel from waste frying oil using a heterogeneous catalyst derived from snail shell. **Bioresource Technology**. 106: 95-100.

Borgman, D. (2007). Bio-fuels and striving for greater energy independence. John Deere bio-fuel white paper: Agricultural. **Moline: John Deere Company.**

Brito, A., Borges, M. E. and Otero, N. (2007). Zeolite Y as a heterogeneous catalyst in biodiesel fuel production from used vegetable oil. **Energy & Fuels**. 21: 3280-3283.

Chen, K. S., Lin, Y. C., Hsu, K. H. and Wang, H. K. (2012). Improving biodiesel yields from waste cooking oil by using sodium methoxide and a microwave heating system. **Energy**. 38: 151-156.

Chen, S. Y., Lao-ubol, S., Mochizuki, T., Abe, Y., Toba, M. and Yoshimura, Y. (2014) Production of Jatropha biodiesel fuel over sulfonic acid-based solid acids. **Bioresource Technology**. 157: 346-350.

Department of Alternative Energy Development and Efficiency-Thailand. (2011). **Energy situation: 2000-2011 annual report**. [Online]. Available: http://www.dede.go.th/download/annual_report/Annua_2555_en.pdf.

Department of Alternative Energy Development and Efficiency-Thailand. (2012). **The renewable and alternative energy development plan for 25 percent in 10 years (AEDP 2012-21)**. [Online]. Available: http://www4.dede.go.th/ dede/images/ stories/pdf/dede_aedp_2012_21.pdf.

Department of Alternative Energy Development and Efficiency-Thailand. (2014). **Thailand biofuel policies 2014**. [Online]. Available: http://www.mtec.or.th/ files/chanpen/1_DEDE.pdf.

Farag, H. A., El-Maghraby, A. and Taha, N. A. (2011). Optimization of factors affecting esterification of mixed oil with high percentage of free fatty acid. **Fuel Processing Technology**. 92: 507-510.

Farooq, M., Ramli, A. and Subbarao. D. (2013). Biodiesel production from waste cooking oil using bifunctional heterogeneous solid catalyst. **Journal of Cleaner Production**. 59: 131-40.

Gade, M. S., Munshi, M. K., Chherawalla, B. M., Rane, V. H. and Kelkar, A. A. (2012). Synthesis of glycidol from glycerol and dimethyl carbonate using ionic liquid as a catalyst. **Catalysis Communications**. 27: 184-188.

Gerpen, J. H. V., Peterson, C. L. and Goering, C. E. (2007). Biodiesel: An alternative fuel for compression ignition engines. **ASABE**. 913CO107: 1-22.

International Energy Agency (IEA). (2015). **Key World Energy Statistics**. [Online]. Available:http://www.iea.org/publications/freepublications/publication/KyeWor ld_Statistics_2015.pdf.

Jagadeeswaraiah, K., Ramesh-Kumar Ch., Sai-Prasad, P. S., Loridant, S. and Lingaiah, N. (2014). Synthesis of glycerol carbonate from glycerol and urea over tin-tungsten mixed oxide catalysts. **Applied Catalysis A: General**. 469: 165-172.

Knothe, G., Van, G. J. H. and Krahl, J. (2005). The biodiesel handbook. **Champaign, Ill: AOCS Press**.

Kumar, S., Salam, P. A., Shrestha, P. and Ackom, E. K. (2013). An assessment of Thailand's biofuel development. **Sustainability**. 5: 1577-1597.

Leung, D. Y. C., Wu, X. and Leung, M. K. H. (2010). A review on biodiesel production using catalyzed transesterification. **Applied Energy**. 87: 1083-1095.

Liu, X., He, H., Wang, Y., Zhu, S. and Piao, X. (2008). Transesterification of soybean oil to biodiesel using CaO as a solid catalyst. **Fuel**. 87: 216-221.

Long, T., Deng, Y., Li, G., Gan, S. and Chen, J. (2011). Application of N-methylimidizolium functionalized anion exchange resin containing NaOH for production of biodiesel. **Fuel Processing Technology**. 92: 1328-1332.

Mahesh, S. E., Ramanathan, A., Begum, K. M. M. S. and Narayanan, A. (2015). Biodiesel production from waste cooking oil using KBr impregnated CaO as catalyst. **Energy Conversion and Management**. 91: 442-450.

Malyaadri, M., Jagadeeswaraiah, K., Sai-Prasad P. S. and Lingaiah, N. (2011). Synthesis of glycerol carbonate by transesterification of glycerol with dimethyl carbonate over Mg/Al/Zr catalysts. **Applied Catalysis A: General**. 401: 153-157.

Marchetti, J. M. (2012). A summary of the available technologies for biodiesel production based on a comparison of different feedstock's properties. **Process Safety and Environmental Protection**. 90: 157-163.

McKendry, P. (2002). Energy production from biomass (part 1): overview of biomass. **Bioresource Technology**. 83: 37-46.

Myint, L. L. (2007). Process analysis and optimization of biodiesel production from vegetable oils. Master's thesis, Chemical Engineering, **Texas A&M University**.

Onoji, S. E., Iyuke, S. E., Igbafe, A. I. and Nkazi, D. B. (2016). Rubber seed oil: A potential renewable source of biodiesel for sustainable development in sub-Saharan Africa. **Energy Conversion and Management**. 110: 125-134.

Pahl, G. (2005). Biodiesel: Growing a new energy economy. White River Junction, Vt: **Chelsea Green Pub**.

Pizarro, A. V. L. and Park, E. Y. (2003). Lipase-catalyzed production of biodiesel fuel from vegetable oils contained in waste activated bleaching earth. **Process Biochemistry**. 38: 1077-1082.

Rastegari, H. and Ghaziaskar, H. S. (2015). From glycerol as the by-product of biodiesel production to value-added monoacetin by continuous and selective esterification in acetic acid. **Journal of Industrial and Engineering Chemistry**. 21: 856-861.

Roschat, W., Kacha, M., Yoosuk, B., Sudyoadsuk, T. and Promarak, V. (2012). Biodiesel production based on heterogeneous process catalyzed by solid waste coral fragment. **Fuel**. 98: 194-202.

Roschat, W., Siritanon, T., Yoosuk, B. and Promarak, V. (2016). Biodiesel production from palm oil using hydrated lime-derived CaO as a low-cost basic heterogeneous catalyst. **Energy Conversion and Management**. 108: 459-467.

Saiyong. P., Liping, Z., Renfeng, N., Shuixin, X., Ping, C. and Zhaoyin, H. (2012). Transesterification of glycerol with dimethyl Carbonate to glycerol carbonate over Na–based zeolites. **Chinese Journal of Catalysis**. 33: 1772-1777.

Salaheldeen, M., Aroua, M. K., Mariod, A. A., Cheng, S. F., Abdelrahman, M. A. and Atabani, A. E. (2015). Physicochemical characterization and thermal behavior

of biodiesel and biodiesel–diesel blends derived from crude *Moringa peregrina* seed oil. **Energy Conversion and Management**. 92: 535-542.

Salis, A., Pinna, M., Monduzzi, M. and Solinas, V. (2008). Comparison among immobilised lipases on macroporous polypropylene toward biodiesel synthesis. **Journal of Molecular Catalysis B: Enzymatic**. 54: 19-26.

Shah, S., Sharma, S. and Gupta, M. N. (2004). Biodiesel preparation by lipase-catalyzed transesterification of Jatropha oil. **Energy & Fuels**. 18: 154-159.

Shieh, C. J., Liao, H. F. and Lee, C. C. (2003). Optimization of lipase-catalyzed biodiesel by response surface methodology. **Bioresource Technology**. 88: 103-106.

Speranza, L. G., Ingram, A. and Leeke, G. A. (2015). Assessment of algae biodiesel viability based on the area requirement in the European Union, United States and Brazil. **Renewable Energy**. 78: 406-417.

Su, C. H. (2013). Recoverable and reusable hydrochloric acid used as a homogeneous catalyst for biodiesel production. **Applied Energy**. 104: 503-509.

Suryaputra, W., Winata, I., Indraswati, N. and Ismadji, S. (2013). Waste capiz (Amusium cristatum) shell as a new heterogeneous catalyst for biodiesel production. **Renewable Energy**. 50: 795-799.

Tan, T., Lu, J., Nie, K., Deng, L. and Wang, F. (2010). Biodiesel production with immobilized lipase: A review. **Biotechnology Advances**. 28: 628-634.

Teng, W. K., Ngoh, G. C., Yusoff, R. and Aroua, M. K. (2014). A review on the performance of glycerol carbonate production via catalytic transesterification: Effects of influencing parameters. **Energy Conversion and Management**. 88: 484-497.

Wattana, S. (2014). Bioenergy development in Thailand: challenges and strategies. **Energy Procedia**. 52: 506-515.

World Bioenergy Association (WBA). (2014). WBA Global Bioenergy Statistics 2014 WBA GBS report. **World Bioenergy Association: Stockholm, Sweden**.

Zabeti, M., Wan-Daud, W. M. A. and Aroua, M. K. (2009). Activity of solid catalysts for biodiesel production: a review. **Fuel Processing Technology**. 90: 770-777.

Zeng, K., Gauthier, D., Li, R. and Flamant, G. (2015). Solar pyrolysis of beech wood: Effects of pyrolysis parameters on the product distribution and gas product composition. **Energy**. 93: 1648-1657.
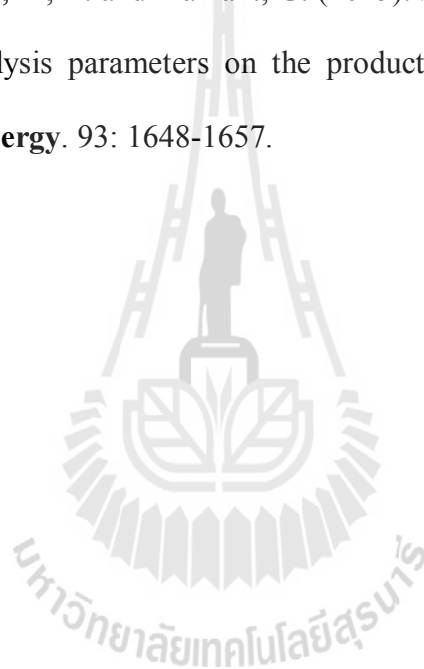
CHAPTER II

RUBBER SEED OIL AS POTENTIAL NON-EDIBLE

FEEDSTOCK FOR BIODIESEL PRODUCTION USING

HETEROGENEOUS CATALYSTS IN THAILAND

2.1 Graphical abstract

Economic plant of Thailand

Rubber seed

❖ Use of rubber seed as a high potential oil feedstock for biodiesel in Thailand.

Rubber tree

Extraction with organic solvent

Transesterification under mild reaction condition

❖ The rubber seed oil biodiesel shows high quality fuel properties.

Rubber seed oil

Rubber seed biodiesel
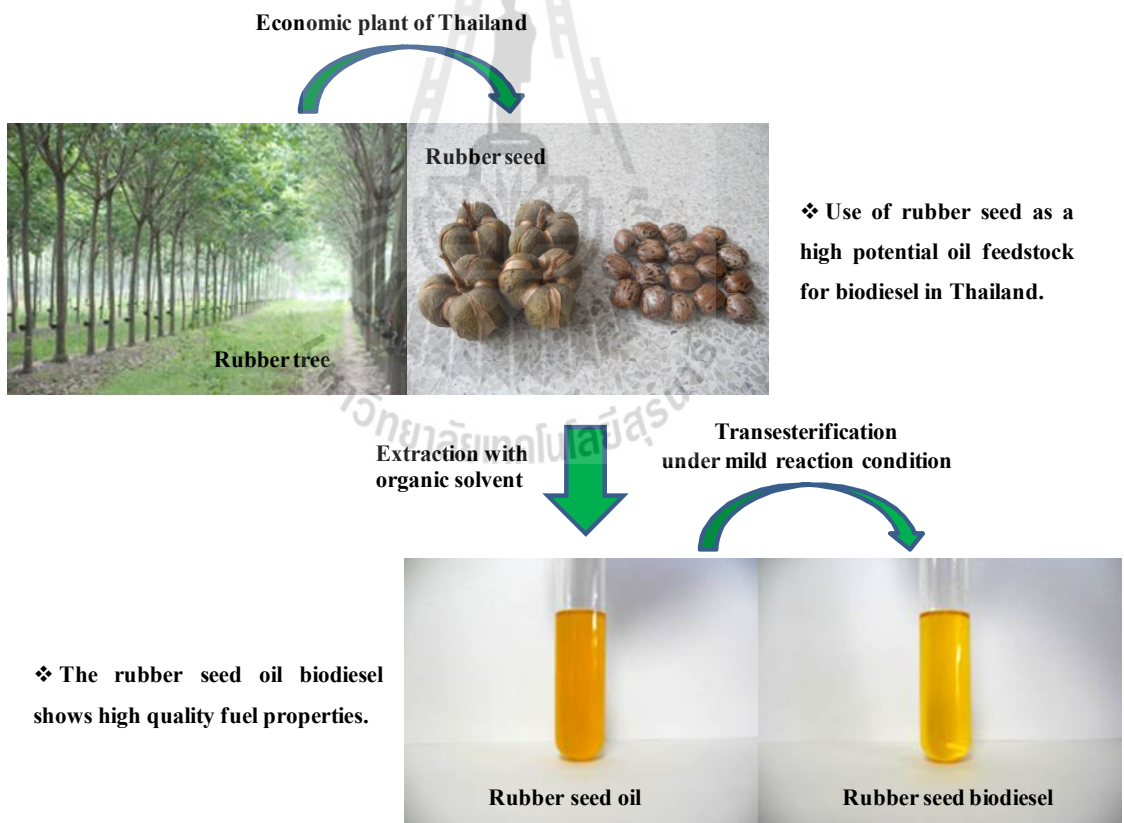
2.2 Highlights

- Rubber seed oil was evaluated as a high potential non-edible feedstock for biodiesel production in Thailand.

- The rubber seed oil was extracted using simple solvent extraction technique and its had lower FFAs contained than previously reported.

- The rubber seed oil was successfully transesterified by various heterogeneous catalyst to biodiesel in high yield and high %FAME of >97% in single step.

2.3 Abstract

This research presents new raw material of rubber seed which is non-edible crops as a source to produce oil for biodiesel production in Thailand. The rubber seed powder was extracted with hexane at room temperature to give rubber seed oil with the yield of 24 wt.%. The composition and key properties of the extracted oil were analyzed including fatty acid compositions, density, kinematic viscosity, flash point, water content and acid value. This high FFAs oil (5.20 wt.%) was successfully transesterified by various heterogeneous catalysts such as CaO-based waste coral fragment, sodium metasilicate and CaO-based eggshell to biodiesel in high yield and high %FAME of >97% in single step. Thermal stability of biodiesel obtained from rubber seed oil was evaluated by using thermogravimetric analysis and compared with petrol-diesel fuels. The biodiesel obtained from rubber seed oil was examined and found to meet the EN 14214 standard for bio-auto fuel.

2.4 Introduction

Biodiesel is an important alternative renewable energy source because it is environmental friendly, non-toxic, and has lower emission gases when used for the combustion (Moser, 2016). Biodiesel is produced from direct transesterification of vegetable oils or animal fat, where the corresponding triglycerides react with small molecule alcohol such as methyl alcohol in the presence of a catalyst (Omidvarborna et al., 2015; Zhang et al., 2016). Currently, more than 95% of biodiesel is produced from edible oils which are easily available on large scale from the agricultural industry. However, continuous and large-scale production of biodiesel from edible oils has recently been of great concern because they compete with food materials – the food versus fuel dispute. There are concerns that biodiesel feedstock may compete with food supply in the long-term. Therefore, non-edible plant oils have been found to be promising crude oils for the production of biodiesel. The use of non-edible oils is very significant in developing countries because of the tremendous demand for edible oils as food and that they are far too expensive to be used as fuel at present (Sanchez-Arreola et al., 2015; Phoo et al., 2014; Araujo et al., 2014).

In Thailand, palm oil is an important raw material for biodiesel production. However, palm oil has been used for essential consumption and food industry. Thus, using palm oil as raw material to produce biodiesel has caused the shortages edible oil consumption and raised palm oil price in the country. At this point, research for non-edible oils or new non-edible crops is crucial for biodiesel production industry in Thailand. Likewise, *Jatropha curcas* plants is promoted as raw material for biodiesel because it plants easily, grows rapidly and offers high yield of oil (Basir et al., 2015; Evon et al., 2013; Portugal-Pereira et al., 2016). However, due to the limited

plantation area for *Jatropha curcas* plants, they are insufficient to be a feedstock in biodiesel production. On the other hand, rubber trees are widely planted in Thailand. Such trees give rubber seed as a by-product which has limited uses in industrials applications.

In 2014, rubber trees cover around 35,482.7 square kilometers (3,548,274 hectare) in Thailand and this number is increasing each year (Office Agricultural 2014). According to the rubber seed production in India which is about 150 kg per hectare, the production of rubber seed in Thailand is expected at 0.532 million tons per year (Ramadhas et al., 2005; Yusup and Khan, 2010). Therefore, using rubber seed as a high potential oil feedstock for biodiesel would increase the value of rubber trees in Thailand. Moreover, many researchers have reported to convert rubber seed kernel as non-edible sources to bio-oil using pyrolysis process (Chin et al., 2014). Chaiya and Reubroycharoen (Chaiya and Reubroycharoen, 2013) found that rubber seed shell and residue give the highest yield of bio-oil which is 38.22% and 34.35%, respectively. Hence, rubber seed shell is a good raw material for liquid bio-fuel production because the extracted oil can be used to produce biodiesel through transesterification reaction, while the residue of rubber seed after extraction oil can be converted to bio-oil by pyrolysis process (Chaiya and Reubroycharoen, 2013; Hassan et al., 2014)

In this work, we report the possibility of using rubber seed collected in Northeastern provinces of Thailand as oil source for biodiesel production. The rubber seed oil was extracted using simple solvent extraction technique. The composition and properties of the extracted rubber seed oil were analyzed. The effect of stored time on free fatty acid (FFAs) content of the rubber seed oil was studied. Single step

transesterification of the extracted oil using heterogeneous catalysts was examined and the fuel properties of the obtained biodiesel were evaluated.

2.5 Material and methods

2.5.1 Materials

Disodium metasilicate (Na_2SiO_3) granule was purchased from Aldrich and the calcium oxide (CaO) AR grade was purchased from Acros. Potassium hydroxide (KOH) used in this work was purchased from Lab-scan. The analytical grade methanol, hexane, acetone, dichloromethane and ethyl acetate were purchased from Fluka. Waste coral fragments collected from Krabi province, Thailand were crushed into small size (0.5-1.0 cm^3) and transformed to CaO-based coral fragment catalyst according to the reported procedure (Roschat et al., 2012). Eggshell was collected from the local restaurant and cleaned by washing with deionized water. After that it was dried at 100 °C for 6 h and transformed to CaO-based eggshell catalyst according to the reported procedure (Viriya-empikul et al., 2012; Joshi et al., 2015). Palm oil was obtained from commercial sources in local market. The rubber seed was collected from the Northeastern provinces of Thailand.

2.5.2 Extraction and characterization of rubber seed oil

Rubber seed has brown color, hard shell, white flesh and oval shape as depicted in Figure 2.1(a). After cleaning with water and air dry, the seed were ground by blender to get rubber seed powder. The powder (1 kg) was added into the solvent, shaked for 30 min, filtered through filter cloth, centrifuged at 2000 rpm for 10 min to obtain a clear liquid, dried with anhydrous Na_2SO_4 and filtered. The solvent was

removed to give a rubber seed oil. Various kinds of solvent were used including hexane, acetone, dichloromethane and ethyl acetate. The solvent to seed powder ratio (v/wt.) was optimized and the total oil content (wt.%) was calculated from weight of extracted oil divided by weight of rubber seed. FFAs content in oil was determined by the reported method (Basir et al., 2015; Bonet-Ragel et al., 2015). The fatty acids component in oil was determined by a gas chromatograph (GC-2010, Shimadzu) equipped with capillary column, DB-WAX (30 m x 0.15 mm) and a flame ionization detector. The methylheptadecanoate was used as the internal standard for quantification, according to EN14103 standard method (Wang et al., 2015).

Figure 2.1 (a) Rubber seeds collected from Northeast provinces of Thailand. (b) Extracted rubber seed oil (right) and biodiesel (left) obtained from the transesterification catalyzed by waste coral fragment.

2.5.3 Transesterification of rubber seed oil

The transesterification was performed in a batch reactor. Rubber seed oil, methanol and catalyst were mixed in a 250 mL 3-neck round bottom flask equipped with a reflux condenser. The reaction mixture was heated at a controlled temperature and stirring rate. The heterogeneous catalysts used for the transesterification of the rubber seed oil were waste coral fragment, sodium silicate granule, CaO-based eggshell and CaO. The optimized conditions for each catalyst are listed in Table 2.3.

To monitor the reaction progress, the mixed solution of 0.5 mL was sampled, and then the excessive amount of methanol was evaporated in an oven before the analysis of biodiesel yield. The conversion of rubber seed oil to biodiesel was determined in terms of percent fatty acid methyl ester (%FAME) as a function of time. The %FAME was determined using proton nuclear magnetic resonance (^{1}H NMR) technique (Xie et al., 2006; Portela et al., 2016; Gurunatha and Ravi, 2015). The %FAME was calculated according the following Eq. 2.1:

$$\%\text{FAME} = \frac{2A_{CH_3}}{3A_{CH_2}} \times 100 \tag{2.1}$$

where A_{CH_3} is an integration of the methoxy protons (CH_3-O) at chemical shift of 3.66 ppm (singlet peak) and A_{CH_2} is an integration of the methylene protons (-CH_2-) at chemical shift of 2.30 ppm (triplet peak). The factors 3 and 2 were derived from the number of attached protons at the methoxy and methylene carbons, respectively. It should be noted that the triplicate experiments are carried out for each combination of reactants and processing conditions, and the errors of %FAME value were typically within 0.5%. %FAME value in biodiesel was finally analyzed again by gas chromatography (Wang et al., 2015; EN-14214, 2008).

2.6 Results and discussion

2.6.1 Oil extraction

Many kinds of solvents were used to extract triglycerides (oil) from the rubber seed powder including hexane, acetone, dichloromethane and ethyl acetate. The results are summarized in Table 2.1. Since higher percentage of FFAs in the oil reduces the yield of the esterification process, this data suggests that hexane is the best solvent for extraction of oil from rubber seed as it gives high yield of oil and less FFAs content. Moreover, hexane is cheaper than others and can be recovered from the process and reused.

The obtained oil and FFAs contents were varied and seem to correlate with the polarity of the extracted solvents which are in the order of hexane << ethyl acetate < acetone ≈ dichloromethane. Less polar solvent can extract high amount of non-polar oil (triglyceride) and less amount of high polar FAAs, and a vice versa. By this method, hexane gives the highest extracted oil content of 24 wt.% (FFAs = 5.2 wt.%) at a solvent to seed ratio of 0.5 v/wt (Figure 2.2). Further increase in the solvent amount does not have any impact on oil yield. Ethyl acetate gives lower oil content of 20 wt.% (FFAs = 8.1 wt.%), while more polar solvents like acetone and dichloromethane give somewhat lower oil content of 16-18 wt.% (FFAs = 10.1-11.8 wt.%). On the basis of this extraction result using hexane and the ability to produce rubber seed in Thailand, it could be expected that oil feedstock from rubber seed (~0.532 million tons per year) will be approximately 128 million liter per year. This amount of oil can give up to about 108.5 million liter of biodiesel per year (transesterification 1 liter of oil yields ~85% of biodiesel and 15% glycerol).

Therefore, the rubber seed could be an efficient source for biodiesel production in Thailand.

Table 2.1 Oil and free fatty acid (FFAs) contents of the extracted rubber seed oils.

Solvent	Oil content (wt.%)	FFAs content (wt.%)
Hexane	24	5.2
Acetone	18	10.1
Dichloromethane	16	11.8
Ethyl acetate	20	8.1
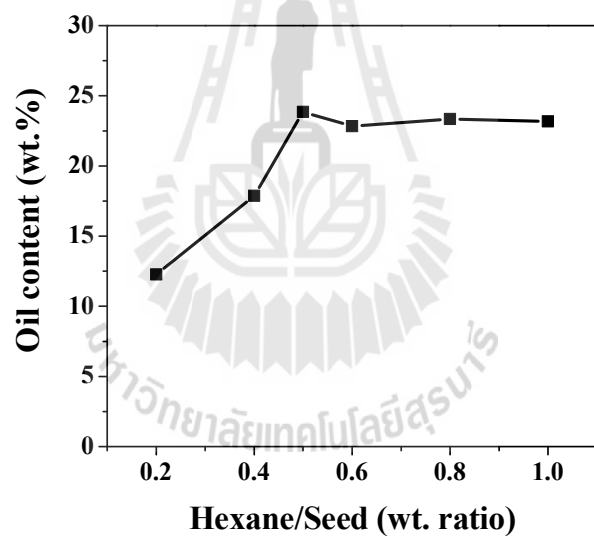
Figure 2.2 Effect of hexane/rubber seed ratio on oil content.

Table 2.2 Properties of rubber seed oil extracted with hexane in comparison with the other reports.

Properties[a]	Rubber seed oil			Palm oil
	This work	Ramadhas[b]	Morshed[c]	this work
Fatty acid composition (%)				
(i) Palmitic acid ($C_{16:0}$)	9.1	10.2	-	37.3
(ii) Stearic acid ($C_{18:0}$)	5.6	8.7	-	3.6
(iii) Oleic acid ($C_{18:1}$)	24.0	24.6	-	45.7
(iv) Linoleic acid ($C_{18:2}$)	46.2	39.6	-	11.2
(v) Linolenic acid ($C_{18:3}$)	14.2	16.3	-	0.4
(vi) other acids	0.9	0.6	-	1.8
Density@15 °C (Kg m^{-3})	894	-	-	901
Average molecular weight of FFAs (g/mol)	275.72	-	278.12	267.06
Kinematic viscosity@ 40 °C (cSt)	7.54	6.62	3.3	7.66
Flash point (°C)	232	198	-	232
Acid value (mg KOH/g oil)	10.60	34	192	0.27
FFAs content (wt.%)	5.20	17	45	0.128
Water content (%w/w oil)	0.013	-	0.93–0.98	0.011

[a]Preformed by biodiesel testing unit, the National Science and Technology Development Agency, Thailand. [b]Ramadhas et al., 2005; [c] Morshed et al., 2011.

2.6.2 GC analysis of rubber seed oil

The rubber seed oil extracted with hexane is a clear yellow liquid. The fatty acid composition and the important physiochemical properties of the rubber seed oil are investigated and compared with other oils, and the results were presented in Table 2.2. Rubber seed oil in this work consists of 15% saturation comprising of palmitic acid ($C_{16:0}$) and stearic acid ($C_{18:0}$) and 85% unsaturation comprising mainly of linoleic

acid ($C_{18:2}$), oleic acid ($C_{18:1}$) and α-linoleic acid ($C_{18:3}$). Saturated fatty acid methyl esters increase the cloud point and cetane number and improve stability whereas more polyunsaturated reduce the cloud point, cetane number and stability. The type and percentage of fatty acids contained in vegetable oil depends on the plant species and on the growth conditions. Though vegetable oils have very low volatility in nature thus quite high flashpoint, it quickly produces volatile combustible compounds upon heating.

2.6.3 Effect of storage time on FFAs content of rubber seed oil

The FFAs content (5.2 wt.%) of the rubber seed oil in this work is significantly lower than that reported by Ramadash et al. (FFAs = 45 wt.%) and Morshed et al. (FFAs = 17 wt.%) (Ramadhas et al., 2005; Morshed et al., 2011). This may come from the difference in extraction method, plant species and growth conditions of the plant. However, the FFAs content in the rubber seed oil is still high when compared with that of *Jatropha* oil (FFAs = 3.3 wt.%), palm oil (FFAs = 0.13 wt.%) and soybean oil (FFAs = 0.09 wt.%) (Roschat et al., 2012; Xie et al., 2006).

Moreover, storage feedstock of oil is an important factor in the process of manufacturing biodiesel but oil can react with air and moisture. Especially when the oil has a high composition of double bonds and get oxidized easily such as rubber seed oil. Consequently, in this research the rubber seed oil was stored for a period of 7 weeks in the bottle and amount of FFAs was analyzed every week. In this case, it was found that FFAs increased only slightly from 10.6 mg KOH/g oil (~5.2 wt.%) in fresh rubber seed oil to 10.7 mg KOH/g oil (~5.4 wt.%) in oil stored for 7 weeks (Figure

2.3). The results demonstrated that rubber seed oil in this study showed high stabilities toward oxidation with air.

The yield of esterification process decreases considerably if FFAs value is greater than 2 wt.%. Canakci and Gerpan (1999; 2001) found that transesterification would not occur if FFAs content in the oil was about 3 wt.%. In order to reduce the high FFAs content in oil, many pretreatment methods have been proposed including refining, extraction by alcohol, esterification by acid-catalysis and multi-step transesterification (Mittelbach and Koncar, 1998; Leung et al., 2010; Prafulla and Shuguang, 2009). Refining of oils increases the overall production cost of the biodiesel due to a high temperature required while extraction by alcohol needs a large amount of solvent and the process is complicated (Leung et al., 2010). Acid esterification is a typical method of producing biodiesel from high FFAs oil (Morshed et al., 2011). A two-step transesterification process can also convert the high FFAs oils to its mono-esters (Ramadhas et al., 2005). The procedure involves acid catalyzed esterification to reduce the FFAs content of the oil to less than 2%. Followed by alkaline catalyze transesterification process to convert the products of the first step to its mono-esters and glycerol. However, both methods require more methanol and are time consuming.

On the other hand, a heterogeneous catalyst offers a significant advantage of simple isolation from the reaction, requires no water, does not cause pollution and is reusable. Therefore, in this study, transesterification of a typical high FFAs type of rubber seed oil to biodiesel using heterogeneous catalysts is investigated.
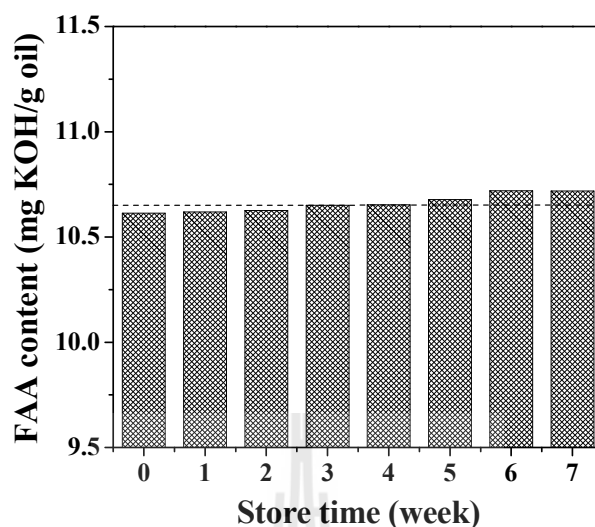
Figure 2.3 Effect of storage time on FFAs content of rubber seed oil.

2.6.4 Heterogeneous transesterification

The heterogeneous catalysts used in the transesterification of rubber seed oil with methanol were CaO-based coral fragment (0.5-1.0 cm^3), disodium metasilicate granule (0.3-1 mm), CaO-based eggshell (>1 μm) and CaO-AR grade (>1 μm). The transesterification conditions for each catalyst are listed in Table 2.3. Figure 2.4 shows the effect of types of catalyst in transesterification of the rubber seed oil to biodiesel. From these data, it was found that all catalysts effectively converted the high FFAs rubber seed oil to biodiesel in a single step. Moreover, no soap formation was observed in all cases.
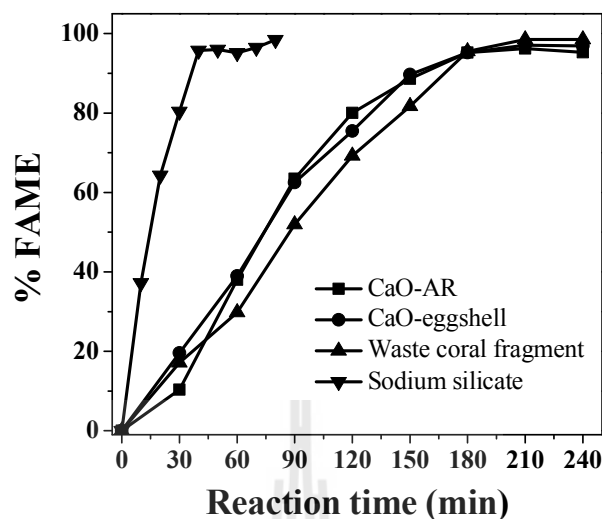
Figure 2.4 Effect of types of catalyst in transesterification of the rubber seed oil to biodiesel (reaction conditions are listed in Table 2.3).

The biodiesel is obtained in high yield and high %FAME of 97-98%. Among these catalysts, the uncalcined disodium metasilicate granule is the most effective catalyst. Under the reaction conditions of catalyst content of 9 wt.%; methanol/oil molar ratio of 9:1; reaction temperature of 65 °C with a constant stirring of 200 rpm, the rubber seed oil is transformed to biodiesel in 40 min. The reaction occurs in high rate. Both CaO-based eggshell and CaO-AR grade particles (catalyst content of 9 wt.%; methanol/oil molar ratio of 15:1; reaction temperature at 65 °C with a constant stirring of 200 rpm) also completely converted the oil to biodiesel in 180 min. While CaO-based coral fragment complete the transesterification in longer time of 210 min and catalyst content of 100 wt.% is required due to its large particle size or low surface area.

However, in an attempt to convert the rubber seed oil to biodiesel using homogeneous KOH catalyst, it was found that the transesterification completed in 40 min with %FAME of 96%, but low yield of biodiesel isolated (45-50%) due to large amount of solid soap forming in the reaction vessel. This side reaction not only reduces the yield of the transesterification product, but also leads to difficulties in the separation of biodiesel from the by-products, which leads to high production cost.

Table 2.3 Heterogeneous transesterification conditions of rubber seed oil catalyzed by different catalyst.

Catalyst	Particle size	Transesterification reaction parameters					
		Catalyst content (wt.%)	MeOH/Oil molar ratio	Temperature (°C)	Stirring rate (rpm)	Reaction time (min)	FAME (%)
CaO-based coral fragment[a]	0.5-1.0 cm^3	100	15:1	65	-	210	98.2
Sodium metasilicate	0.3-1 mm	9	9:1	65	200	40	98.5
CaO-based eggshell[b]	>1 μm	10	12:1	60	200	180	97.6
CaO-AR grade	>1 μm	6	15:1	65	200	180	97.9

[a]Roschat et al., 2012.

[b]Viriya-empikul et al. 2012.

2.6.5 Physicochemical properties of the biodiesel synthesized from rubber seed oil

2.6.5.1 ^{1}H NMR analysis

Biodiesel obtained from all these reactions after removing of the catalyst by simple filtration without any treatment and cleaning processes is a light yellow liquid (Figure 2.1(b)). The ^{1}H NMR analysis of biodiesel and oil was done to investigate their purity. Figure 2.5(A and C) show the expanded ^{1}H NMR spectra of the rubber seed oil and rubber seed biodiesel in the region of 0–6.0 ppm. The characteristics of oil can be observed by the present of glyceridic protons (-OCO-CH_2-CH(OCO-)-CH_2-OCO-) of triglycerides assigned in the range of 4.0–5.2 ppm. While the formation of biodiesel (methyl ester) is characterized by the presence of the protons of the methyl ester moiety (CH_3-OCO-) and the α-carbonyl methylene groups (R-CH_2-OCO-) at chemical shifts approximately 3.66 ppm and 2.30 ppm, respectively. It can be clearly seen that the glyceride backbone of triglyceride is totally absent in the biodiesel sample. Moreover, the present of a strong signal at chemical shift of around 5.3 ppm assigned to the alkene protons (-$CH=CH$-) in ^{1}H-NMR spectra of both oil and biodiesel signifies that their main components are unsaturated fatty acid and methyl ester, respectively.

2.6.5.2 ^{13}C NMR analysis

The ^{13}C NMR spectra of the rubber seed oil and biodiesel obtained from rubber seed oil are depicted in Figure 2.6(A and B). The signal at δ 173.28 ppm and δ 172.87 ppm represent the carboxyl carbon of the ester molecules in triglyceride (rubber seed oil) while the prepared biodiesel only shows the signal of the carboxyl

carbon at δ 174.30 ppm. The signal at δ 68.90 ppm and δ 62.12 ppm in the ^{13}C NMR

spectrum of rubber seed oil is due to the carbonyl methylene groups. Whereas, the

methoxy carbon of methyl esters of rubber seed oil biodiesel illustrates the signal at δ

51.42 ppm. These data confirm that the glyceride backbone of triglyceride is absent in

the biodiesel product. Moreover, the olefinic carbons of triglyceride both in rubber

seed oil and biodiesel (FAME) are similar and can be observed at δ 127.76, 127.90,

128.10, 128.31, 129.72, 130.02 and 130.24 ppm. The methylene and methyl carbons

of fatty acid moiety appear in the range from δ 14.11 to 34.10 ppm. The ^{13}C NMR

clearly show the differences between molecular structure of triglyceride in rubber

seed oil and methyl ester in biodiesel which confirms that rubber seed oil was

successfully transformed to biodiesel.
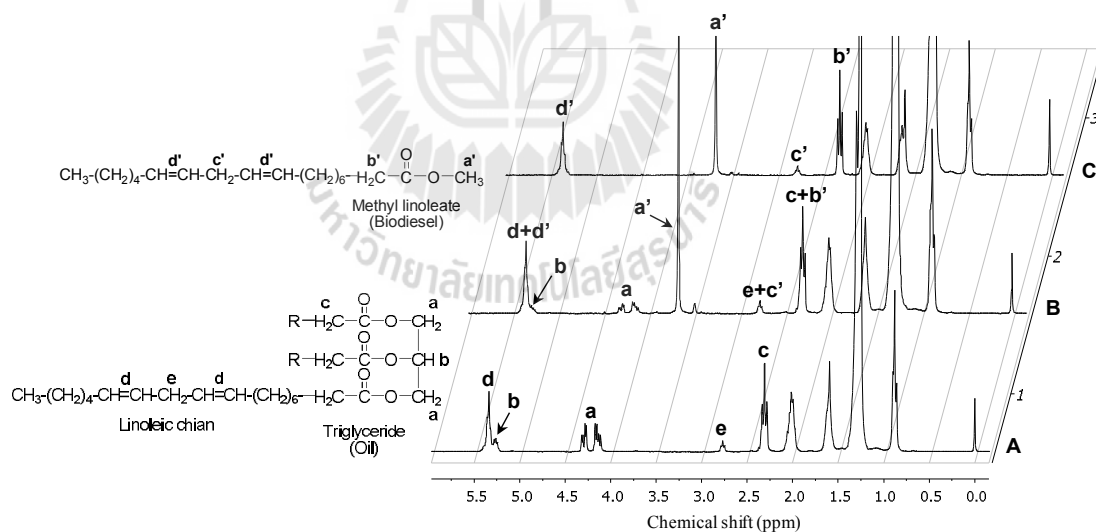
Figure 2.5 ^{1}H NMR spectra of A) extracted rubber seed oil (triglyceride), B) uncompleted transesterification (triglyceride + biodiesel) and C) completed transesterification (biodiesel).
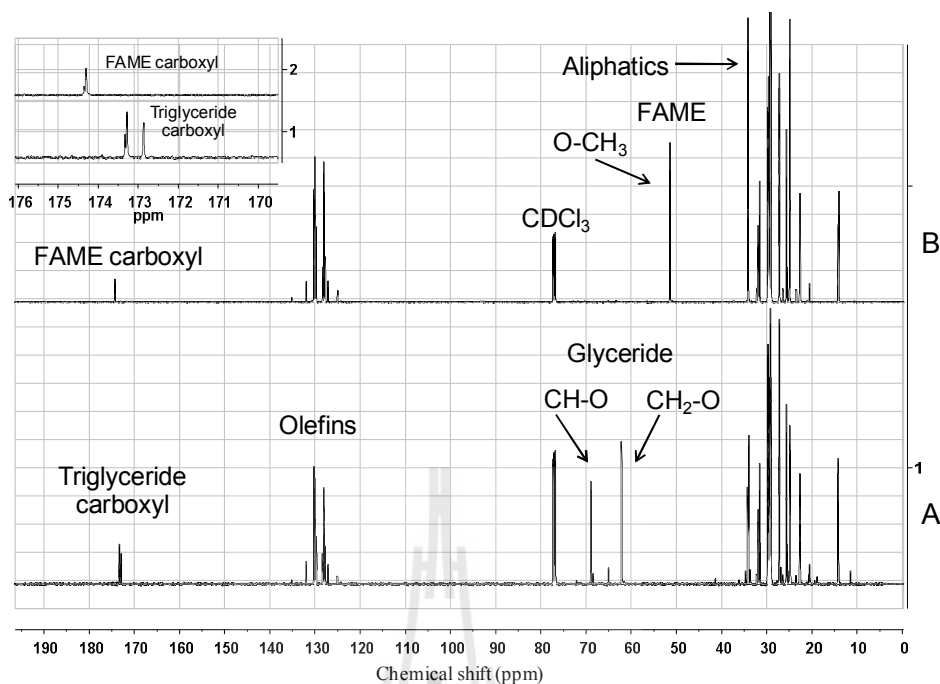
Figure 2.6 ^{13}C NMR spectra of A) rubber seed oil (triglyceride) and B) FAME synthesized from rubber seed oil (biodiesel).

2.6.5.3 FT-IR analysis

FT-IR spectra of the petroleum diesel oil, rubber seed oil and biodiesel synthesized from rubber seed oil are shown in Figure 2.7(a), (b) and (c) respectively. The petroleum diesel oil illustrate only hydrocarbon peaks consist of two strong peaks at 2924 cm^{-1} and 2855 cm^{-1} which are the symmetric and asymmetric vibrations of C-H stretching in CH$_2$ and CH$_3$ group, respectively. The bending vibration of CH$_3$, and CH$_2$ groups appeared at 1462 cm^{-1} and 1378 cm^{-1}. While the small peak at 725 cm^{-1} is rocking vibration of the (CH$_2$)$_n$ in aliphatic group (Ahmad et al., 2014).

On the other hand, rubber seed oil and biodiesel obtained from rubber seed oil show similar observable characteristic peaks of ester compound at ~1740 cm^{-1} which is stretching of carbonyl group (C=O) and the C-O-C symmetric and anti-

symmetric stretching vibrations are observed at ~1300-1000 cm^{-1}. Moreover, C-H of CH$_2$ and CH$_3$ groups have stretching vibration at ~3020-2850 cm^{-1} while bending vibrations appeared at ~1470-1435, ~1360 cm^{-1} and the rocking vibration of the (CH$_2$)$_n$ corresponds to peak at ~720 cm^{-1} (Ahmad et al., 2014; Reshad et al., 2015). However, the FT-IR spectra of the rubber seed oil (Figure 7(b)) show a peak at ~3470 cm^{-1} corresponding to the hydrogen bond stretching and bending vibration of free fatty acid (-OH). While, biodiesel product synthesized from rubber seed oil has no stretching and bending vibration of O-H bonds. This result corresponds to the acid value of 0.35 mg KOH/g oil in biodiesel which is reduced from 10.6 mg KOH/g oil in rubber seed oil extract.

The FT-IR spectra of both rubber seed oil and its biodiesel product are very similar due to the similar chemical structure. However, they have some small different peaks around at ~3020-2850 cm^{-1} which are broader in rubber seed oil, while C-H of methoxy group of biodiesel show strong stretching. In addition, rubber seed oil has only single peak at 1459 cm^{-1} due to the bending vibration of CH$_2$ and CH$_3$ group but biodiesel product shows double peaks at 1460 and 1440 cm^{-1}. The FT-IR clearly showed that rubber seed oil was successfully converted to biodiesel consistent with the ^{1}H and ^{13}C-NMR results.
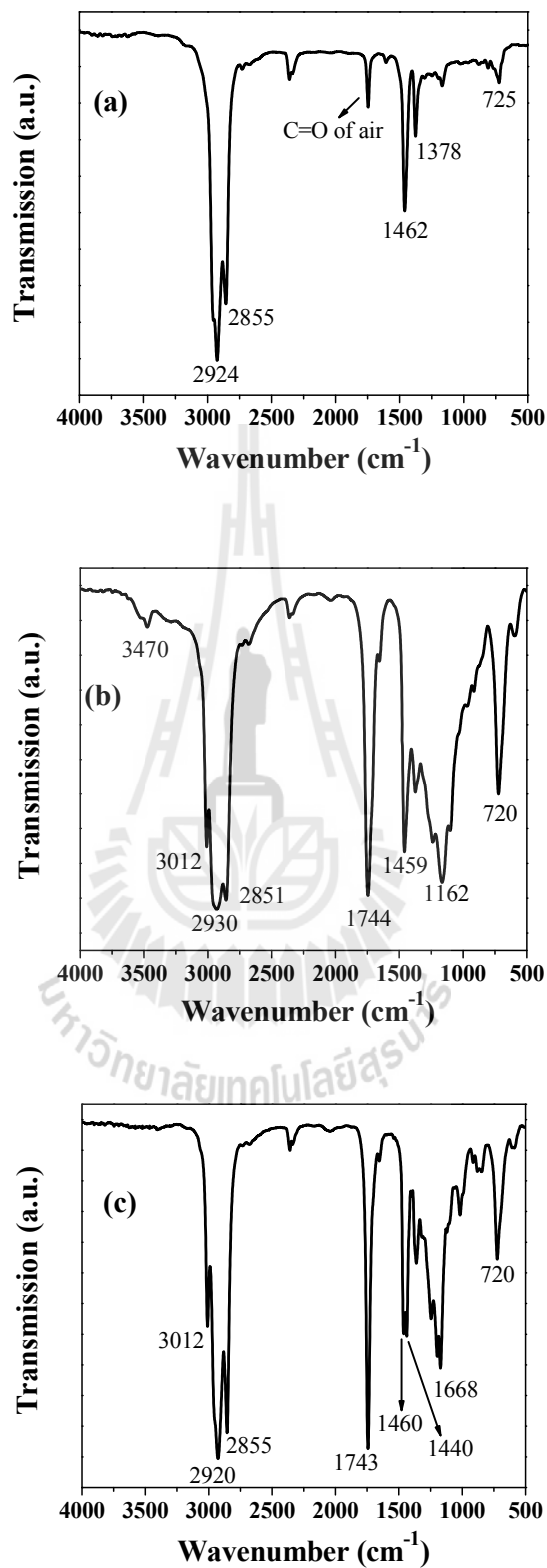
Figure 2.7 FT-IR spectrum of (a) petrol-diesel oil (b) rubber seed oil and (c) synthesized biodiesel from rubber seed oil.

2.6.5.4 Thermo gravimetric analysis

The TGA results of the rubber seed oil and biodiesel from rubber seed oil compared with petroleum diesel oil were depicted in Figure 2.8. The TGA showed that the rubber seed oil is thermally stable up to 230 °C. The TGA curves also confirm the absence of water and solvent contamination in the oil sample. The weight loss of rubber seed oil starts at 230 °C and significantly after 300 °C increases. Rubber seed oil completely degraded at the temperature 550 °C with mass loss of over 99%. Likewise, the synthesized biodiesel shows similar degradation. The mass loss of biodiesel appears at ~125 °C and the biodiesel completely decomposed at ~450 °C. After completely decompose both rubber seed oil and biodiesel show no residual weight. On the other hand, petroleum diesel oil evaporation begins at 70 °C and deplete at ~300 °C.

Biodiesel is known as an ester compound which has high boiling point and is less volatile than petroleum diesel oil. However, the process to compress air without fuel in a cylinder of engine is at temperature of 800 °C (Sivakumar et al., 2011). Therefore, the combustion of biodiesel prepared by transformation of the rubber seed oil within the engine as an alternative fuel is not a problem. In addition, TGA data confirms that the biodiesel from rubber seed oil is clean fuel because it is completely decompose to H_2O, CO_2 and CO (Reshed et al., 2015; Borugadda and Goud, 2012).
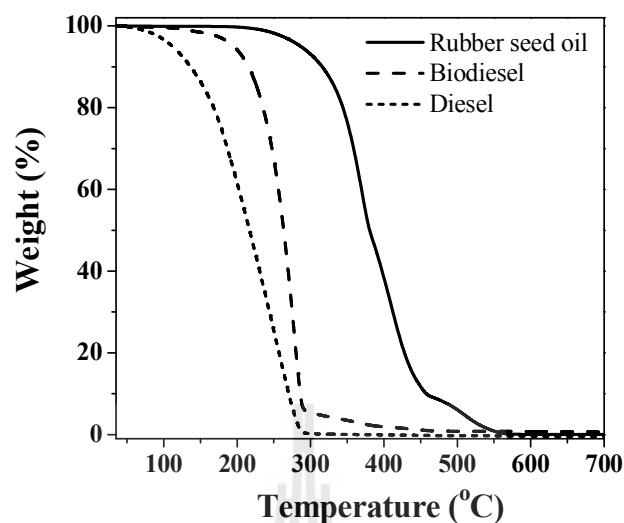
Figure 2.8 Thermogravimatric curve of petroleum diesel oil, rubber seed oil and synthesized biodiesel from rubber seed oil.

2.6.6 Properties of biodiesel

The fuel properties of the rubber seed oil biodiesel were evaluated according to the EN 14214 and ASTM standards and compared with biodiesel, high-speed diesel standards and biodiesel prepared from palm oil (EN-14214, 2008; Reyes-Trejo et al., 2014). The results are summarized in Table 2.4. Most of the physicochemical properties of rubber seed oil biodiesel meet those of biodiesel and diesel standards and are comparable to palm oil biodiesel.

The rubber seed oil biodiesel has methyl ester content of 97.7%. Kinematic viscosity of 4.84 cSt is standing within the acceptable range of the standard biodiesel (3.5-5.0 cSt), but it is slightly higher than that of the high-speed diesel standard (1.8-4.1 cSt). The water content of 0.023 %w/w and acid number of 0.35 mg KOH/g oil are lower than the limit of the standards and palm oil biodiesel. The total

contamination defined as the impurity content in the rubber seed oil biodiesel collected without any treatment and cleaning processes is 12 ppm which is lower than the acceptant value of 24 ppm. The heating value or heat of combustion of the obtained rubber seed oil biodiesel (9563 kcal/kg) is higher than that of palm oil biodiesel (9488 kcal/kg) and closer to that of the diesel (10840 kcal/kg). The oxidation number of rubber seed oil biodiesel is less than palm oil biodiesel because the rubber seed oil contains higher unsaturated fatty acid than palm oil. However, the oxidation number, which indicates a durability of the biodiesel when reacts with oxygen and water in the air to form carboxylic acid compounds, of the obtained biodiesel (9.82 h) is still higher than that of the standard biodiesel (6 h).
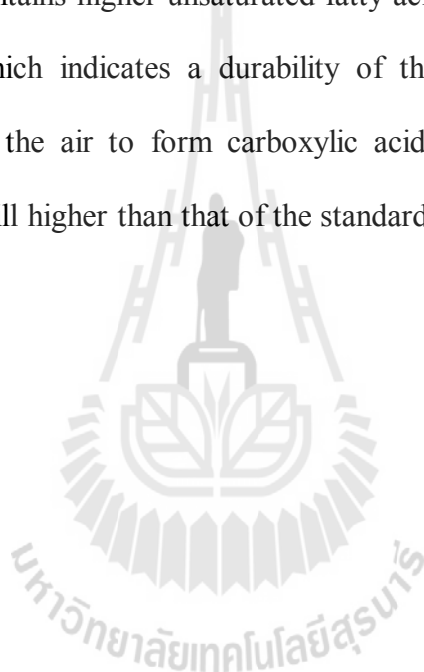
Table 2.4 Properties of rubber seed oil biodiesel in comparison with the standards and other biodiesels.

Fuel properties[a]	Standard biodiesel[b]	High-speed diesel	Palm oil biodiesel[c]	Rubber seed oil biodiesel[c]
Density@15 °C (Kg m^{-3})	860-900	810-870	874	880
Kinematic viscosity @ 40 °C (cSt)	3.5-5.0	1.8-4.1	4.33	4.84
Flash point (°C)	>120	≥52	187	184
Acid number (mg KOH/g oil)	<0.5	-	0.25	0.35
Water content (%w/w oil)	<0.050	≤0.05	0.025	0.023
Copper strip corrosion	Number 1	≤1	1	1
Methyl ester content (%)	96.5	-	96.8	97.74
Oxidation number (hour)	>6	-	12.68	9.82
Total contamination (ppm)	>24	-	7	12
Heating value (kcal/kg)	-	10840	9488	9563

[a]Preformed by biodiesel testing unit, the National Science and Technology Development Agency, Thailand.

[b]EN-14214, 2008

[c]This work

2.7 Conclusions

Rubber seed, non-edible crops, collected from the Northeast province of Thailand can be used as a new raw material to produce oil for biodiesel production. The 24 wt.% of oil is successfully extracted from the rubber seed powder using hexane (0.5 v/wt of solvent/seed ratio). The extracted rubber seed oil contains low FFAs content of 5.2 wt.% and unsaturated fatty acids (linoleic acid ($C_{18:2}$) 46.2%, oleic acid ($C_{18:1}$) 24.0%, α-linoleic acid ($C_{18:3}$) 14.2%) as the major fatty acid components. This high FFAs oil (>3 wt.%) is successfully transesterified by various heterogeneous catalysts such as CaO-based waste coral fragment, sodium metasilicate and CaO-based eggshell to biodiesel in high yield and high %FAME. Under optimum conditions of catalyst content of 9 wt.%; methanol/oil molar ratio of 9:1; reaction temperature of 65 °C with a constant stirring of 200 rpm, sodium metasilicate can convert the rubber seed oil to yield biodiesel with a %FAME exceeding 97% in 40 min. The rubber seed oil biodiesel collected without any treatment and cleaning process shows high quality fuel properties that satisfy all EN 14214 and high-speed diesel standards. The capability to use oil extracted from rubber seed as inexpensive feedstock in combination with utilization of these heterogeneous catalysts would additionally improve the economic aspect of overall biodiesel production, making cost-efficient biodiesel in Thailand.

2.8 References

Ahmad, J., Yusup, S., Bokhari, A. and Kamil, R. M. N. (2014). Study of fuel properties of rubber seed oil based biodiesel. **Energy Conversion and Management**. 78: 266-275.

Araújo, F. D. S., Araújo, I. C., Costa, I. C. G., Moura, C. V. R., Chaves, M. H. and Araújo, C. E. C. (2014). Study of degumming process and evaluation of oxidative stability of methyl and ethyl biodiesel of *Jatropha curcas* L. oil from three different Brazilian states. **Renewable Energy**. 71: 495-501.

Basir, F. Al., Datta, S. and Roy, P. K. (2015). Studies on biodiesel production from *Jatropha Curcas* oil using chemical and biochemical methods – A mathematical approach. **Fuel**. 158: 503-511.

Bonet-Ragel, K., Canet, A., Benaiges, M. D. and Valero, F. (2015). Synthesis of biodiesel from high FFA *alperujo* oil catalysed by immobilised lipase. **Fuel**. 161: 12-17.

Borugadda, V. B. and Goud, V. V. (2012). Biodiesel production from renewable feedstocks: Status and opportunities. **Renewable & Sustainable Energy Reviews**. 16: 4763-4784.

Canakci M. and Gerpan, J. V. (2011), Biodiesel production from oils and fats with high free fatty acids. **Transactions of the ASAE**. 44: 1429-1436.

Canakci, M. and Gerpan, J. V. (1999). Biodiesel production via acid catalysis. **Transactions of the American Society of Agricultural Engineers**. 42: 1203-1210.

Chaiya, C. and Reubroycharoen, P. (2013). Production of Bio Oil from Para rubber seed using Pyrolysis Process. **Energy Procedia**. 34: 905-911.

Chin, B. L. F., Yusup, S., Shoaibi, A. Al., Kannan, P., Srinivasakannan, C. and Sulaiman, S. A. (2014). Kinetic studies of co-pyrolysis of rubber seed shell with high density polyethylene. **Energy Conversion and Management**. 87: 746-753.

EN-14214. (2008). Automotive Fuels-Fatty Acid Methyl Esters (FAME) for Diesel Engines–Requirements and test methods. [Online]. Available: https://www.en. wikipedia.org/wiki/EN_14214.

Evon, Ph., Kartika, A. I., Cerny, M. and Rigal, L. (2013). Extraction of oil from *jatropha* seeds using a twin-screw extruder: Feasibility study. **Industrial Crops and Products**. 47: 33-42.

Gurunatha, B. and Ravi, A. (2015). Process optimization and kinetics of biodiesel production from neem oil using copper doped zinc oxide heterogeneous nanocatalyst. **Bioresource Technology**. 190: 424-428.

Hassan, S. N. A. M., Ishak, M. A. M., Ismail, K., Ali, S. N. and Yusop, M. F. (2014). Comparison Study of Rubber Seed Shell and Kernel (*Heve brasiliensis*) as Raw Material for Bio-Oil Production, **Energy Procedia**. 52: 610-617.

Joshi, G., Rawat, D. S., Lamba, B. Y., Bisht, K. K., Kumar, P., Kumar, N. and Kumar, S. (2015). Transesterification of *Jatropha* and Karanja oils by using waste egg shell derived calcium based mixed metal oxides. **Energy Conversion and Management**. 96: 258-267.

Leung, D. Y. C., Xuan, W. and Leung, K. M. H. (2010). A review on biodiesel production using catalyzed transesterification. **Applied Energy**. 87: 1083-1095.

Mittelbach, M. and Koncar, M. (1998). Method for the preparation of fatty acid alkyl esters. **United States patent 5849939**. [Online]. Available: http://www. freepatentsonline.com/5849939.html.

Morshed, M., Ferdous, K., Ferdous, M. R., Mazumder, M. S. I., Islam, M. A. and Uddin, Md. T. (2011). Rubber seed oil as a potential source for biodiesel production in Bangladesh. **Fuel**. 90: 2981-2986.

Moser, B. R. (2016). Fuel property enhancement of biodiesel fuels from common and alternative feedstocks via complementary blending. **Renewable Energy**. 85: 819-825.

Office Agricultural Economics. (2014). Forecasting agricultural crop year 2557/58. **Journal Forecasting Agricultural Output**. 27: 1-83. [Online]. Available: https//www.oae.go.th/ download/download_journal/2558/yearbook57.pdf.

Omidvarborna, H., Kumar, A. and Kim, D. S. (2015). NO_x emissions from low-temperature combustion of biodiesel made of various feedstocks and blends. **Fuel Processing Technology**. 140: 113-118.

Phooa, Z. W. M. M., Razona, L. F., Knothec, G., Ilhamb, Z., Goembirab, F., Madrazoa, C. F., Rocesa, S. A. and Sakab, S. (2014). Evaluation of Indian milkweed (*Calotropis gigantea*) seed oil as alternative feedstock for biodiesel. **Industrial Crops and Products**. 54: 226-232.

Portela, N. A., Oliveira, E. C. S., Neto, A. C., Rodrigues, R. R. T., Silva, S. R. C., Castro, E. V. R. and Filgueiras, P. R. (2016). Quantification of biodiesel in petroleum diesel by ^{1}H NMR: Evaluation of univariate and multivariate approaches. **Fuel**. 166: 12-18.

Portugal-Pereira, J., Nakatani, J., Kurisu, K. and Hanaki, K. (2016). Life cycle assessment of conventional and optimised *Jatropha* biodiesel fuels. **Renewable Energy**. 86: 585-593.

Prafulla D. P. and Shuguang, D. (2009). Optimization of biodiesel production from edible and non-edible vegetable oils. **Fuel**. 88: 1302-1306.

Ramadhas, A. S., Jayaraj, S. and Muraleedharan, C. (2005). Biodiesel production from high FFAs rubber seed oil. **Fuel**. 84: 335-340.

Reshad, A. S., Tiwari, P. and Goud, V. V. (2015). Extraction of oil from rubber seeds for biodiesel application: Optimization of parameters. **Fuel**. 150: 636-644.

Reyes-Trejo, B., Guerra-Ramírez, D., Zuleta-Prada, H., Cuevas-Sánchez, J. A., Reyes, L., Reyes-Chumacero, A. and Rodríguez-Salazar, J. A. (2014). *Annona diversifolia* seed oil as a promising non-edible feedstock for biodiesel production. **Industrial Crops and Products**. 52: 400-404.

Roschat, W., Kacha, M., Yoosuk, B., Sudyoadsuk, T. and Promarak, V. (2012). Biodiesel production based on heterogeneous process catalyzed by solid waste coral fragment. **Fuel**. 98: 194-202.

Sanchez-Arreola, E., Martin-Torres, G., Lozada-Ramírez, J. D., Hernandez, L. R., Bandala-Gonzalez, E. R. and Bach, H. (2015). Biodiesel production and de-oiled seed cake nutritional values of a Mexican edible *Jatropha curcas*. **Renewable Energy**. 76: 143-147.

Sivakumar, P., Anbarasu, K. and Renganathan, S. (2011). Bio-diesel production by alkali catalyzed transesterification of dairy waste scum. **Fuel**. 90: 147-151.

Viriya-empikul, N., Krasae, P., Nualpaeng, W., Yoosuk, B. and Faungnawakij, K. (2012). Biodiesel production over Ca-based solid catalysts derived from industrial wastes. **Fuel**. 92: 239-244.

Wang, M., Nie, K., Yun, F., Cao, H., Deng, L., Wang, F. and Tan, T. (2015). Biodiesel with low temperature properties: Enzymatic synthesis of fusel alcohol fatty acid ester in a solvent free system. **Renewable Energy**. 83: 1020-1025.

Xie, W., Peng, H. and Chen, L. (2006). Transesterification of soybean oil catalyzed by potassium loaded on alumina as a solid-base catalyst. **Applied Catalysis A: General**. 300: 67-74.

Yusup, S. and Khan, M. (2010). Basic properties of crude rubber seed oil and crude palm oil blend as a potential feedstock for biodiesel production with enhanced cold flow characteristics. **Biomass & Bioenergy**. 10: 1523-1526.

Zhang, P., Liu, Y., Fan, M. and Jiang, P. (2016). Catalytic performance of a novel amphiphilic alkaline ionic liquid for biodiesel production: Influence of basicity and conductivity. **Renewable Energy**. 86: 99-105.

CHAPTER III

A SIMPLE ANALYSIS METHOD FOR BIODIESEL

PRODUCT BY THIN LAYER CHROMATOGRAPHY

(TLC) VISUALIZED UV LIGHT

3.1 Graphical abstract
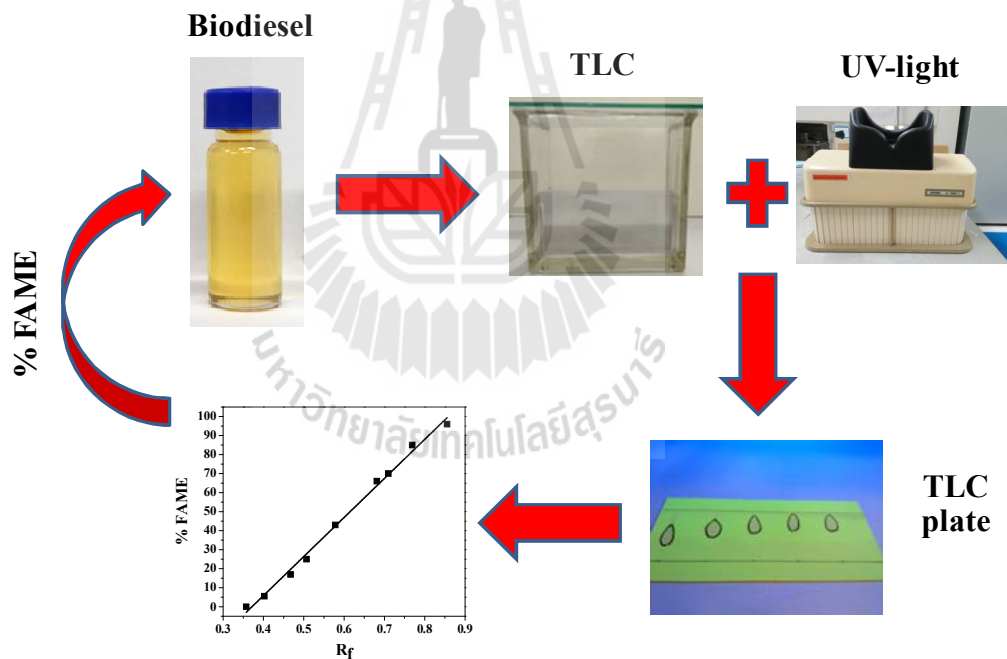
The TLC visualized UV light is an efficient, economical, convenient, rapid, and simple method to evaluate %FAME of biodiesel product.

3.2 Highlights

- TLC visualized UV light analysis method is used to evaluate %FAME of biodiesel product.

- Types of catalysts have no effects on the results obtained from TLC visualized UV light analysis.

- TLC visualized UV light is an efficient and simple method for screening and monitoring the biodiesel production process.

3.3 Abstract

This work demonstrates the use of thin layer chromatography (TLC) visualized UV light as a potential analysis method for cursory screening and monitoring the biodiesel production process via transesterification of palm oil with methanol. The synthesized biodiesel samples were examined %FAME by using gas chromatography (GC) and ^{1}H NMR, and physicochemical properties were confirmed by using ^{13}C NMR, TG-DTA and FT-IR, respectively. The relation between %FAME obtained by GC and R_f value was plotted, and displayed a linear relationship of the two values following the equation $y = 205x - 76$, where y and x are %FAME and R_f value, respectively. The TLC visualized UV light is a good analysis method and show similarity of %FAME determined by GC and ^{1}H NMR techniques with a marginally ±2-4% difference. Hence, TLC visualized UV light is an efficient, economical, convenient, rapid, and simple method for determining of %FAME in the biodiesel production process, both qualitatively and quantitatively.

3.4 Introduction

Biodiesel is a renewable and clean fuel produced from vegetable oil and animal fats via transesterification reaction with alcohols. Generally, methanol or ethanol is used to form fatty acid methyl ester (FAME) or fatty acid ethyl ester (FAEE) (Azeem et al., 2016; Alhassan et al., 2014; Habibullah et al., 2015). Biodiesel is promoted in many countries especially in European countries and the United States where biodiesel is encouraged to be used in automobiles (Speranza et al., 2015). In Thailand, biodiesel has been used to blend with petro-diesel in the ratio of 5% (B5 fuel) and the Royal Thai Government for development has stated that the ratio should reach 25% within 10 years (Department of Alternative Energy Development and Efficiency-Thailand, 2012).

According to the European standard (EN 14214; test-method EN 14103), the most common way to examine biodiesel fuel is based on gas chromatography (GC) (EN-14214, 2008; Maneerung et al., 2015). However, this method has some disadvantages as it requires a long time to analyze (about 30-45 min per sample) and the use of standard solution (methyl heptadecanoate) which results in the expensive testing process. In addition, a long analyzing process also limits the ability to study kinetics in transesterification reaction which is important to the design and control of production process in the large scale. Another method commonly used in probing transesterification reaction is proton nuclear magnetic resonance (^{1}H NMR). The technique is more suitable for kinetic study as it requires a relatively short time to analyze (approximately 3-5 min per sample) (Roschat et al., 2016; Killner et al., 2015). Nevertheless, the uses of ^{1}H NMR to examine biodiesel are limited by the high cost of both the instrument and its maintenance.

The other analytical methods such as Fourier transform infrared spectroscopy (FT-IR) and gas chromatography mass spectrometry (GC/MS) can be used to identify the chemical functional group and composition of the synthesized biodiesel. However, they only give qualitative results thus are mainly used only to support other techniques (Farooq et al., 2013; Basumatary and Deka, 2012; Bradley, 2010). Chand et al., reports the use of thermogravimetric and differential thermal analysis (TG-DTA) to monitor biodiesel production (Chand et al., 2009). They found that TGA analysis is correlated with the ^{1}H NMR method and can be used to estimate the percentage of biodiesel with an error of 1.5%. However, this method still involves an expensive instrument, takes a long time to analyze, and also requires N_2 atmosphere in process.

In addition, high performance thin layer chromatography (HP-TLC) and thin layer chromatography coupled with flame ionization detection (TLC-FID) have been employed to assess the progress of transesterification (Chattopadhyay et al., 2011; Yang et al., 2013). Both methods are widely used for biodiesel analysis because they are simple and more convenient than GC. However, both techniques require complicate instruments including UV–VIS spectrophotometer and flame ionization detector. Thin layer chromatographies (TLC) have been utilized to monitor the progress of transesterification. Supamathanon et al. and Sukhawanit et al., used TLC plate strained with iodine to qualitatively analyze the biodiesel product. In this case, lack of ability to analyze the biodiesel product quantitatively limits the applications of the technique (Supamathanon et al., 2011; Sukhawanit et al., 2014)

The current study demonstrates the development of TLC method visualized by UV light as an easy, convenient, and very low-cost technique to monitor the reaction

progress of biodiesel production. Moreover, the possibility to use such technique in a quantitative way is discussed in comparison with other established techniques like GC and ^{1}H NMR.

3.5 Materials and methods

3.5.1 Materials

Reagent grade chemicals including CaO and NaOH were purchased from Acros, while methanol, petroleum ether, acetone, and glacial acetic acid were obtained from Fluka. Palm oil purchased from commercial sources in the local market was used in the preparation of biodiesel. Silica gel-coated TLC plates applied in this study were purchased from SILICYCLE Ultra Pure SILICA GELS, Canada.

3.5.2 Preparation of biodiesel samples

All biodiesel samples in this work were prepared by transesterification reaction carried out in a 250 mL 3-neck round bottom flask equipped with a reflux condenser. For reaction with CaO heterogeneous catalyst, the temperature and stirring rate were controlled at 60 °C and 200 rpm, respectively. 10 wt.% of CaO catalyst loading and methanol to oil molar ratio of 12:1 were used (Viriya-empikul et al., 2012). NaOH was used as a homogeneous catalyst; 0.3 wt.% of catalyst, methanol to oil molar ratio of 6:1, reaction temperature of 50 °C and stirring rate of 200 rpm were used (Arzamendi et al., 2007). In this work, two sets of biodiesel samples were prepared. The first set composing of samples was prepared with CaO catalyst at the previously described conditions with varied reaction time in order to get samples with different %FAME (samples A1-A9). This set of sample was used to generate a standard curve

of the TLC method. The second set composed of two samples prepared with CaO and NaOH catalysts. These two samples were used as unknown samples whose reaction progresses were probed with TLC method. To do so, 0.5 mL of each solution mixture was sampled at different reaction times, heated to remove excess methanol and analyzed to determined %FAME.

3.5.3 Biodiesel analysis

3.5.3.1 Analysis by gas chromatography

The yield and compositions of biodiesel were analyzed by a gas chromatograph (GC-2010, Shimadzu) equipped with a capillary DB-WAX column (30 m × 0.15 mm) and connected with a flame ionization detector. Temperature of the column was programmed from 180 to 230 °C with a heating rate of 5 °C/min. Methyl heptadecanoate was used as an internal standard for quantitative analysis according to EN14103 standard method and the errors for methyl ester content were typically within ±2.0 wt.% (Viriya-empikul et al., 2012). Methyl ester content (C) was calculated according to Eq. 3.1:

$$C = \frac{(\Sigma A) - (AEI)}{AEI} \times \frac{CEI \times VEI}{m} \times 100\% \tag{3.1}$$

where $\sum A$ is total peak area of the methyl ester from C_{14} to $C_{22:1}$. AEI is the peak area of methyl heptadecanoate internal standard. CEI is a concentration of the methyl heptadecanoate solution (mg/mL). VEI is the volume of the methyl heptadecanoate solution (mL) and m is the mass of the biodiesel sample (mg) (EN-14214, 2008; Maneerung et al., 2015; Shan et al., 2015).

3.5.3.2 Nuclear magnetic resonance spectroscopy

The biodiesel sample was analyzed by using nuclear magnetic resonance technique (500 MHz of NMR spectrometer, Bruker) using CDCl₃ (99.8%) as a solvent. The biodiesel yield was calculated in term of %FAME according to Eq 3.2:

$$\%FAME = \frac{2A_{CH_3}}{3A_{CH_2}} \times 100 \qquad (3.2)$$

where A_{CH_3} is an integration of the methoxy protons of the methyl ester moiety (*CH₃*–OCO–) at 3.66 ppm chemical shift. A_{CH_2} is an integration of the proton in α-carbonyl methylene groups (R–*CH₂*–OCO–) both in triglyceride and methyl ester at chemical shift of 2.30 ppm. The factors 3 and 2 were derived from the number of attached protons at the methoxy and α-carbonyl methylene carbons, respectively (Roschat et al., 2016). It should be noted that the error from this method was typically within ±1-2%. In addition, the conversion of triglyceride into biodiesel can be detected by the presence of characteristic methylene proton peaks of *C1* and methine proton peak of *C2* in triglyceride (–OCO–¹*CH₂*–²*CH*(OCO–)–¹*CH₂*–OCO–) at chemical shift 4.16 ppm, 4.30 ppm and 5.30 ppm as shown in Figure 3.2, respectively.

Moreover, ¹³C NMR was used to characterize biodiesel product in the term of qualitative analysis. The difference of triglyceride as a starting material and the biodiesel product could be observed as the chemical shift at 172-174 ppm is an identity of the carboxyl carbon. The triglyceride would be shown two positions peak of central and terminal carbonyl carbon, whereas biodiesel product can be seen only one peak of carbonyl carbon. In addition, chemical shift at 68 ppm and 62 ppm is

related to carbonyl methylene groups of triglyceride and at 51 ppm belong to methoxy carbon of biodiesel product.

3.5.3.3 Thermogravimetric and differential thermal analysis

The biodiesel products were analyzed by thermogravimetric/ differential thermal analyzer carried out on a Mettler Toledo thermal analyzer (TGA/DSC1). In this technique, 10-15 mg of sample was heated at a constant heating rate of 10 °C/min under atmosphere of nitrogen gas mixed with oxygen gas at a constant flow rate of 50 mL/min (Vega-Lizama et al., 2015). The applied temperature range was 35-700 °C.

3.5.3.4 Fourier transform infrared spectroscopy analysis

Fourier transforms infrared spectroscopy on a Perkin–Elmer FTIR spectrometer and spectrum GX spectrometer was employed to characterize biodiesel in the range of 4000–400 cm^{-1} with resolution of 4 cm^{-1}. The sodium chloride cell was used as a salt plate to place the sample in the light beam of the instrument.

3.5.3.5 Thin layer chromatography visualized UV light analysis

TLC visualized UV light was employed to analyze a quantity of biodiesel product to compared with the results from GC and ^{1}H NMR. The biodiesel samples from the reaction after removing excess methanol were spotted on a TLC plate and the TLC plate was then put in a developing container which contained a mixed solvent of petroleum ether/acetone/glacial acetic acid with a ratio of 85:15:1 v/v/v, respectively. After that, the TLC plate was removed from the developing container and the solvent front was immediately marked with a pencil. Finally, the dried TLC

plate was put under a UV lamp to detect the spots of the sample. Spot circle was marked lightly with a pencil. The distance traveled by the solvent front and that traveled by the sample were measured and used to calculate retention factor, R_f, according to Eq. 3.3:

$$R_f = \frac{\text{distance traveled by the sample (cm)}}{\text{distance traveled by the solvent front (cm)}} \tag{3.3}$$

3.6 Results and discussion

3.6.1 Construction of a standard curve

3.6.1.1 Gas chromatography analysis

The biodiesel products from palm oil were produced in nine samples and analyzed by GC. Figure 3.1 shows an example of profile for the sample A9 (96.12% of FAME). The GC chromatograms correspond to the different compositions of fatty acid methyl esters listed in Table 3.1. The results show that the major compositions of reference biodiesel product synthesized from palm oil with CaO, were methyl oleate (C18:1), methyl palmitate (C16:0) and methyl linoleate (C18:2). The results agree well with those reported by Viriya-empikul et al. (Viriya-empikul et al., 2012). As a result in Table 3.2, shows %FAME of all biodiesel samples A1 to A9 obtained from analysis by GC technique.

Table 3.1 Fatty acid methyl ester composition of biodiesel sample A9.

Retention Time (min)	FAME
9.452	Methyl myristate (C14:0)
11.183	Methyl palmitate (C16:0)
12.042	Methyl heptadecanoate (C17:0)
12.987	Methyl stearate (C18:0) + Methyl oleate (C18:1)
13.298	Methyl linoleate (C18:2)
13.720	Methyl linolenate (C18:3)
14.463	Methyl arachidate (C20:0)
17.782	Methyl erucate (22:1)
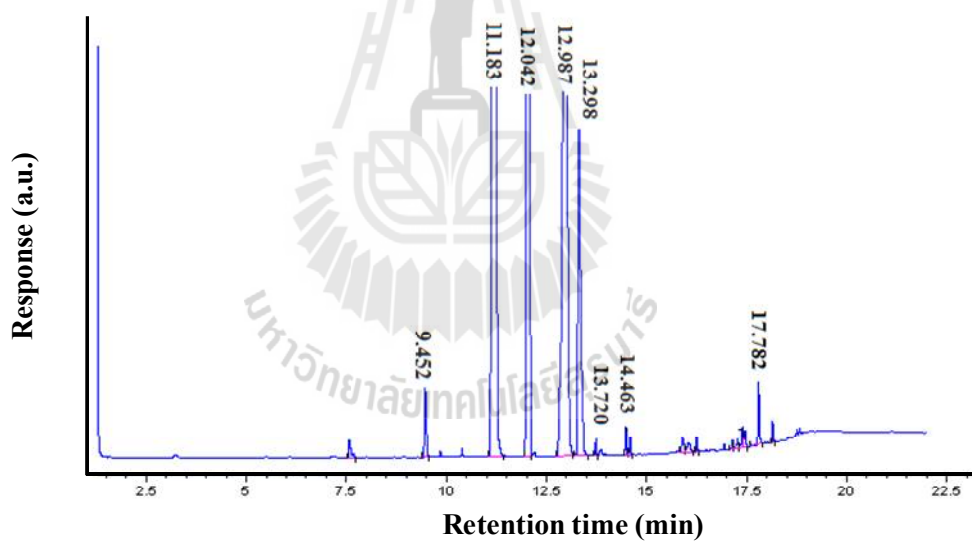
Figure 3.1 GC chromatogram of biodiesel sample A9.
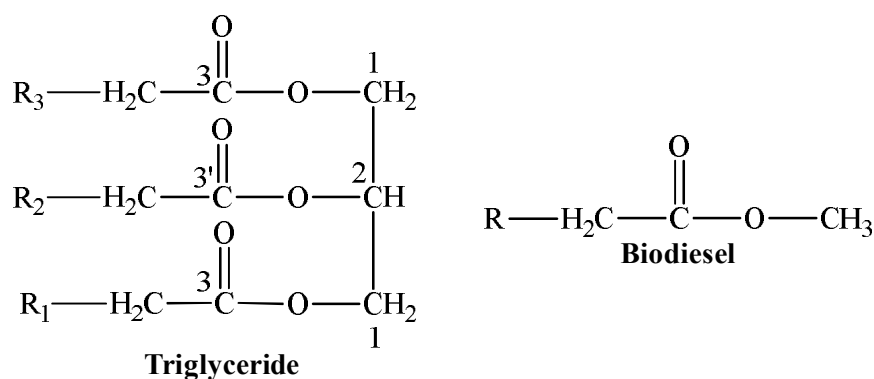
Figure 3.2 Chemical structures of triglyceride and biodiesel product.

3.6.1.2 Nuclear magnetic resonance spectroscopy

^{1}H NMR spectra of the palm oil and the obtained biodiesel are depicted in Figure 3.3(a). The palm oil (spectrum a) shows two peaks between 4.16-4.30 ppm and the small peak at 5.30 ppm assigned to glyceridic protons but does not show a methoxy proton peak at 3.66 ppm (-OCO-CH_2-CH(OCO-)-CH_2-OCO-). When %FAME increased (spectra b, c and d), the methoxy proton (CH_3-OCO-) peak at 3.66 ppm is increased. On the other hand, peaks area at 4.16-4.30 ppm and 5.30 ppm decrease and disappear when the conversion of triglyceride was completed (spectrum e). The %FAMEs of all biodiesel samples were analyzed by ^{1}H-NMR as shown in Table 3.2.

To confirm the results, ^{13}C NMR was used to identify the sample as shown in Figure 3.3(b) and (c), respectively. Palm oil (spectrum a) shows important carbon peaks corresponding to triglyceride at 172.9 ppm and 173.4 ppm correlated with central carbonyl carbon ($^{3'}C$) and terminal carbonyl carbon (^3C), respectively. The peak at 62.11 ppm is a characteristic of ^1C terminal carbon of triglyceride, while the ^2C central carbon shows peak at 68.89 ppm as depicted chemical structure of

triglyceride in Figure 3.2. When methyl ester is generated from palm oil, carbonyl carbon ($-COOCH_3-$) at 174.26 ppm and methoxy carbon ($-OCH_3$) at 51.40 ppm can be seen along with carbon peaks of triglyceride (spectra b, c and d). After palm oil is completely transformed into biodiesel, carbonyl carbon peak, terminal carbon of $-CH_2-O-$ bond and central carbon of $-CH-O-$ bond of triglyceride (^1C, ^2C) are absent but carbonyl carbon and methoxy carbon of methyl ester appear (spectrum e).
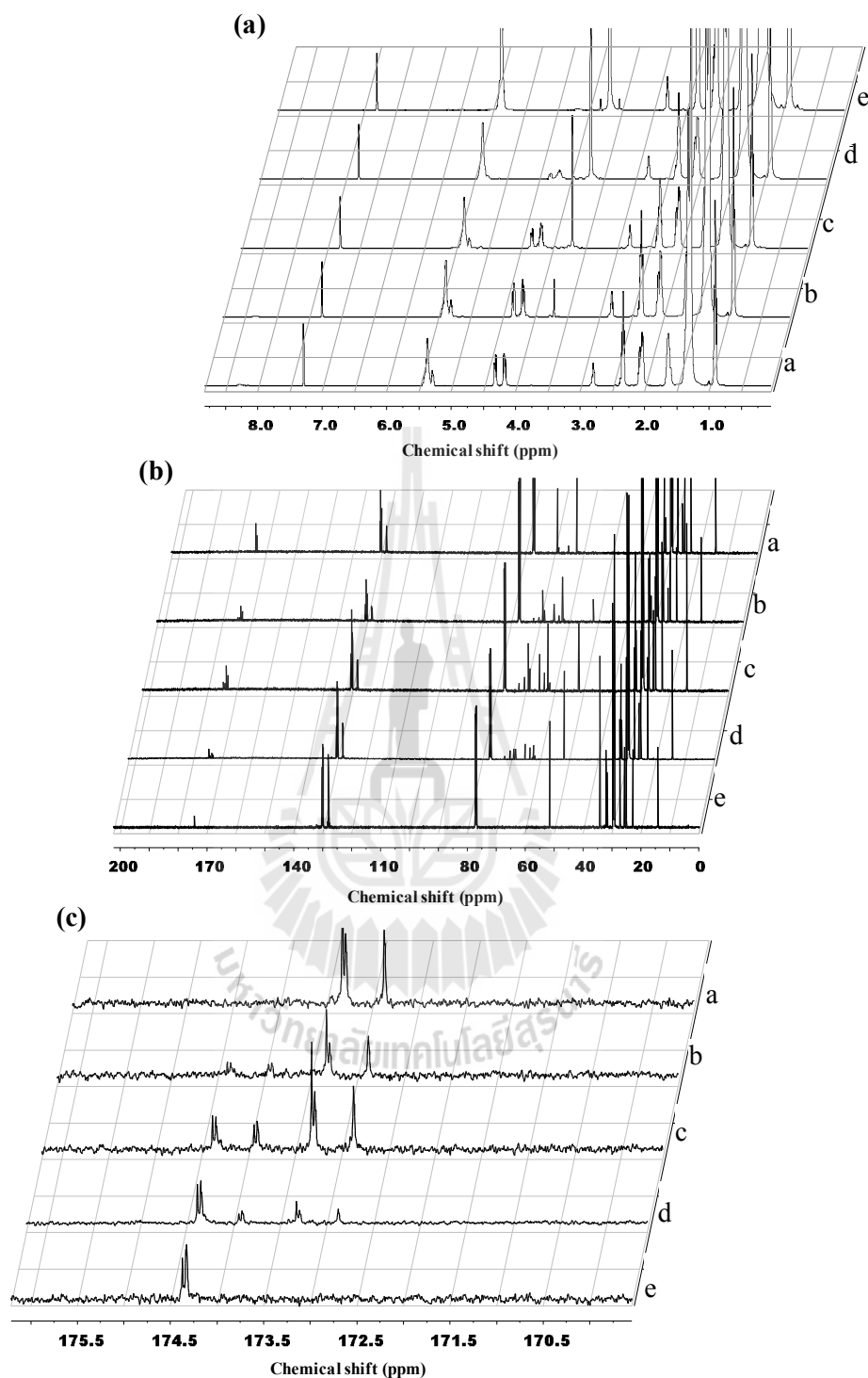
Figure 3.3 (a) ^{1}H NMR, (b) ^{13}C NMR and (c) expanded ^{13}C-NMR spectra: spectrum a (sample A1) is palm oil; spectra b, c and d (samples A3, A5 and A7) are uncompleted transesterification (triglyceride + biodiesel); spectrum e (sample A9) is biodiesel.

To compare %FAME evaluated by GC and ^{1}H NMR spectroscopy, the results from both techniques were plotted as shown in Figure 3.4. The linear fitting graph illustrates R^2 value of 0.9992 with a slope of 1.0024. These two methods for measuring biodiesel were in good agreement to quantify %FAME because %FAME error from these methods is typically within ±1%.
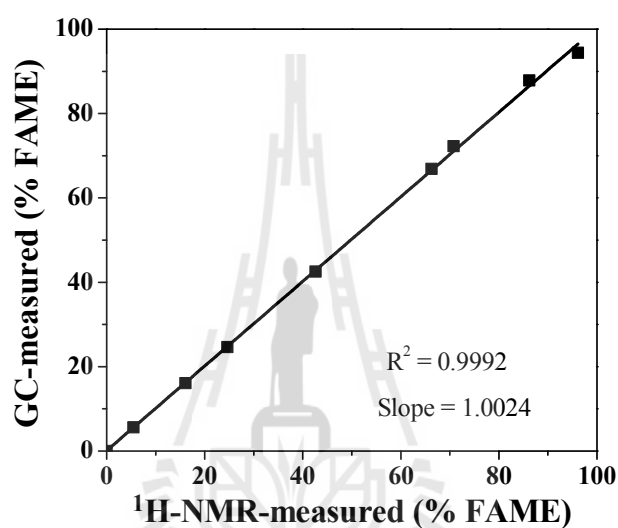
Figure 3.4 The linear fit graph of %FAME of biodiesel samples obtained from GC against ^{1}H NMR method.

Table 3.2 Comparison %FAME of biodiesel samples obtained from difference analysis method.

Biodiesel sample	%FAME		
	GC analysis method	^{1}H NMR analysis method	TLC visualized UV light
A1	0	0	0
A2	5.49	5.62	7.28
A3	16.09	16.09	17.22
A4	34.65	34.65	36.50
A5	42.64	42.54	42.51
A6	66.26	66.86	64.93
A7	70.76	72.25	68.14
A8	86.21	87.82	84.19
A9	96.12	94.41	97.97

3.6.1.3 Thermogravimetric and differential thermal analysis

In this case, TG-DTA was employed to characterize biodiesel in the term of qualitative analysis and the results were used for supporting information with other techniques. Figure 3.5(a) shows thermal stability of palm oil with 0 %FAME (sample A1) from 30 °C up to about 260 °C, the thermal degradation only involves one decomposition step. The mass of palm oil starts to decrease after 260 °C and continues to decrease rapidly until the palm oil decomposes completely at 540 °C. The overall mass loss is over 99.5%. While the reference sample A9 with 96.12 %FAME, shows degradation in two steps. The first step is the decomposition of methyl ester compound starting at approximately 150 °C and complete at about 300 °C with the weight change over 95%. The second step is mass loss of triglyceride

compound after 300 °C which completely volatilized at 500 °C with total mass change of 99.95%.

Figure 3.5(a) reveals thermogravimetric curves of other samples. The curves show similar degradable step of methyl ester compound with biodiesel sample A9. According to DTA curves illustrated in Figure 3.5(b), biodiesel sample A9 (96.12 %FAME) decomposes between 150-300 °C and the maximum rate change of thermal decomposition is at 276 °C. Similarly, triglyceride demonstrates range of mass loss at 260-540 °C with the maximum rate at 381 °C. Both results of TG and DTA of this study, can confirm qualitative information of all biodiesel samples.

(a)

(b)
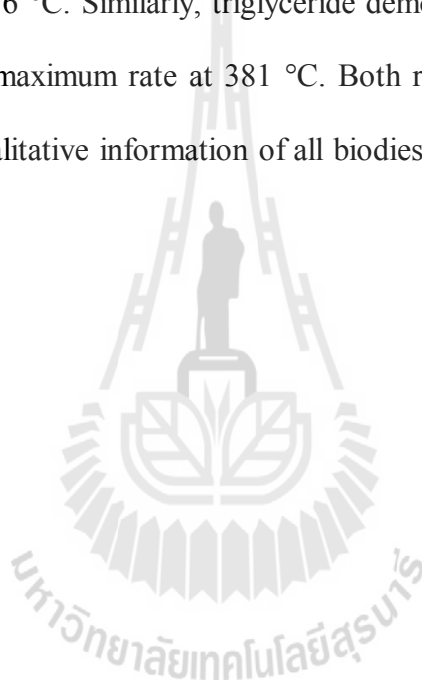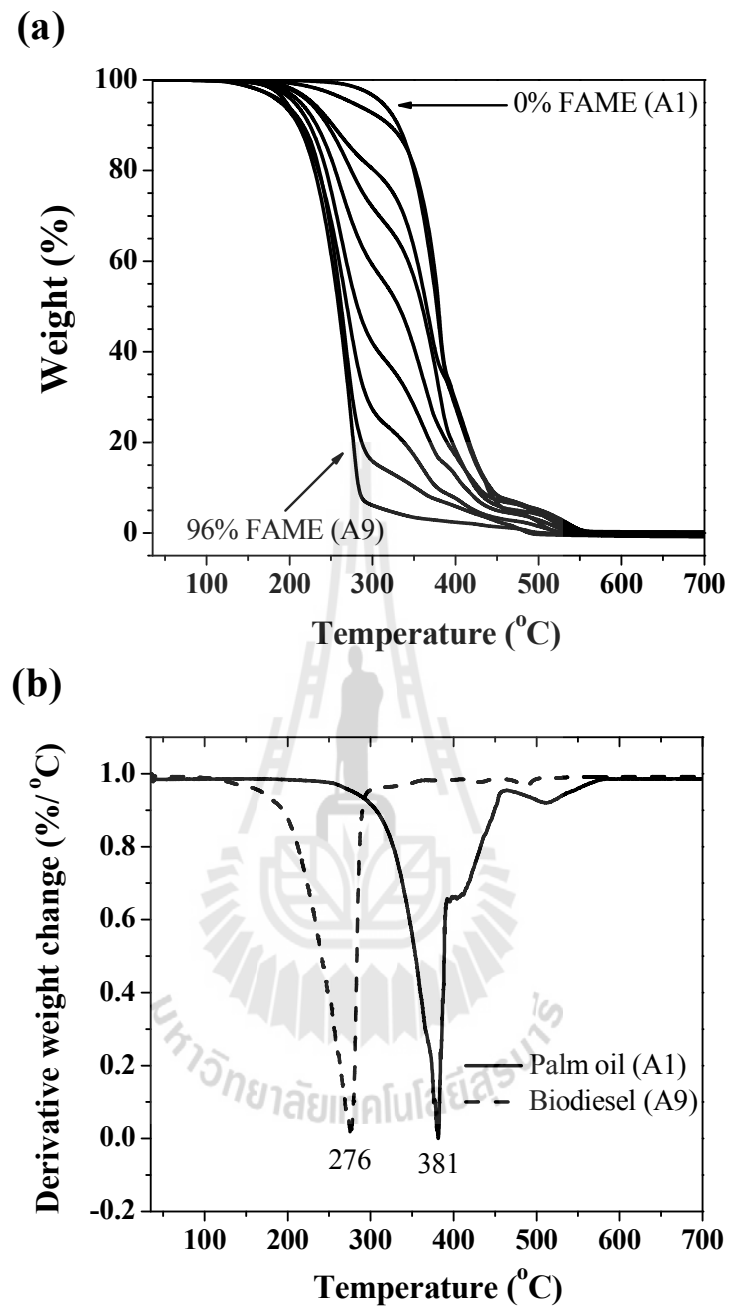
Figure 3.5 (a) TGA curves of the biodiesel samples A1 to A9 measured %FAME by

GC. (b) DTA curves of biodiesel sample A9 (96.12 % FAME) and palm oil (A1).

3.6.1.4 Fourier-transform infrared spectroscopy analysis

FT-IR spectra of palm oil and the biodiesel products are depicted in Figure 3.6. The peaks at 2926 cm^{-1} and 2855 cm^{-1} are assigned to the asymmetric and symmetric stretching vibration of aliphatic CH_2 and terminal CH_3 group, respectively. It should be noted that peaks of biodiesel sample becomes sharper from 0 %FAME (palm oil) to 96.12 %FAME. The main peaks of ester group at 1747 cm^{-1} is the stretching vibration of the carbonyl group ($C=O$). Peaks at 1300-1000 cm^{-1} correspond to $C–O$ stretching vibrations (Bradley, 2010). In addition, the $C–O$ stretching vibration of palm oil is broader than that of other samples with more %FAME. Moreover, FT-IR spectra also show the bending vibration in the range 1350-1480 cm^{-1} which is a characteristic of CH$_3$, CH$_2$ and CH group.

The FT-IR spectra of both palm oil and biodiesel are due to the similar ester compounds. Figure 3.7 shows the close-up of FT-IR spectra in the range 1400-1500 cm^{-1}. It can be observed that another peak appeared at ~ 1430 cm^{-1} when %FAME increased. This peak reflects the methyl esters of all types of fatty acids in the biodiesel (O'Donnell et al., 2013). This is the small difference between triglyceride compound in as a starting material and biodiesel product. Hence, the FT-IR analysis is suitable to use for the referring data and in giving supporting qualitative information.
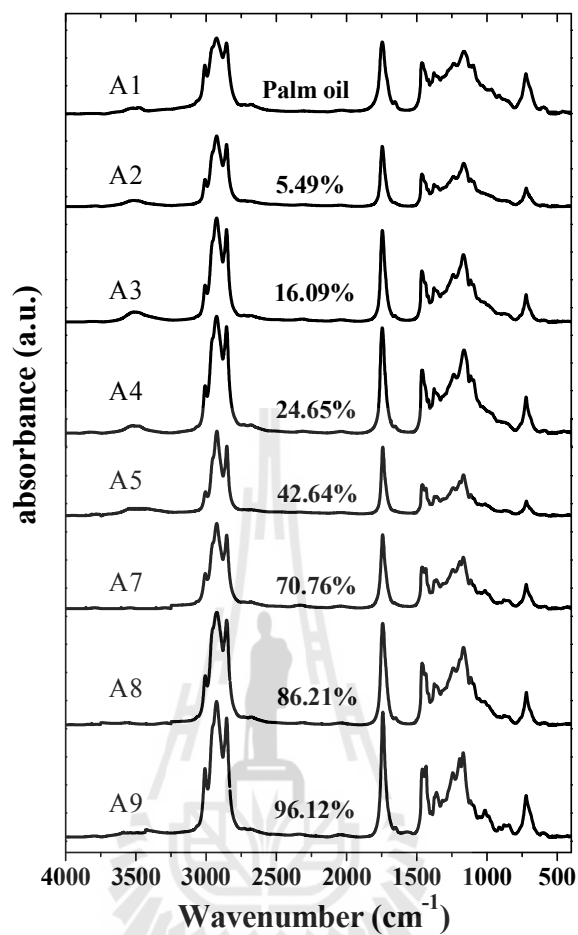
Figure 3.6 FT-IR spectra of biodiesel samples obtained %FAME by GC analysis.
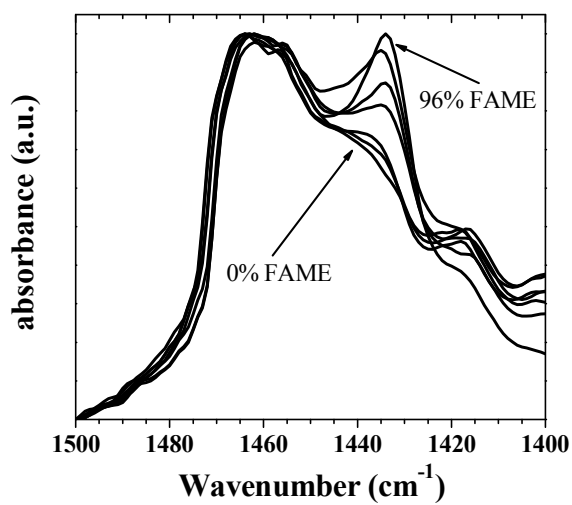
Figure 3.7 FT-IR spectra of reference biodiesel in the range 1400-1500 cm^{-1}.

3.6.1.5 Thin layer chromatography visualized UV light

TLC profiles of palm oil and biodiesel samples are depicted in Figure 3.8. The TLC profiles of all biodiesel samples were luminous under UV-light because they have chromophore group in the molecule especially ester group (R_1–$COOR_2$) and double bond of carbon atoms (–C=C–). Both of palm oil and its biodiesel products can absorb UV-light and show pink-purple spots (Dantas et al., 2011; Insausti et al., 2012). Additionally, each of biodiesel products can travel different distances depending on the molecular size and polarity. Under the optimized mixed solvent of petroleum ether/acetone/glacial acetic acid (85:15:1 v/v/v) conditions, triglyceride is larger and more polar than methyl ester compound thus it can travel shorter distance than biodiesel sample and give different R_f values. As a result, TLC method can be applied to indicate %FAME of the sample. Figure 3.9 shows a standard curve of %FAME of the biodiesel samples against R_f value of each reference biodiesel sample which can be fitted with a linear relationship as described by Eq. 3.4:

$$y = 205x - 76 \tag{3.4}$$

where y and x are %FAME and R_f value, respectively. The numeral 205 and 76 are the constant values. The R^2 value of the fit is 0.9940. The linear fit between the two data series suggests that this method can determine %FAME of biodiesel product.

The %FAME obtained from this method was calculated against and compared with those obtained from ^{1}H-NMR spectroscopy and GC analysis as shown in Table 3.2. The average difference of %FAME by using TLC method compared to GC and ^{1}H NMR is ±2-4%. As the results obtained by TLC method agree well with those of GC and ^{1}H NMR, TLC shows high potential as a reliable method for %FAME investigation.
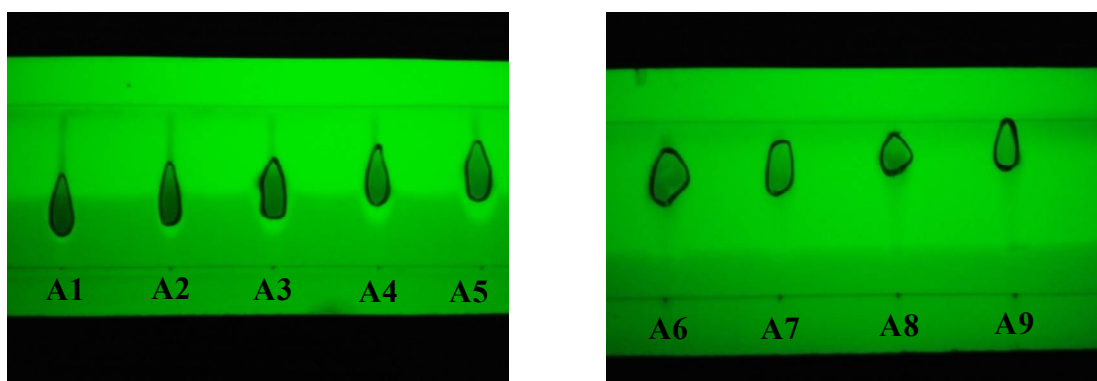
Figure 3.8 TLC plates of biodiesel samples (A1, A2, A3, A4, A5, A6, A7, A8, and A9 are 0%, 5.49%, 16.09%, 34.65%, 42.64%, 66.26%, 70.76%, 86.21% and 96.12% of FAME, respectively).
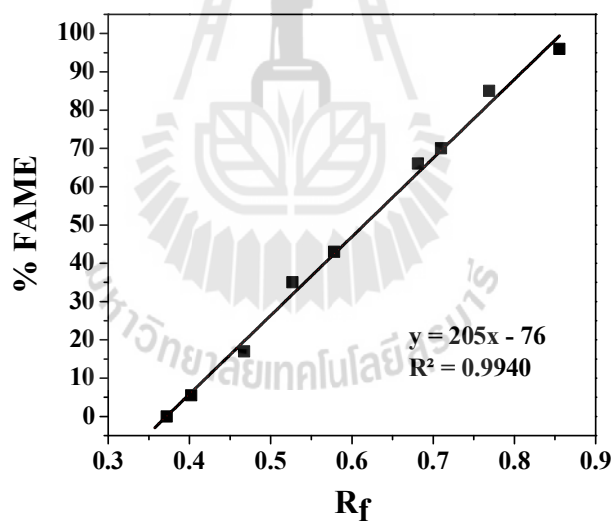
Figure 3.9 R_f values of biodiesel sample from TLC visualized UV light analytical method plotted against the actual %FAME of biodiesel obtained by GC chromatography.

3.6.2 Unknown biodiesel products analysis

3.6.2.1 Comparison %FAME obtained by TLC and ^{1}H NMR analysis

Determination of %FAME in unknown biodiesel sample by transesterification using NaOH as a homogeneous basic catalyst was investigated. Figure 3.10(a) shows comparison of %FAME in such sample obtained from TLC and ^{1}H-NMR methods. The correlations between both analysis methods are excellent. Examples of a TLC plate using for screening %FAME in a homogeneous catalyzed reaction are shown in Figure 3.10(b). Spot (A) is a biodiesel sample at the reaction time of 5 min, which palm oil was transformed incompletely. %FAME calculated by using R_f value was 82.00%, while that obtained from ^{1}H-NMR spectroscopy was 82.99%. On the other hand, spots (B) and (C) are biodiesel samples of reaction times of 15 min and 30 min, respectively. As their R_f is equal to that of biodiesel standard (spot D), the transesterification in these two samples were completed.

Similarly, %FAME in CaO catalyzed samples were investigated using TLC and ^{1}H-NMR as shown in Figure 3.11(a). It can be observed that both techniques give consistent results. These results show that type of catalyst (homogeneous and heterogeneous) has no effects on analyzing biodiesel contents with TLC method. Therefore, the potential to apply TLC visualized UV light method for testing biodiesel production, both qualitatively and quantitatively, is very high.
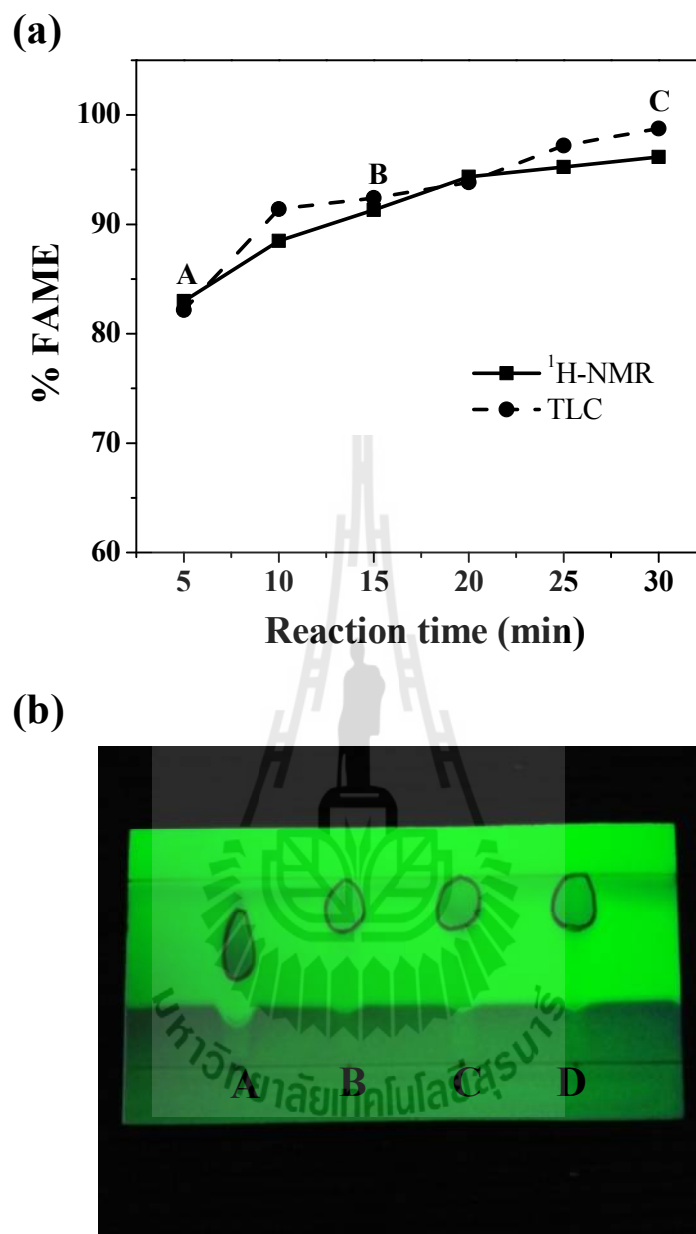
Figure 3.10 (a) %FAME of biodiesel determined by TLC and ^{1}H-NMR in the biodiesel samples obtained by using NaOH catalyzed reaction. (b) Example of TLC plate of biodiesel product from transesterification at various reaction times of (A) 5 min, (B) 15 min, (C) 30 min and (D) biodiesel standard 96.12% of FAME.

(a)

(b)
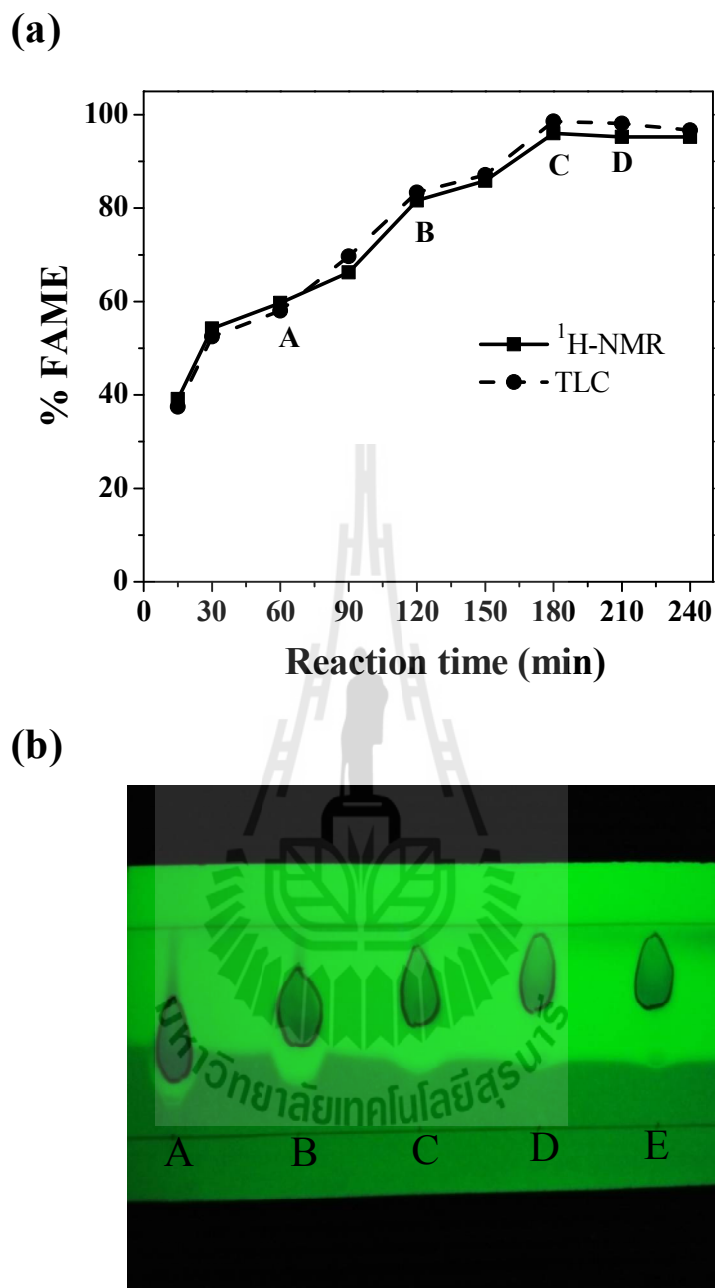
Figure 3.11 (a) %FAME of biodiesel determined by TLC and ^{1}H-NMR in the biodiesel samples obtained by using CaO catalyzed reaction. (b) Example of TLC plate of biodiesel product from transesterification at various reaction times of (A) 60 min, (B) 120 min, (C) 180 min (D) 210 and (E) methyl ester standard 96.12% of FAME.

3.6.2.2 Physicochemical properties of the unknown biodiesel products

Fuel properties of the unknown biodiesel products obtained from synthesized palm oil using NaOH and CaO catalyst were evaluated according to the European Standard EN 14214 methods for bio-fuel. The results are summarized in Table 3.3 which indicates that the final biodiesel products are found to be within the standard. Additionally, the table also shows that the methyl ester content analyzed by GC, TLC, and ^{1}H NMR are similar. This result supports that TLC visualized UV light is efficient and suitable to use in terms of screening and monitoring %FAME of biodiesel production process.

Table 3.3 Physicochemical properties of the biodiesel synthesized by using NaOH and CaO as catalyst and screening cursorily %FAME with TLC visualized UV light analysis method.

Property	Unit	EN 14214	Synthesized biodiesel	
			NaOH	CaO
Methyl ester content[a]	%	96.5	96.78	97.12
Methyl ester content[b]	%	-	98.54	99.43
Methyl ester content[c]	%	-	98.75	95.94
Kinematic viscosity at 40 ºC	mm^2/s	3.50-5.00	4.44	4.50
Density (15 ºC)	Kg/m^3	860-900	880	884
Flash point	ºC	>120	188	190
Acid value	mg KOH/g	<0.5	0.30	0.24
Water content	%w/w oil	<0.050	0.022	0.033
Copper strip corrosion	-	Number 1	1	1
Oxidation number	h	>6	14.32	15.23

[a]obtained by GC, [b]obtained by ^{1}H-NMR spectroscopy, [c]obtained by TLC visualized UV light method.

3.7 Conclusions

TLC visualized UV light can be utilized as a potential screening and monitoring technique in biodiesel production by transesterification process. This method has a small error of %FAME within ±2-4% compared with ^{1}H-NMR and GC spectroscopy. The results show that type of catalyst including homogeneous (NaOH) and heterogeneous (CaO) has no effects on analyzing biodiesel contents with TLC method. Therefore, TLC visualized UV light is an efficient, low-cost and simple method for people who have no access to complicate instruments to evaluate %FAME of biodiesel product.

3.8 References

Alhassan, Y., Kumar N., Bugaje I. M., Pali H. S. and Kathkar, P. (2014). Co-solvent transesterification of cotton seed oil into biodiesel: effects of reaction condition on quality of fatty acids methyl esters. **Energy Conversion and Management**. 84: 640-648.

Arzamendi, G., Campo, I., Arguinarena, E., Sanchez, M., Montes, M. and Gandia, L. M. (2007). Synthesis of biodiesel with heterogeneous NaOH/alumina catalysts: Comparison with homogeneous NaOH. **Chemical Engineering Journal**. 134: 123-130.

Azeem, M. W., Hanif, M. A., Al-Sabahi, J. N., Khan A., Naz S. and Ijaz, A. (2016). Production of biodiesel from low priced renewable and abundant date seed oil. **Renewable Energy**. 86: 124-132.

Basumatary, S. and Deka, D. C. (2012). Identification of fatty acid methyl esters in biodiesel from *Pithecellobium monadelphum* seed oil. **Der Chemica Sinica Journal**. 3(6): 1384-1393.

Bradley, M. (2012). Biodiesel (FAME) Analysis by FT-IR. Thermo Fisher Scientific. Thermo Electron Scientific Instruments LLC, Madison, WI USA is ISO Certified. [Online]. Available: http://www.thermoscientific.com/content/dam/tfs /ATG/CMD/CMD%20Documents/Application%20&%20Technical%20Notes/ AN-51258-Biodiesel-FAME-Analysis-by-FT-IR.pdf>.

Chand, P., Reddy, Ch. V., Verkade, J. G, Wang, T. and Grewell, D. (2009). Thermogravimetric quantification of biodiesel produced via alkali catalyzed transesterification of soybean oil. **Energy & Fuels**. 23: 989-992.

Chattopadhyay, S., Das, S. and Sen, R. (2011). Rapid and precise estimation of biodiesel by high performance thin layer chromatography. **Applied Energy**. 88: 5188-5192.

Dantas, M. B., Albuquerque, A. R., Barros, A. K., Rodrigues-Filho, M. G., Antoniosi-Filho, N. R., Sinfronio, F. S. M., Rosenhaim, R., Soledade, L. E. B., Santos, I. M. G. and Souza, A. G. (2011). Evaluation of the oxidative stability of corn biodiesel. **Fuel**. 90: 773-778.

Department of Alternative Energy Development and Efficiency of Thailand. (2012). The Renewable and alternative energy development plan for 25 percent in 10 years. [Online]. Available: https//www4.dede.go.th/dede/images/stories/pdf/ dede _aedp_ 2012_21.pdf.

EN-14214 (2008). Automotive Fuels – Fatty Acid Methyl Esters (FAME) for Diesel Engines – Requirements and test methods. Euro Committ for Standardization, Brussels. [Online]. Available: https://en.wikipedia.org/wiki/EN_14214.

Farooq, M., Ramli, A. and Subbarao, D. (2013). Biodiesel production from waste cooking oil using bifunctional heterogeneous solid catalysts. **Journal of Cleaner Production**. 59: 131-140.

Habibullah, M., Masjuki, H. H., Kalam, M. A., Rahman, S. M. A., Mofijur, M., Mobarak, H. M. and Ashraful, A. M. (2015). Potential of biodiesel as a renewable energy source in Bangladesh. **Renewable & Sustainable Energy Reviews**. 50: 819–834.

Insausti, M., Gomes, A. A., Cruz, F. V., Pistonesi, M. F., Araujo, M. C. U., Galvao, R. K. H., Pereira, C. F. and Band, B. S. F. (2012). Screening analysis of

biodiesel feedstock using UV–vis, NIR and synchronous fluorescence spectrometries and the successive projections algorithm. **Talanta**. 97: 579-583.

Killner, M. H. M., Linck, Y. G., Danieli, E., Rohwedder, J. J. R. and Blumich, B. (2015). Compact NMR spectroscopy for real-time monitoring of a biodiesel production. **Fuel**. 139: 240-247.

Maneerung, T., Kawi, S. and Wang, C. H. (2015). Biomass gasification bottom ash as a source of CaO catalyst for biodiesel production via transesterification of palm oil. **Energy Conversion and Management**. 92: 234-243.

O'Donnell, S., Demshemino, I., Yahaya, M., Nwadike, I. and Okoro, I. (2013). A review on the spectroscopic analyses of biodiesel. **European International Journal of Science and Technology**. 2: 137-146.

Roschat, W., Siritanon, T., Yoosuk, B. and Promarak, V. (2016). Biodiesel production from palm oil using hydrated lime-derived CaO as a low-cost basic heterogeneous catalyst. **Energy Conversion and Management**. 108: 459-467.

Shan, R., Chen, G., Yan, B., Shi, J. and Liu, C. (2015). Porous CaO-based catalyst derived from PSS-induced mineralization for biodiesel production enhancement. **Energy Conversion and Management**. 106: 405-413.

Speranza, L. G., Ingram, A. and Leeke, G. A. (2015). Assessment of algae biodiesel viability based on the area requirement in the European Union, United States and Brazil. **Renewable Energy**. 78: 406-417.

Sukhawanit, C., Srinophakun, P. and Matsumura, M. (2014). Biodiesel Production from Crude Sunflower Oil. **Journal of Research in Engineering and Technology**. 1: 141-148.

Supamathanon, N., Wittayakun, J. and Prayoonpokarach, S. (2011). Properties of Jatropha seed oil from Northeastern Thailand and its transesterification catalyzed by potassium supported on NaY zeolite. **Journal of Industrial and Engineering Chemistry**. 17: 182-185.

Vega-Lizama, T., Diaz-Ballote, L., Hernandez-Mezquita, E., May-Crespo, F., Castro-Borges, P., Castillo-Atoche, A., Gonzalez-Garcia, G. and Maldonado, L. (2015). Thermogravimetric analysis as a rapid and simple method to determine the degradation degree of soy biodiesel. **Fuel**. 156: 158-162.

Viriya-empikul, N., Krasae, P., Nualpaeng, W., Yoosuk, B. and Faungnawakij, K. (2012). Biodiesel production over Ca-based solid catalysts derived from industrial wastes. **Fuel**. 92: 239-244.

Yang, B. J., Zheng, L., Han, X. T. and Zheng, M. G. (2013). Development of TLC–FID technique for rapid screening of the chemical composition of microalgae diesel and biodiesel blends. **Fuel**. 111: 344-349.

CHAPTER IV

BIODIESEL PRODUCTION FROM PALM OIL USING

HYDRATED LIME-DERIVED CaO AS A LOW-COST

BASIC HETEROGENEOUS CATALYST

4.1 Graphical abstract
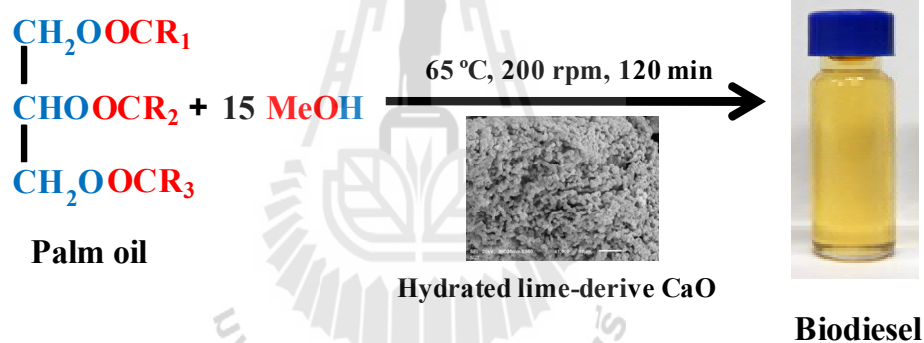
$$CH_2OOCR_1$$
$$CHOOCR_2 + 15\ MeOH \xrightarrow{65\ ^{\circ}C,\ 200\ rpm,\ 120\ min}$$
$$CH_2OOCR_3$$

Palm oil

Hydrated lime-derive CaO

Biodiesel

Hydrated lime-derived CaO can be utilized as high efficient heterogeneous solid catalyst for transesterification of palm oil to biodiesel product.

4.2 Highlights

- CaO catalyst was successfully prepared from hydrated lime using a simple method.

- Hydrated lime-derived CaO were used as a catalyst in transesterification of palm oil to biodiesel.

- Over 97% FAME yield was achieved from transesterificaion of palm oil within 2 h.

- This CaO has high potential for applications as green and low-cost catalyst.

4.3 Abstract

In this study, hydrated lime-derived calcium oxide (CaO) was used as a catalyst for the transesterification of palm oil. The catalyst was characterized by TG-DTA, XRD, XRF, FT-IR, SEM, Hammett indicator method, TPD-CO_2 and BET by N_2 adsorption. Under the optimal conditions at catalyst loading of 6 wt.%, methanol/oil molar ratio of 15:1, reaction temperature 65 °C, and stirring rate of 200 rpm; 97% yield of biodiesel could be achieved in 2 h. Effects of water amount were investigated and the catalyst could tolerate high water content of 5 wt.%. The kinetic of the reaction followed pseudo-first order with the activation energy (Ea) of 121.12 kJ/mol and frequency factor (A) of 1.203 x 10^{17} min^{-1}. After treatments, high quality biodiesel was obtained which indicated that the very cheap hydrated lime-derived CaO showed excellent catalytic activity and high potential for applications in biodiesel production.

4.4 Introduction

Nowadays, the petroleum oil consumption is increasing due to the economic development and incremental population of the world. However, this energy source is limited, expensive and polluted to the environment (Huang et al., 2015). In order to solve these problems, biodiesel is used as an alternative energy source for diesel engines. Biodiesel has gained lots of attention as it is renewable, clean,

biodegradable, global friendly, non-toxic and inexpensive (Zabeti et al., 2009; Taufiq-Yap et al., 2014). It is generally known that fatty acid methyl esters (FAME) are a biodiesel product which can be obtained by transesterification reaction of vegetable oil or animal fat with methanol in the presence of catalysts (Alhassan et al., 2014; Somnol et al., 2014). In general, 1 mol of triglyceride and 3 mol of methanol generate 3 mol of fatty acid methyl esters and 1 mol of glycerol by-product.

Transesterification with homogeneous basic catalysts such as NaOH, KOH and NaOCH$_3$ usually involves heating at 60-80 °C for about 1 h. After that, large amount of water is required to eliminate the catalysts which will otherwise contaminate the biodiesel product. Therefore, to use homogeneous catalysts for transesterification reaction, one has to consider the production cost, environmental effect, reactor corrosion and catalysts reuse ability (Kawashima et al., 2008; Mahesh et al., 2015; Meher et al., 2006).

On the other hand, heterogeneous catalysts are promoted as a green process because they can be easily separated from the reaction mixture and reused several times. Moreover, the biodiesel product obtained from heterogeneous catalyzed reaction does not require further cleaning process (Takase et al., 2014; Reyero et al., 2014). In addition, the reaction usually results in pure glycerol by-product (Lo′pez et al., 2007). There are several works reported on biodiesel production using heterogeneous catalysts. Kim et al. reported Na/NaOH/γ-Al$_2$O$_3$ as a catalyst applied for the production of biodiesel from vegetable oil (Kim et al., 2004). Takase et al. investigated the application of zirconia modified with KOH as a heterogeneous solid basic catalyst to produce biodiesel from new non-edible oil (Takase et al., 2014). Soetaredjo et al. used KOH/bentonite as a catalyst for transesterification of palm oil

to biodiesel (Soetaredjo et al., 2011). Brito et al. applied Zeolite Y as a heterogeneous catalyst in biodiesel fuel production from used vegetable oil (Brito et al., 2007). Nevertheless, some of these materials still have to be improved as they show low catalytic activity, high sensitivity to moisture and dissolution in methanol. Many heterogeneous catalysts are also complicated to generate.

Among the heterogeneous catalysts, calcium oxide (CaO) has been the most studied catalyst material for biodiesel production because it has high basicity, high transesterification activity in mild reaction condition, less solubility in methanol and non-toxicity. In addition, CaO can be prepared from natural calcium carbonate ($CaCO_3$) sources such as waste eggshells (Somnul et al., 2014; Wei et al., 2009), mollusk shells (Somnul et al., 2014), ostrich eggshells (Chen et al., 2014), meretrix venus shells and golden apple snail shells (Viriya-empikul et al., 2012), crab shell (Correia et al., 2014), capiz shell (Suryaputra et al., 2013) and clam shell (Asikin-Mijan et al., 2015) which further reduces the cost.

In the rural areas of Thailand, hydrated lime is produced using traditional methods where golden apple snail shells and smaller portions of other kinds of shells are thermally decomposed in the ground hole using heat from wood combustion. After 3 hours of the decomposition, the product is collected and mixed with water to obtain hydrated lime. An important focus in this present work is to study the possible usage of hydrated lime as a cost-effective heterogeneous catalyst for biodiesel production. The simple modification process was applied to enhance the catalytic activity while the optimum condition of the reaction was investigated using palm oil and methanol as starting reagents. The effects of water on the catalytic activity and the efficiency of reused catalyst were carefully studied to demonstrate the stability of

the catalyst. The fuel properties of the obtained biodiesel after purification and treatment processes were evaluated by using American Society for Testing and Material (ASTM D6751) methods and European Standard methods (EN14214) for bio-auto fuels. In addition, reaction kinetics of transesterification using CaO obtained from calcined hydrated lime was also investigated.

4.5 Experimental

4.5.1 Materials and catalyst preparation

Palm olein oil (FFAs of 0.29 mg KOH g^{-1}) was purchased from Morakot Industries PCL., Thailand. The composition of fatty acid in palm oleic oil was analyzed by gas-chromatography (GC) and the results are given in Table 4.1 (refer to EN14214 Standard method).

Table 4.1 Fatty acid composition of palm olein oil used as a starting material.

Fatty acid	Composition (wt.%)
Lauric acid (C12:0)	0.4
Maristic acid (C14:0)	0.8
Palmitic acid (C16:0)	37.3
Stearic acid (C18:0)	3.6
Oleic acid (C18:1)	45.7
Linoleic acid (C18:2)	11.1
Linoleic acid (C18:3)	0.4
Linoleic acid (C18:3)	0.4
Arachidic acid (C20:0)	0.2
Eicosenoic acid (20:1)	0.1

Methanol (analytical reagent grade) was obtained from Fluka. Hammett indicators namely phenolphthalein, thymolphthalein, indigo carmine, 2,4-dinitroaniline, and 4-nitroaniline of analytical grade were obtained from Aldrich and Fluka. The hydrated lime was purchased from Thai markets, dried overnight in an oven at 100 °C and then crushed and sieved. The resulting materials were calcined in a furnace at designated temperature (700, 800 and 900 °C) in air for 3 h.

4.5.2 Catalyst characterization

Thermal decomposition of the hydrated lime was analyzed by thermo-gravimetric/differential thermal analyzer (TG-DTA) using a Rigaku TG-DTA 8120 thermal analyzer under air flow with a heating rate of 10 °C/min. Both the original hydrated lime and modified hydrated lime were examined by X-ray powder diffraction (XRD) using a PHILIPS X'Pert-MDP X-ray diffractometer with Cu Kα radiation ($\lambda = 1.5418$ Å) at 1600W, 40 kV and 40 mA. The elemental compositions of all samples were analyzed by a PHILIPS Magi X diffuse wavelength X-ray Fluorescence (XRF) spectrophotometer with 1 kW Rh Kα radiation. The samples were characterized by Fourier transforms infrared (FT-IR) spectroscopy technique using a Perkin–Elmer FT-IR spectroscopy spectrum RXI spectrometer in the range of 400–4000 cm^{-1} with resolution of 4 cm^{-1} and potassium bromide (KBr) was used as a matrix. Scanning electron microscopy (SEM) was operated using JEOL JSM 6010LV scanning electron microscope at an accelerated voltage of 10 kV.

Brunauer-Emmett-Teller (BET) was used to investigate surface area and pore volume. The analyst BET is used to determine isotherm of low temperature adsorption and desorption of N$_2$ gas using He as carrier gas on a Bel-sorp-mini II

(Bel-Japan). The basic site property of the catalysts was analyzed by temperature programmed desorption method (TPD) using Chemisorption Analyzer (Belcat B) with CO_2 as an investigation molecule and He as a carrier gas. The basic strength was tested by Hammett indicator method using the following indicators with different acidity functions ($H\_$); phenolphthaleine ($H\_ = 9.8$), indigo carmine ($H\_ = 12.2$), 2,4-dinitroaniline ($H\_ = 15.0$) and 4-nitroaniline ($H\_ = 18.4$).

4.5.3 Catalytic tests and product analysis

The transesterification reaction of palm oil was conducted in a three-neck round bottom batch reactor equipped with a reflux condenser, a magnetic stirrer and a thermocouple. A mixture of methanol (MeOH) and catalyst were preheated at designed temperature (30, 50, 55, 60, 65 and 70 °C) and added to the oil of 30 mL. The transesterification reaction was carried out with various MeOH to oil molar ratios of 3:1 to 21:1 and catalyst loading amount of 2 wt.% to 10 wt.% relative to oil weight for the required reaction times. The effect of water content on the catalytic performance was studied by comparing the reactions containing small amount of water (1, 3, 5, 7, 9 and 11 wt.%) catalyzed by the prepared catalysts to the same reactions catalyzed by KOH.

To monitor reaction progress, 0.5 mL of the solution was sampled every specific period of time, dried to evaporate all methanol and analyzed for the yield. The conversion of the palm oil to biodiesel was evaluated by proton nuclear magnetic resonance (^{1}H NMR) using a Brüker AVANCE 300 MHz spectrometer as shown in Figure 4.1. Tetramethylsilane (TMS) and $CDCl_3$ were used as the internal reference

and a solvent, respectively. The conversion of the palm oil to biodiesel (denoted as %FAME) was calculated according to the following equation 4.1:

$$\%\text{FAME} = \frac{2A_{CH_3}}{3A_{CH_2}} \times 100 \qquad (4.1)$$

where %FAME is the FAME yield. A_{CH_3} is an integration of the methoxy protons of the methyl ester moiety (*CH₃-OCO-*) at chemical shift of 3.68 ppm. A_{CH_2} is an integration of the proton in α-carbonyl methylene groups (*R-CH₂-OCO-*) both in triglyceride and methyl ester at chemical shift of 2.31 ppm. The factors 3 and 2 were derived from the number of attached protons at the methoxy and α-carbonyl methylene carbons, respectively (Meher et al., 2006; Roschat et al., 2012; Samart et al., 2009).
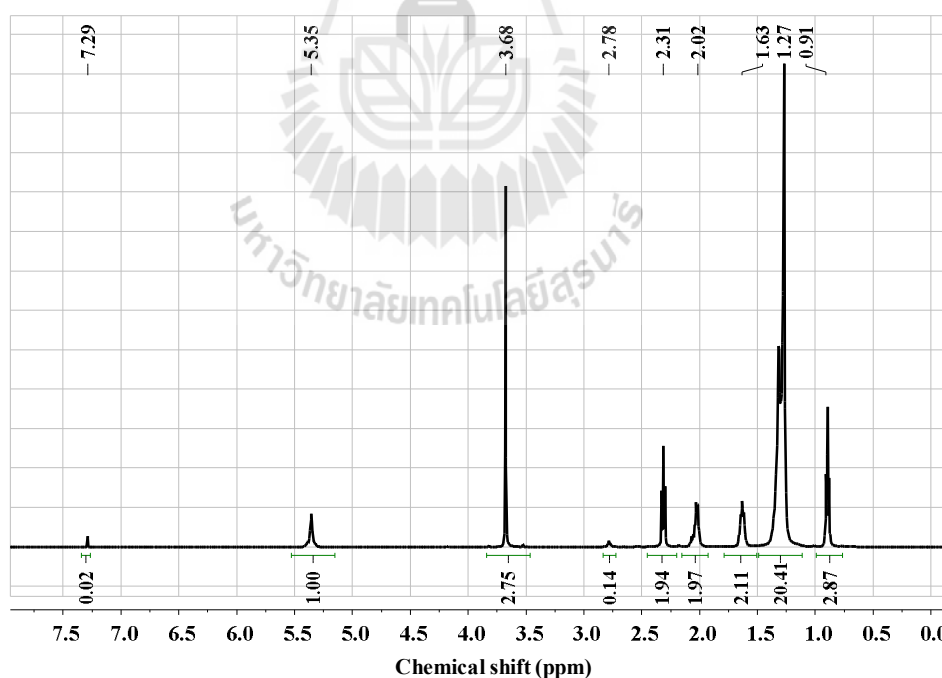
Figure 4.1 Analysis of biodiesel produced from the transesterification of palm oil and methanol using ¹H NMR.

Methyl ester content of the final biodiesel product was determined according to EN14214 standard method. The yield and compositions of biodiesel were analyzed by a gas chromatograph (GC-2010, Shimadzu) equipped with capillary DB-WAX column (30 m × 0.15 mm) and connected with a flame ionization detector. Temperature of the column was programmed from 180 to 230 °C with the heating rate of 5 °C/min and methylheptadecanoate was used as an internal standard. Methyl esters content (C) was calculated according to the following equation 4.2:

$$C = \frac{(\sum A) - (AEI)}{AEI} \times \frac{CEI \times VEI}{m} \times 100\% \qquad (4.2)$$

where $\sum A$ is total peak area of the methyl ester from C_{12} to $C_{20:1}$. AEI is peak area of methylheptadecanoate as an internal standard. CEI is concentration of the methylheptadecanoate solution (mg/mL). VEI is volume of the methylheptadecanoate solution (mL) and m is mass of the biodiesel sample (mg) (Viriya-empikul et al., 2012; Yoosuk et al., 2010).

The obtained biodiesel product was purified by removing excess methanol, filtrated to separate catalyst and treated with cation-exchange resin. The purified biodiesel was then tested according to ASTM and EN 14214 standards for bio-auto fuels (Meher et al., 2006; Roschat et al., 2012).

4.6 Results and discussion

4.6.1 Characterization of hydrated lime and CaO catalysts

In order to obtain the optimal calcination temperature, the hydrated lime was analyzed by TG/DTA and the results are presented in Figure 4.2. The weight loss occurred in the range of 30–350 °C which suggested that water and organic compounds were removed. In the range of 350–450 °C and 600–750 °C, the weight

losses correspond to removal of water molecules from $Ca(OH)_2$ and the decomposition of $CaCO_3$ to CaO and CO_2, respectively (Viriya-empikul et al., 2012; Correia et al., 2014; Yoosuk et al., 2010). Based on TGA results, the calcinations temperature of 700, 800 and 900 °C were selected to determine a suitable condition for CaO catalyst generation.
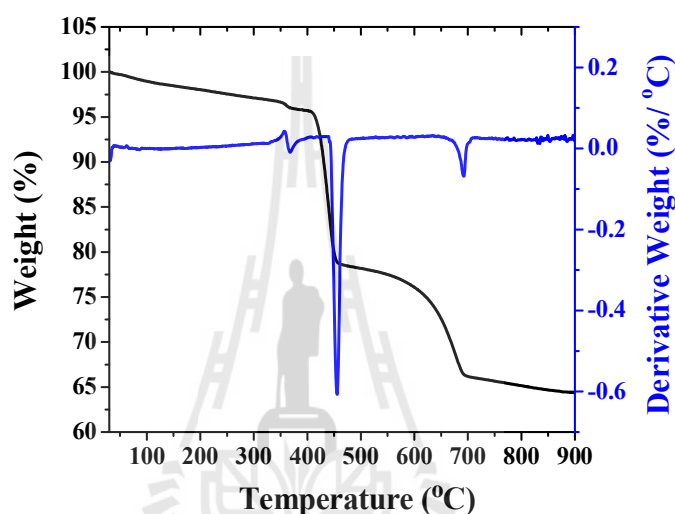
Figure 4.2 TG/DTA thermograms of hydrated lime.

XRD patterns of hydrated lime are shown in Figure 4.3(a). The results revealed that there were two major components; $Ca(OH)_2$ and $CaCO_3$, in the hydrated lime material. $CaCO_3$ is a result of uncompleted decomposition of shells as the hydrated lime was prepared at low temperature which was insufficient to completely decompose $CaCO_3$ in the shells. Figure 4.3(b) shows XRD patterns of hydrated lime calcined at different temperatures. The sample calcined at 700 °C for 3 h contained a mixture of CaO, $Ca(OH)_2$ and $CaCO_3$ crystalline phase while those calcined at 800 and 900 °C for 3 h demonstrated CaO as a major phase. As a result, it was concluded that the temperature of at least 800 °C is required to completely convert calcium

carbonate into calcium oxide. The similar results were also obtained in reports of Nakatani et al., Muhammad and Anita, and Chakraborty et al. (Nakatani et al., 2009; Muhammad and Anita, 2015; Chakraborty et al., 2011)
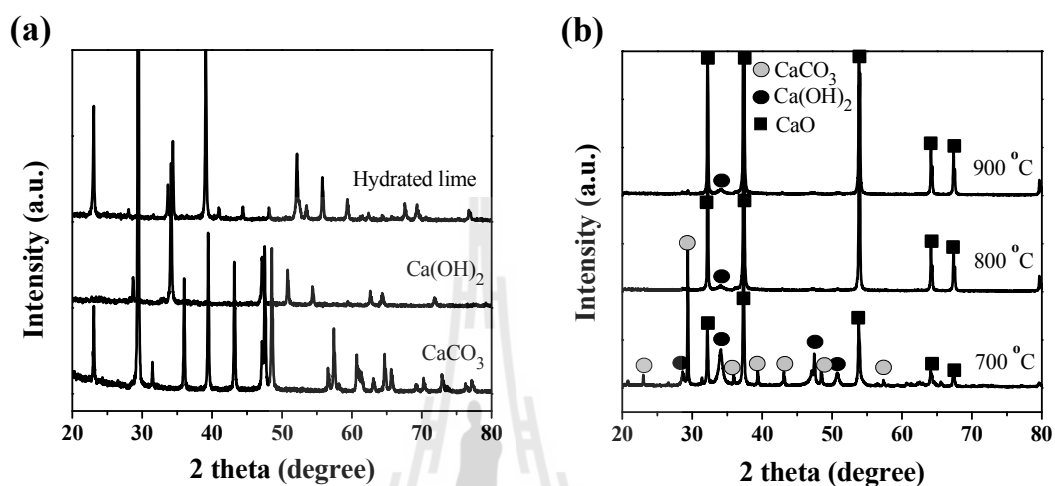
Figure 4.3 (a) XRD patterns of original hydrated lime, $Ca(OH)_2$, and $CaCO_3$. (b) XRD patterns of hydrated lime calcined at 700, 800 and 900 °C for 3 h.

The components of calcined hydrated lime were investigated by FT-IR as shown in Figure 4.4(a) which reveals only a band of Ca-O stretching at 523 cm^{-1} and a very small hydroxyl group stretching at 3637 cm^{-1}. These results indicated that after calcination at 800 °C for 3 h, $CaCO_3$ and $Ca(OH)_2$ were completely transformed to CaO. XRF spectroscopy showed that CaO derived from hydrated lime was composed of 96.9 wt.% CaO, 1.1 wt.% SiO_2 and 2 wt.% of other oxides. The morphology of the obtained CaO was probed by SEM as illustrated in Figure 4.4(b). The SEM images of hydrated lime calcined at 800 °C for 3 h displays aggregation of regular rod-like particles with high porosity.
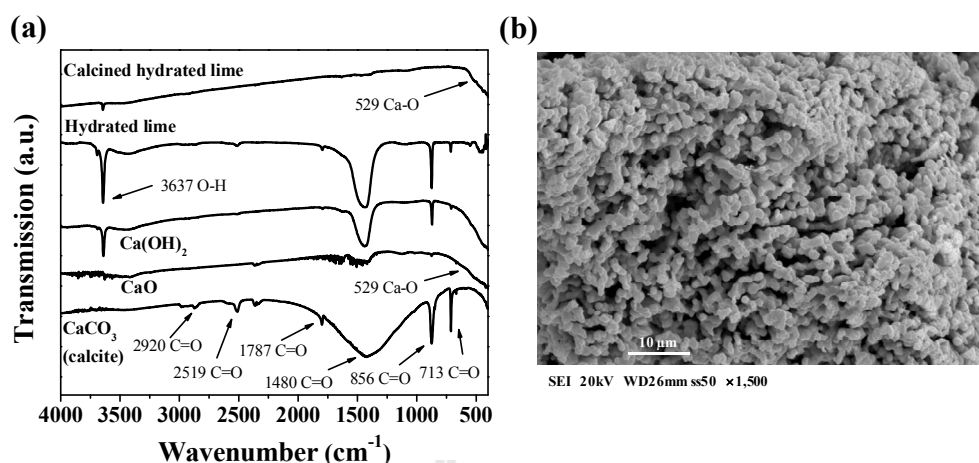
Figure 4.4 (a) IR spectra of the calcined hydrated lime at 800 °C for 3 h, hydrated lime, $Ca(OH)_2$, CaO and $CaCO_3$. (b) SEM images of the hydrated lime calcined at 800 °C for 3 h.

The surface morphologies of the catalyst directly affect the productivity of biodiesel because triglyceride molecules would reacted with methanol molecules absorbed on active sites. Thus, a higher surface area of catalyst would generally enhance the reaction yield. As listed in Table 4.2, CaO obtained from calcined hydrated lime showed greater BET surface area and pore volume than commercial CaO and CaO reported in many works suggesting a high potential as a heterogeneous catalyst. Such large surface area and pore volume are expected as both H_2O and CO_2 were eliminated during thermal decomposition of $Ca(OH)_2$ and $CaCO_3$ in hydrated lime leaving a porous CaO (Asikin-Mijan et al., 2015). Similar strategy has also been used by Yoosuk et al., who rehydrated CaO before calcination to increase its surface area and basicity (Yoosuk et al., 2010).

Table 4.2 Comparison of BET surface area, pore volume and total basic site of CaO prepared from different sources at difference conditions.

Source of catalyst	Calcined temperature (°C) and time (h)	BET surface area (m^2/g)	Pore volume (cm^3/g)	Total basic site (μmol/g)
Hydrated lime, This work	800, 3	15.0	0.2174	326.4
Eggshell[a]	800, 4	1.1	0.005	172.2
Golden apple snail shell[a]	800, 4	0.9	0.004	207.8
Meretrix venus shell[a]	800, 4	0.5	0.002	176.4
Waste eggshells[b]	800, 4	1	0.005	194
Ostrich eggshell[c]	800, 4	8.6	0.037	-
Commercial calcium carbonate[c]	800, 4	7.5	0.030	-

[a]Viriya-empikul et al., 2012; [b]Kusdiana and Saka, 2014; [c]Chen et al., 2014.

Furthermore, the basic strengths of CaO catalyst produced by calcining hydrated lime at 800 °C for 3 h was measured by Hammett indicator method which showed $H\_$ values in the range of 15.0-18.4 as evidenced by their coloration ability with 2,4-dinitroaniline (pKa = 15) but not with 4-dinitroaniline. Parent hydrated lime, on the other hand, showed basic strength values of 9.8-12.2 (Mosaddegh and Hassankhani, 2014). Moreover, the total basic site was also evaluated by CO_2-TPD which showed that CaO catalyst derived from hydrated lime had strong basic sites with total basic amount of 326.4 μmol/g as shown in Figure 4.5 and Table 4.2. These results suggest that BET surface area correlates with the basic site of CaO. Higher surface area usually results in higher basic sites; both properties are preferred in heterogeneous catalyst for biodiesel production (Viriya-empikul et al., 2010).
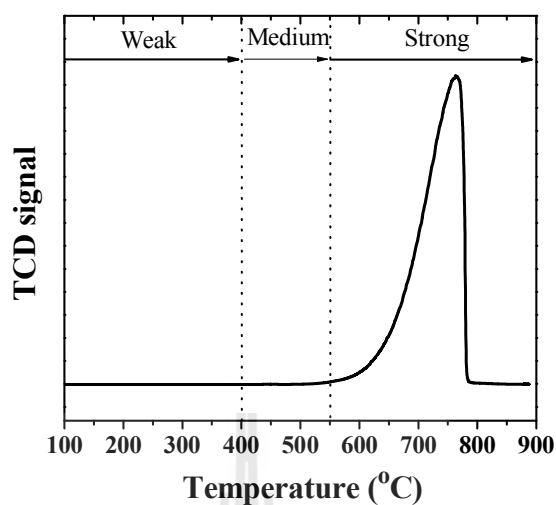
Figure 4.5 CO_2-TPD of CaO catalyst obtained from calcination hydrated lime at 800 °C for 3 h.

The nitrogen adsorption/desorption isotherm of the hydrated lime-derived CaO catalyst and commercially available CaO are shown in Figure 4.6(a) and (b), respectively. Hydrated lime-derived CaO sample displayed type IV isotherm which is a characteristic of mesoporous materials based on IUPAC's classification (Yoosuk et al., 2010; Kusdiana and Saka, 2004). While commercially available CaO displays a type II isotherm which is produced with a low slope in the middle region of the isotherm and a desorption line almost overlapping with an adsorption line. In particular, this isotherm is represented unrestricted monolayer–multilayer adsorption and attributed to a nonporous or macroporous material (Khemthong et al., 2012). The hydrated lime-derived CaO exhibited the small hysteresis loop corresponding to H3-type which indicated the slit shaped mesopores. The same feature was not observed in commercial CaO.
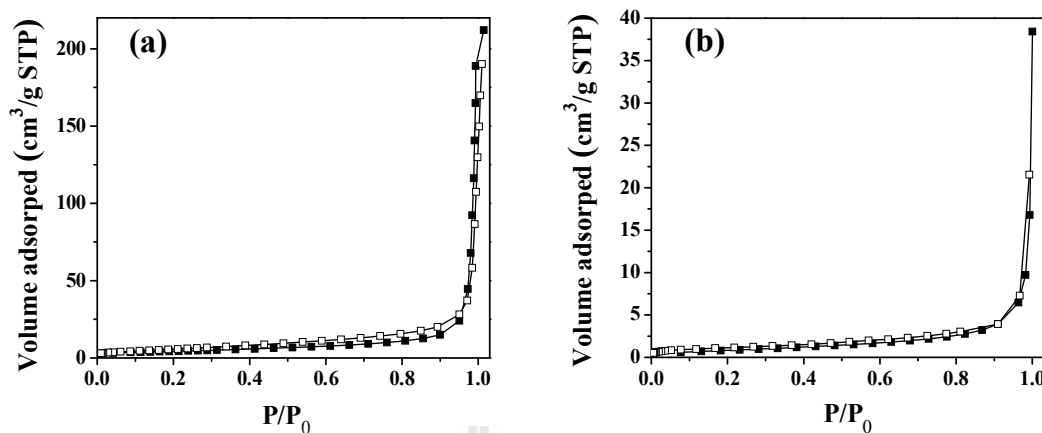
Figure 4.6 N_2 adsorption/desorption isotherms of (a) hydrated lime-derived CaO and (b) commercial CaO.

4.6.2 Catalytic activity in the transesterification

4.6.2.1 Effects of calcining temperature of hydrated lime

Catalytic activity of all samples was investigated as shown in Figure 4.7. The results showed that original hydrated lime had lower activity than calcined hydrated lime. In addition, FAME yield significantly increased from 70.07% to 97.20% at reaction time 180 min when calcining temperature of hydrated lime was increased from 700 to 800 °C. Hydrated lime calcined at 900 °C resulted in a slightly lower FAME yield (94.34%) which can be described by the lowering of the surface area resulting from sintering effect during the calcinations (Alonsoa et al., 2010; Khemthong et al., 2012; Kouzu et al., 2008; Ngamcharussrivichai et al., 2010). Therefore, the optimal calcining temperature to prepare CaO catalyst was 800 °C.
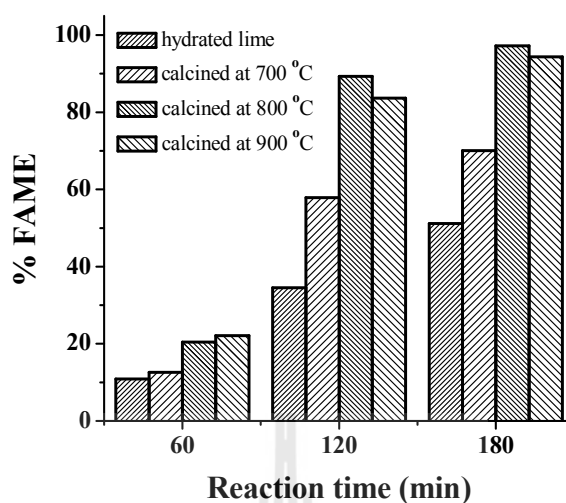
Figure 4.7 %FAME obtained in transesterification using hydrated lime and calcined hydrated lime at various temperature for 3 h (Reaction condition: amount of catalyst loading = 6 wt.%, methanol/oil molar ratio = 12:1, reaction temperature = 60 °C, stirring speed = 300 rpm and reaction time = 3 h).

4.6.2.2 Effects of catalyst loading amount

The optimal catalyst loading was determined by varying mass ratio of catalyst from 2 wt.% to 10 wt.%. As shown in Figure 4.8(a), the yield of biodiesel increased when loading amount was increased from 2 wt.% to 6 wt.%. With 6 wt.% of catalyst, 95.63% of triglycerides were transformed to biodiesel in 3 h. In general, basic sites of CaO generate methoxide anion from methanol. As a higher reactive nucleophilic molecule, methoxide anion attack electrophilic carbonyl carbon in triglyceride to give biodiesel. Consequently, increase of catalyst content will enhance the biodiesel product (Chen et al., 2015; Li et al., 2013). However, loading amount of catalyst more than 6 wt.% did not give higher biodiesel yields because of the limitations related to the mass transfer of reactants to the catalyst which became the

rate determining step. In addition, high amount of catalyst increases viscosity of the system to the point that the adequate mixing is not reached (Chen et al., 2014; Nakatani et al., 2009). Hence, the optimal catalyst loading for transformation of palm oil to biodiesel in this study was 6 wt.%.
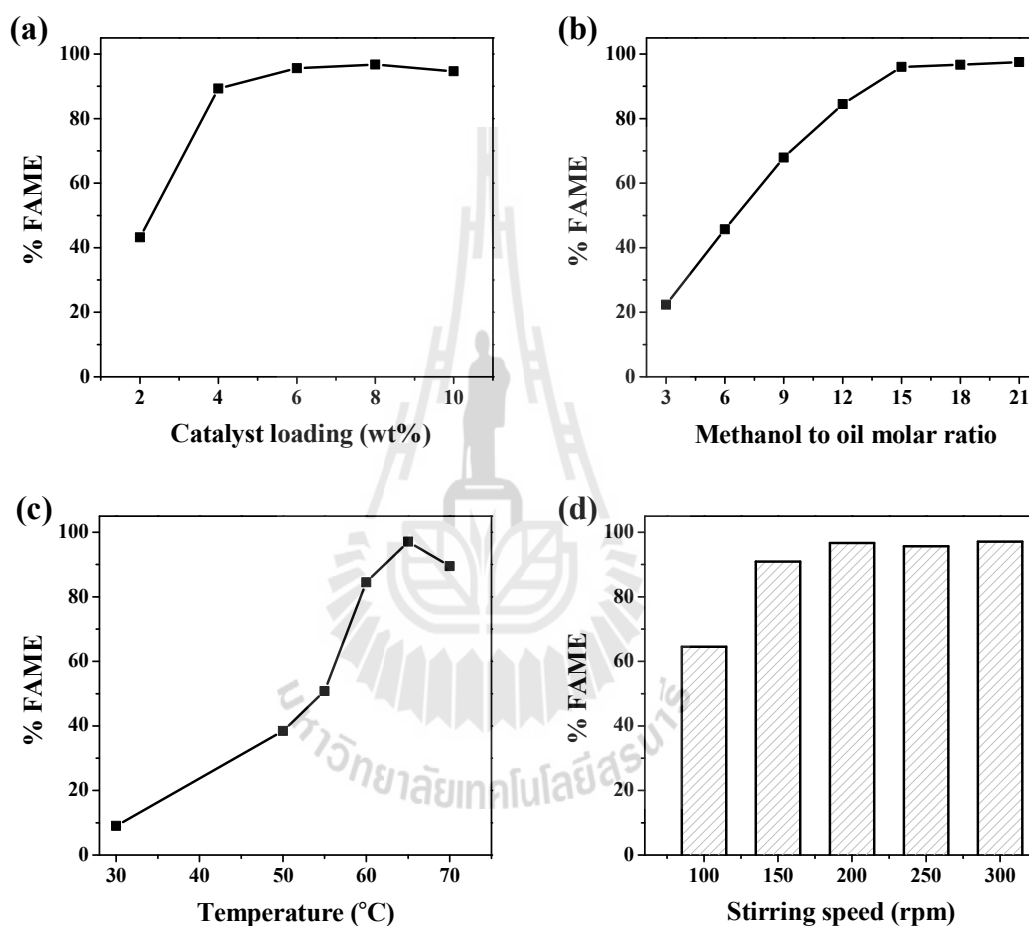
Figure 4.8 Effect of reaction conditions on %FAME. (a) Catalyst loading (methanol/oil molar ratio of 15:1, 65 °C, 200 rpm and 3 h). (b) Methanol to oil molar ratio (catalyst loading 6 wt.%, 65 °C, 200 rpm and 3 h). (c) Reaction temperature (methanol/oil molar ratio of 15:1, catalyst loading 6 wt.%, 200 rpm and 3 h). (d) Stirring speed (methanol/oil molar ratio of 15:1, catalyst loading 6 wt.%, 65 °C and 3 h).

4.6.2.3 Effects of methanol to oil ratio

The methanol to palm oil molar ratio is one of the most important factors that directly affect the biodiesel yield. Although stoichiometric ratio requires three moles of methanol for each mole of triglyceride (Takase et al., 2014). The transesterification is commonly carried out with extra amount of methanol in order to shift the equilibrium towards the direction of methyl ester formation. The effects of methanol to palm oil molar ratios were investigated as shown in Figure 4.8(b). The result clearly displayed that when molar ratio of methanol to oil was increased from 3:1 to 15:1, FAME yield was increased from 22.35% to 96.12%. The methanol to palm oil molar ratio of 15:1 was sufficient to complete the reaction. Beyond 15:1, biodiesel yield did not change due to the dissolution of glycerol by-product in excessive methanol which inhibited the reaction of methanol with catalyst and oil. Thus, the optimal methanol to palm oil molar ratio in the present reaction was 15:1, which was more than that of the practical methanol to oil molar ratio (6:1) for homogeneous catalyzed transesterification (Li et al., 2013).

4.6.2.4 Effects of reaction temperature

The effects of reaction temperature on transesterification were investigated by varying the temperature from 30 °C to 70 °C with a constant reaction time of 3 h. FAME yield increased from 9.04% to 97.23% when the reaction temperature was increased from 30 °C to 65 °C as presented in Figure 4.8(c). Such a result is expected as reaction temperature directly affects kinetic of the transesterification. However, at 70 ºC which exceeded the boiling point of methanol (64.7 °C), methanol vaporized and caused a problem involving the three phase system

including palm oil as liquid phase, methanol as gas phase and CaO catalyst as solid phase reducing the FAME yield (Liu et al., 2007; Liu et al., 2008).

4.6.2.5 Effects of stirring speed

In order to find the optimal condition for the reaction, effects of stirring reaction mixture were also investigated. The phase separation between hydrophilic methanol, hydrophobic oil and solid catalyst is generally known to be the major problem in heterogeneous reactions. Therefore, a proper mixing of the reaction by stirring is required (Chen et al., 2014; Nakatani et al., 2009). Results in Figure 4.8(d) show that stirring speed of 200 rpm is sufficient to get 97.12% yield of FAME. Higher speed had no further effects on the yield.

4.6.2.6 Comparison of hydrated lime-derived CaO against original hydrated lime

Figure 4.9 shows comparison of catalytic activity between hydrated lime-derived CaO and original hydrated lime using optimum reaction condition. The results showed that hydrated lime-derived CaO had higher catalytic activity than the original hydrated lime which is consistent with the basic property of each material. FAME yield reached 97.22% after 2 h for reaction catalyzed by CaO obtained from hydrated lime, while reaction catalyzed by original hydrated lime only reached 62.28% yield of FAME after 4 h and took 6 h to complete. Kouzu et al., reported that the catalytic activity for transesterification of triglyceride to form methyl ester was in the order of $CaO > Ca(OH)_2 >> CaCO_3$ (Kouzu et al., 2008). In this study, it was found that hydrated lime contained a mixture of $Ca(OH)_2$ and $CaCO_3$ which show

lower catalytic activity. Hence, after calcinations, hydrated lime was converted to CaO and the catalytic performance was then greatly improved.
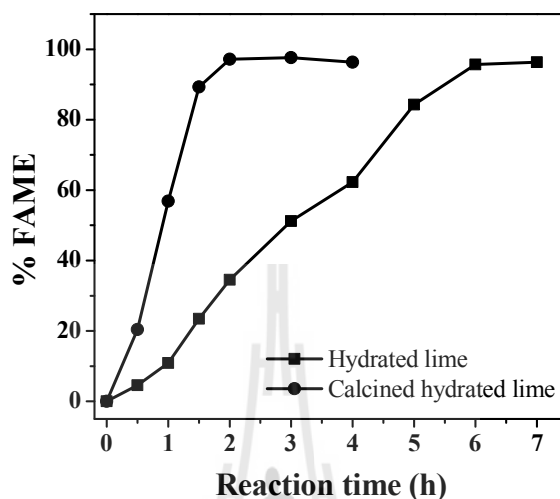
Figure 4.9 Comparison of catalytic activity between CaO derived from hydrated lime and original hydrated lime. Reaction condition: methanol/oil molar ratio of 15:1, catalyst loading amount of 6 wt.%, reaction temperature of 65 °C and stirring speed 200 rpm.

4.6.3 Effects of water on catalytic performance

Water has a significant effect on the yield of the biodiesel production especially when CaO is as a catalyst. The water content is the main cause of soap formation and transformation of CaO to $Ca(OH)_2$ with reduced efficiency. The presence of water in a reaction has more negative effect than the presence of free fatty acids. In present work, the transesterification catalyzed by CaO obtained from calcined hydrated lime showed excellent tolerance to water in the palm oil as presented in Figure 4.10. The FAME yield was maintained at 96.36% when the water content in the oil was less than 5 wt.% which is similar to the results reported in Liu et al. (Liu et al., 2008). In

this case, low amount of water in reaction mixture may improve catalytic activity of CaO as OH group can be generated which accelerates methoxide anion formation in the transesterification (Liu et al., 2008).
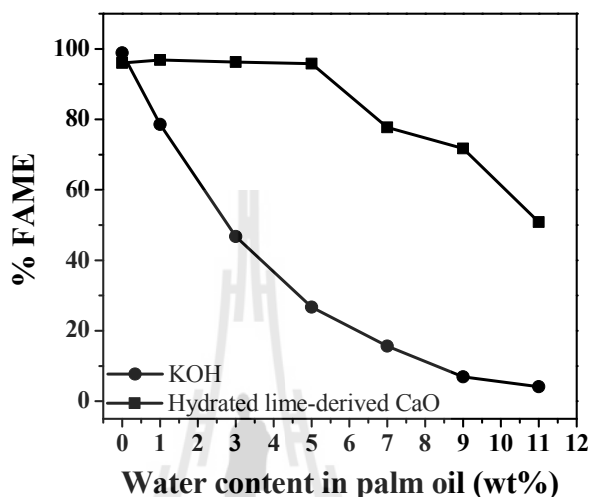
Figure 4.10 Effect of water content to %FAME of CaO catalyst prepared from calcined hydrated lime and KOH catalyst. Reaction condition of CaO catalyst: catalyst loading amount of 6 wt.%, methanol/oil molar ratio of 15:1, reaction time 2 h, reaction temperature 65 °C and stirring speed 200 rpm. Reaction condition of KOH catalyst: catalyst loading amount of 0.5 wt.%, methanol/oil molar ratio of 9:1, reaction time 1 h, reaction temperature 65 °C and stirring speed 200 rpm.

However, above 5 wt.% water contain, the yield of FAME was decreased to 78.2% because the excessive water content in the reaction could produce soap formation. Furthermore, this result confirmed that KOH as a homogeneous catalyst, had high sensitivity to water content as FAME yield significantly reduced from 98.91% to 78.63% when the water content was increased to 1 wt.% and violently decreased to 26.79% in 5 wt.% water (Atadashi et al., 2012).

4.6.4 Reusability of hydrated lime-derived CaO catalyst

Reusability of the catalyst is an important factor in biodiesel production process. After the reaction completed, the catalyst was filtrated from the solution mixture and washed with methanol and hexane. As shown in Figure 4.11(a) after being used for 5 times the catalyst still yielded more than 90% yield of FAME. Beyond 5 times, the activity of this catalyst reduced gradually. This phenomenon was investigated by FT-IR as shown in Figure 4.11(b). After being used for 10 times, the catalyst reacted with water and CO_2 forming $Ca(OH)_2$ and $CaCO_3$ whose absorption bands were observed at 3646 cm^{-1} (CaO—H stretching) and 1418 cm^{-1} (C=O stretching in $CaCO_3$) (Kusdiana and Saka, 2004; Atadashi et al., 2012).
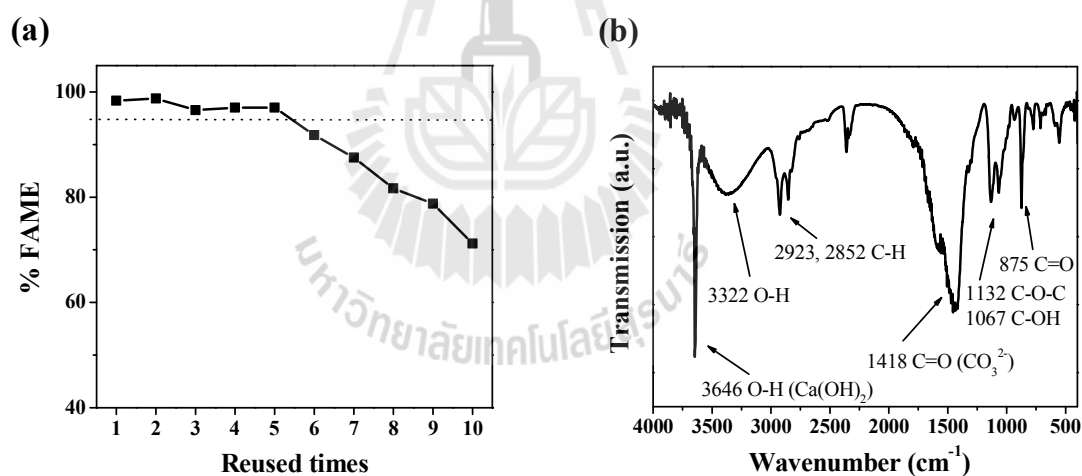
Figure 4.11 (a) Reusability study of hydrated lime-derived catalyst; reaction condition: catalyst loading amount of 6 wt.%, methanol/oil molar ratio of 15:1, reaction temperature 65 °C, reaction time 2 h and stirring speed 200 rpm. (b) IR spectra of catalyst after reused 10 times.

Furthermore, IR spectra also indicated that liquid compounds in the process namely palm oil, biodiesel, glycerol and methanol covered the surface of the catalyst showing stretching band of O—H at 3320 cm^{-1}, C—H at 2923 and 2852 cm^{-1}, C=O at 1418 cm^{-1}, C—O—C at 1132 cm^{-1}, C—OH at 1067 cm^{-1}, and C=O bending at 875 cm^{-1} as observed by Lee et al. using SEM (Lee et al., 2015). In addition, strength of the basic sites *(H_)* decreased to 9.8-12.2 which is similar to that of parent hydrated lime.

4.6.5 Biodiesel properties

Fuel properties of the obtained biodiesel after purification and treatment process were evaluated according to the ASTM and EN14214 standard methods under the optimum reaction conditions and depicted in Table 4.3. This study found that the obtained biodiesel has high quality standard properties specifically methyl ester content, viscosity, flash point, acid value, water content, sulfated ash, calcium content, total contamination, carbon residue, copper strip corrosion, density and oxidation number. The obtained values are comparable to those reported by Boey et al., Baroutian et al. and Tang et al. (Boey et al., 2011; Baroutian et al., 2010; Tang et al., 2013).

Table 4.3 Fuel properties of biodiesel obtained from the transesterification of palm oil at optimum conditions of hydrated lime-derived CaO catalyst after purification and treatment process.

Fuel properties	Unit	Standard	Boey[a]/ Baroutian[b]/ Tang[c]	This work
Density	kg/m^3	860-900	884 / 877 / 890	875
Kinematic viscosity	mm^2/s	3.5-5.0	4.2 / 5.16 / 4.6	4.20
Flash point	°C	>120	- / 188 / 164	186
Acid number	mg KOH/g	≤0.5	- / 0.33 / -	0.24
Water content	%w/w oil	≤0.050	- / - / -	0.031
Copper strip corrosion	-	Number 1	- / - /-	Number 1
Methyl ester content	%	96.5	98.8 / - / 91.8-99.8	97.61
Oxidation number	hour	>6	- / - / -	15.44
Total contamination	mg/kg (ppm)	≤24	- / -/-	15.7
Calcium content	ppm	≤5	- / - / -	1.073
Sulfated ash	% w/w oil	≤0.02	- / - / -	0.0156
Carbon residue	% w/w oil	≤0.05	- / - / -	0.0395

[a]Boey et al., 2011; [b]Baroutian et al., 2010; [c]Tang et al., 2013.

4.6.6 Kinetics of palm oil to biodiesel production

The transesterification is assumed to be a single step, and the rate law can be explained by equation 4.3:

$$r = \frac{-d[TG]}{dt} = k'[TG]\,[ROH]^3 \qquad (4.3)$$

where [TG] and [ROH] are triglyceride and alcohol concentration, respectively. In this case, three mol equivalent of methanol react with 1 mol equivalent of triglyceride and k' is the rate constant (Vujicic et al., 2010). As excess methanol was used, methanol

concentration is assumed to be constant. Therefore, the reaction could be considered pseudo-first order (Freedman et al., 1986). Integrating and rearranging the equation 4.3 results in following equation 4.4:

$$\ln[TG]_0 - \ln[TG]_t = k\,t \tag{4.4}$$

$\ln[TG]_0$ is initial concentration of triglyceride which is assumed to be 1 molar, therefore $\ln[TG]_0 = 0$, t = reaction time and $\ln[TG]_t = 1 - X_{ME}$, where X_{ME} is the yield of FAME. Finally, the rearranged equation 4.4 becomes equation 4.5:

$$-\ln[1 - X_{ME}] = k\,t \tag{4.5}$$

Following equation 4.5, plot of $-\ln[1 - X_{ME}]$ against t is shown in Figure 4.12(a). The slope is equal to rate constant (k) which increases with reaction temperature. The Arrhenius plot of ln k against 1/T is presented in Figure 4.12(b) (Birla et al., 2012). The obtained activation energy (Ea) and the frequency factor (A) were 121.12 kJ/mol and 1.203×10^{17} min^{-1}, respectively. The obtained activation energy is smaller than that reported by Vujicic (162.1 kJ/mol) (Vujicic et al., 2010). The obtained kinetic data may be used to optimize the condition to produce biodiesel. Nevertheless, all results in this work indicated that CaO catalyst prepared from calcined hydrated lime shows good catalytic activity and should be promoted for biodiesel production industry.
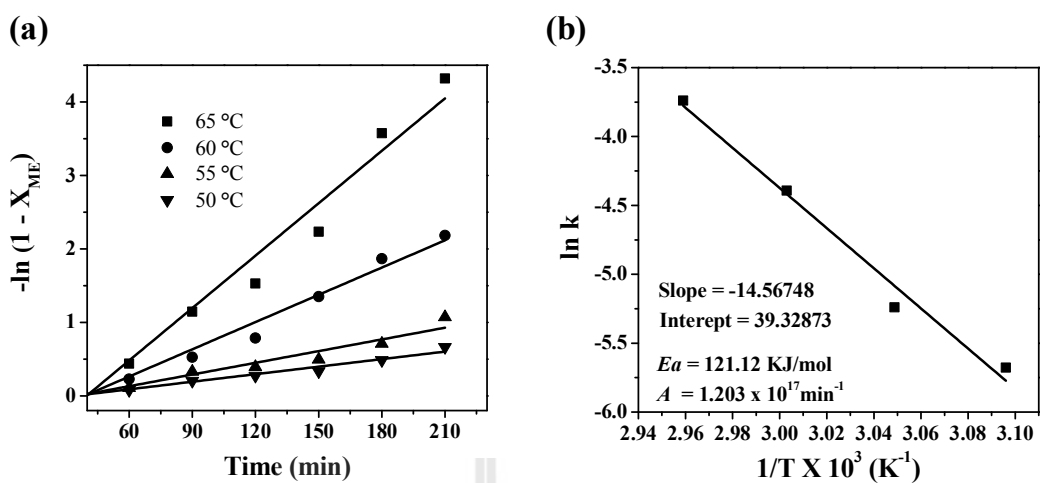
Figure 4.12 (a) -ln(1-X_{ME}) versus reaction time plot at different temperatures; reaction condition: catalyst loading amount of 6 wt.%, methanol/oil molar ratio of 15:1 and stirring speed 200 rpm. (b) Arrhenius plot ln k versus 1/T $\times$ 10^3 (K^{-1}) for transesterification of palm oil using CaO derived from calcined hydrated limes.

4.7 Conclusion

Hydrated lime-derived CaO was investigated as a catalyst in the transesterification of palm oil for biodiesel synthesis. The results indicated that calcination was an appropriate method to improve catalytic activity of hydrated lime. The hydrated lime-derived CaO catalyst showed very high activity and provides FAME yield of 97.2% after only 2 h. This CaO catalyst could be reused for at least 5 times and tolerated a maximum of 5 wt.% water content. The kinetics data was investigated where activation energy (*Ea*) of 121.12 kJ/mol and the frequency factor (*A*) of 1.203 $\times$ 10^{17} min^{-1} were obtained. After purification and treatments, high quality biodiesel could be obtained. Therefore, hydrated lime-derived CaO catalyst

has high potential for applications as green, low-cost and renewable catalyst for biodiesel production in the industrial scale.

4.8 References

Alhassan, Y., Kumar, N., Bugaje, I. M., Pali, H. S. and Kathkar, P. (2014). Co-solvent transesterification of cotton seed oil into biodiesel: Effects of reaction condition on quality of fatty acids methyl esters. **Energy Conversion and Management.** 84: 640-648.

Alonsoa, D. M., Vila, F., Mariscal, R., Ojeda, M., Granados, M. L. and Santamaria-Gonzalez, J. (2010). Relevance of the physicochemical properties of CaO catalysts for the methanolysis of triglycerides to obtain biodiesel. **Catalysis Today**. 158: 114-120.

Asikin-Mijan, N., Lee, H. V. and Taufiq-Yap, Y. H. (2015). Synthesis and catalytic activity of hydration–dehydration treated clamshell derived CaO for biodiesel production. **Chemical Engineering Research and Design**. 102: 368-377.

Atadashi, L. M., Aroua, M. K., Abdul-Aziz, A. R. and Sulaiman, M. N. M. (2012). The effects of water on biodiesel production and refining technologies: A review. **Renewable & Sustainable Energy Reviews**. 16: 3456-3470.

Baroutian, S., Aroua, M. K., Raman, A. A. A. and Sulaiman, N. M. N. (2010). Potassium hydroxide catalyst supported on palm shell activated carbon for transesterification of palm oil. **Fuel Processing Technology**. 91: 1378-1385.

Birla, A., Singh, B., Upadhyay, S. N. and Sharma, Y. C. (2012). Kinetics studies of synthesis of biodiesel from waste frying oil using a heterogeneous catalyst derived from snail shell. **Bioresource Technology**. 106: 95-100.

Boey, P. L., Maiam, G. P. and Hamid, S. A. (2011). Performance of calcium oxide as a heterogeneous catalyst in biodiesel production: A review. **Chemical Engineering Journal**. 168: 15-22.

Brito, A., Borges, M. E. and Otero, N. (2007). Zeolite Y as a heterogeneous catalyst in biodiesel fuel production from used vegetable oil. **Energy & Fuels**. 21: 3280-3283.

Chakraborty, R., Bepari, S. and Banerjee, A. (2011). Application of calcined waste fish (Labeorohita) scale as low-cost heterogeneous catalyst for biodiesel synthesis. **Bioresource Technology**. 102: 3610-3618.

Chen, G., Shan, R., Shi, J. and Yan, B. (2014). Ultrasonic-assisted production of biodiesel from transesterification of palm oil over ostrich eggshell-derived CaO catalysts. **Bioresource Technology.** 171: 428-432.

Chen, G., Shan, R., Shi, J., Liu, C. and Yan, B. (2015). Biodiesel production from palm oil using active and stable K doped hydroxyapatite catalysts. **Energy Conversion and Management**. 98: 463-469

Correia, L. M., Saboya, R. M. A., de Sousa Campelo, N., Cecilia, J. A., Rodriguez-Castellon, E., Cavalcante, C. L. and Vieira, R. S. (2014). Characterization of calcium oxide catalysts from natural sources and their application in the transesterification of sunflower oil. **Bioresource Technology**. 151: 207-213.

Freedman, B., Butterfield, O. R. and Pryde, H. E. (1986). Transesterification kinetics of soybean. **Journal of the American Oil Chemists' Society**. 63: 1375-1380.

Huang, R., Cheng, J., Qiu, Y., Li, T., Zhou, J. and Cen, K. (2015). Using renewable ethanol and isopropanol for lipid transesterification in wet microalgae cells to

produce biodiesel with low crystallization temperature. **Energy Conversion and Management**. 105: 791-797.

Kawashima, A., Matsubara, K. and Honda, K. (2008). Development of heterogeneous base catalysts for biodiesel production. **Bioresource Technology**. 99: 3439-3443.

Khemthong, P., Luadthong, C., Nualpaeng, W., Changsuwan, P., Tongprem, P, Viriya-empikul, N. and Faungnawakij, K. (2012). Industrial eggshell wastes as the heterogeneous catalysts for microwave assisted biodiesel production. **Catalysis Today**. 190: 112-116.

Kim, H. J., Kang, B. S., Kim, M. J., Park, Y. M., Kim, D. K., Lee, J. S. and Lee, K. Y. (2004). Transesterification of vegetable oil to biodiesel using heterogeneous base catalyst. **Catalysis Today**. 93: 315-320.

Kouzu, M., Kasuno, T., Tajika, M., Sugimoto, Y., Yamanaka, S. and Hidaka, J. (2008). Calcium oxide as a solid base catalyst for transesterification of soybean oil and its application to biodiesel production. **Fuel**. 87: 2798-2806.

Kusdiana, D. and Saka, H. (2004). Effects of water on biodiesel production by supercritical methanol treatment. **Bioresource Technology**. 91: 289-295.

Lee, S. L., Wong, Y. C., Tan, Y. P. and Yew, S. Y. (2015). Transesterification of palm oil to biodiesel by using waste obtuse horn shell-derived CaO catalyst. **Energy Conversion and Management**. 93: 282-288.

Li, M., Chen, D. and Zhu, X. (2013). Preparation of solid acid catalyst from rice husk char and its catalytic performance in esterification. **Chinese Journal of Catalysis**. 34: 1674-1682.

Liu, X., He, H., Wang, Y. and Zhu, S. (2007). Transesterification of soybean oil to biodiesel using SrO as a solid base catalyst. **Catalysis Communications**. 8: 1107-1111.

Liu, X., He, H., Wang, Y., Zhu, S. and Piao, X. (2008). Transesterification of soybean oil to biodiesel using CaO as a solid base catalyst. **Fuel**. 87: 216-221.

Loʹpez-Granados, M. L., Zafra-Poves, M. D., Martı́n-Alonso, D., Mariscal, R., Cabello-Galisteo, F., Moreno-Tost, R., Santamarı́a, J. and Fierro, J. L. G. (2007). Biodiesel from sunflower oil by using activated calcium oxide. **Applied Catalysis B: Environmental**. 73: 317-326.

Mahesh, S. E., Ramanathan, A., Begum, K. M. M. S. and Narayanan, A. (2015). Biodiesel production from waste cooking oil using KBr impregnated CaO as catalyst. **Energy Conversion and Management**. 91: 442-450.

Meher, L. C., Vidya-Sagar, D. and Naik, S. N. (2006). Technical aspects of biodiesel production by transesterification a review. **Renewable & Sustainable Energy Reviews**. 10: 248-268.

Mosaddegh, E. and Hassankhani, A. (2014). Preparation and characterization of nano-CaO based on eggshell waste: Novel and green catalytic approach to highly efficient synthesis of pyrano[4,3-*b*]pyrans. **Chinese Journal of Catalysis**. 35: 351-356.

Muhammad, F. and Anita, R. (2015). Biodiesel production from low FFA waste cooking oil using heterogeneous catalyst derived from chicken bones. **Renewable Energy**. 76: 362-368.

Nakatani, N., Takamori, H., Takeda, K. and Sakugawa, H. (2009). Transesterification of soybean oil using combusted oyster shell waste as a catalyst. **Bioresource Technology**. 100: 1510-1513.

Ngamcharussrivichai, C., Nunthasanti, P., Tanachai, S. and Bunyakiat, K. (2010). Biodiesel production through transesterification over natural calciums. **Fuel Processing Technology**. 91: 1409-1415.

Reyero, I., Arzamendi, G. and Gandía, L. M. (2014). Heterogenization of the biodiesel synthesis catalysis: CaO and novel calcium compounds as transesterification catalysts. **Chemical Engineering Research and Design**. 9(2): 1519-1530.

Roschat, W., Kacha, M., Yoosuk, B., Sudyoadsuk, T. and Promarak, V. (2012). Biodiesel production based on heterogeneous process catalyzed by solid waste coral fragment. **Fuel**. 98: 194-202.

Samart, C., Sreetongkittikul, P. and Sookman, C. (2009). Heterogeneous catalysis of transesterification of soybean oil using KI/mesoporous silica. **Fuel Processing Technology**. 90: 922-925.

Soetaredjo, F. E., Ayucitra, A., Ismadji, S. and Maukar, A.L. (2011). KOH/bentonite catalysts for transesterification of palm oil to biodiesel. **Applied Clay Science**. 53: 341-346.

Somnul, K., Niseng, S. and Prateepchaikul, G. (2014). Optimization of high free fatty acid reduction in mixed crude palm oils using circulation process through static mixer reactor and pilot-scale of two-step process. **Energy Conversion and Management**. 80: 374-381.

Suryaputra, W., Winata, I., Indraswati, N. and Ismadji, S. (2013). Waste capiz (Amusium cristatum) shell as a new heterogeneous catalyst for biodiesel production. **Renewable Energy**. 50: 795-799.

Takase, M., Zhang, M., Feng, W., Chen, Y., Zhao, T., Cobbina, S. J., Yang, L. and Wu, X. (2014). Application of zirconia modified with KOH as heterogeneous solid base catalyst to new non edible oil for biodiesel. **Energy Conversion and Management**. 80: 117-125.

Tang, Y., Xu, J., Zhang, J. and Lu, Y. (2013). Biodiesel production from vegetable oil by using modified CaO as solid basic catalysts. **Journal of Cleaner Production**. 42: 198-203.

Taufiq-Yap, Y. H., Teo, S. W., Rashid, U., Islam, A., Hussien, M. Z. and Lee, K. T. (2014). Transesterification of Jatropha curcas crude oil to biodiesel on calcium lanthanum mixed oxide catalyst: effect of stoichiometric composition. **Energy Conversion and Management**. 88: 1290-1296.

Viriya-empikul, N., Krasae, P., Nualpaeng, W., Yoosuk, B. and Faungnawakij, K. (2012). Biodiesel production over Ca-based solid catalysts derived from industrial wastes. **Fuel**. 92: 239-244.

Viriya-empikul, N., Krasae, P., Puttasawat, B., Yoosuk, B., Chollacoop, N. and Faungnawakij, K. (2010). Waste shells of mollusk and egg as biodiesel production catalysts. **Bioresource Technology**. 101: 3765-3767.

Vujicic, Dj, Comic, D., Zarubica, A., Micic, R. and Boskovic, G. (2010). Kinetics of biodiesel synthesis from sunflower oil over CaO heterogeneous catalyst. **Fuel**. 89: 2054-2061.

Wei, Z., Xu, C. and Li, B. (2009). Application of waste eggshell as low-cost solid catalyst for biodiesel production. **Bioresource Technology**. 100: 2883-2885.

Yoosuk, B., Udomsap, P., Puttasawat, B. and Krasae, P. (2010). Modification of calcite by hydration–dehydration method for heterogeneous biodiesel production process: The effects of water on properties and activity. **Chemical Engineering Journal**. 162: 135-141.

Zabeti, M., Wan-Daud, W. M. A. and Aroua, M. K. (2009). Activity of solid catalysts for biodiesel production: a review. **Fuel Processing Technology**. 90: 770-777.
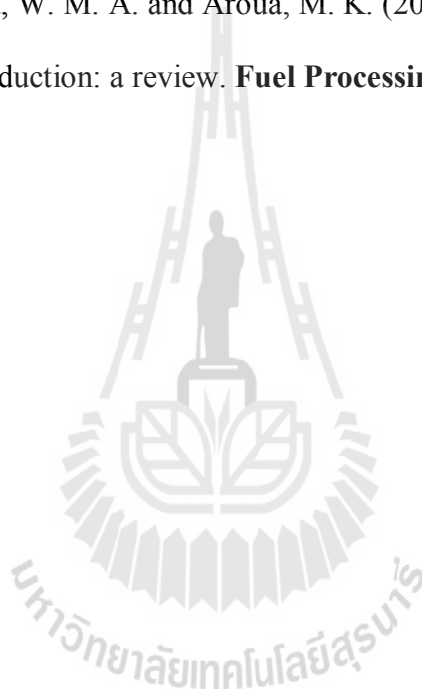
CHAPTER V

ECONOMICAL AND GREEN BIODIESEL

PRODUCTION PROCESS USING RIVER SNAIL

SHELLS-DERIVED CaO CATALYST AND

CO-SOLVENT METHOD

5.1 Graphical abstract
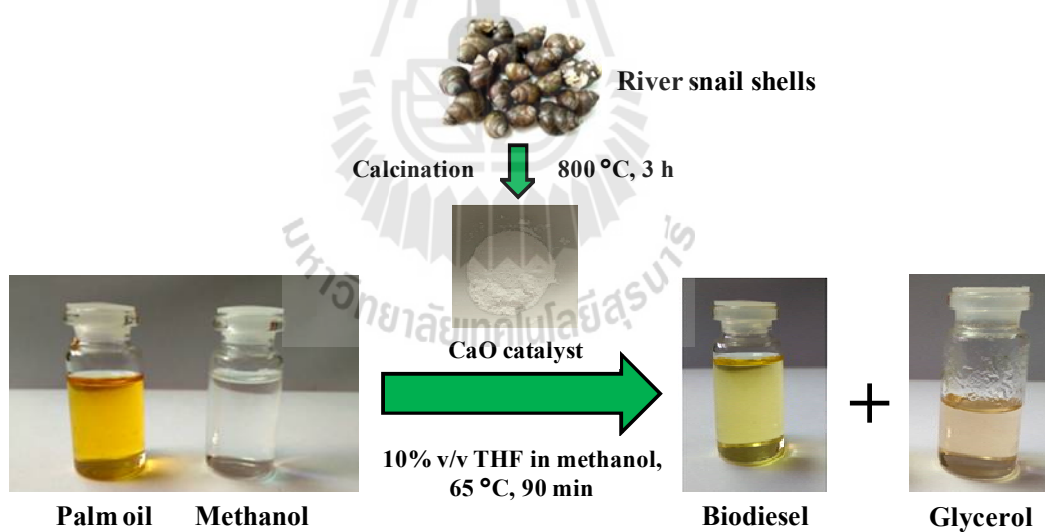
River snail shells-derived CaO catalysts and THF co-solvent are both capable of improving transesterification of palm oil in biodiesel production.

5.2 Highlights

- River snail shells-derived CaO catalyst was synthesized for the first time.

- Over 98.5% (±1.5) FAME yield is achieved from transesterification of palm oil in 90 min under the use10 %v/v of THF in methanol.

- The transesterification reaction mechanism is experimentally demonstrated.

- The co-solvent method of THF/methanol successfully decreases activation energy of reaction.

5.3 Abstract

River snail shells-derived CaO was used as a heterogeneous catalyst to synthesize biodiesel via transesterification of palm oil with methanol. The shell materials were calcined in air at 600-1000 °C for 3 h. Physicochemical properties of the resulting catalysts were characterized by TGA-DTG, XRD, SEM, BET,XRF, FT-IR and TPD. CaO catalyzed transesterification mechanism of palm oil into biodiesel was verified. The effects of adding a co-solvent on kinetic of the reaction and %FAME yield were investigated. %FAME yield of 98.5% ±1.5 was achieved under the optimal conditions of catalyst/oil ratio of 5 wt.%; methanol/oil molar ratio of 12:1; reaction temperature of 65 °C; 10% v/v of THF in methanol and reaction time of 90 min. The results ascertained that river snail shells is a novel raw material for preparation of CaO catalyst and the co-solvent method successfully decreases the reaction time and biodiesel production cost.

5.4 Introduction

Biodiesel is known to be an alternative to diesel fuel derived from petroleum source. It can be used on its own or mixed with diesel in any diesel-engine vehicles. Advantages of biodiesel are biodegradability, non-toxicity, and lower CO_2 and sulfur emission (Wang et al., 2015). Biodiesel is composed of long chain fatty acid alkyl esters typically produced from a reaction between a triglyceride in fats or oils and short chain alcohols, mainly methanol (Leung et al., 2010).

Generally, biodiesel production via transesterification reaction requires a catalyst to promote the reaction. Commonly, homogeneous catalysts such as KOH and NaOH are widely used because they give high biodiesel yield under mild reaction condition and short reaction time (Lee et al., 2015). However, the use of these catalysts has drawbacks as large amount of water is required to wash the produced biodiesel to eliminate the catalyst and soaps. Homogeneous catalysts are also difficult to be reused and they can corrode reactors (Farooq et al., 2013). Such disadvantages of homogeneous catalysts increase the cost of biodiesel production. On the other hand, heterogeneous basic catalysts have many advantages as they are cheap, environmentally friendly and non-toxic. It is possible to reuse and recycle heterogeneous basic catalysts without employing water to clean the biodiesel product. Moreover, the reaction usually results in pure glycerol as a by-product (Farooq et al., 2005; Reyero et al., 2014).

Several articles report the use of solids and composites as a heterogeneous catalyst for biodiesel production. Na/NaOH/γ-Al$_2$O$_3$ was applied as a catalyst for the biodiesel production from vegetable oil (Kim et al., 2004). Mo-Mn/γ-Al$_2$O$_3$-MgO has been used to transform waste cooking oil to biodiesel fuel (Farooq et al., 2014). The

uses of zeolites in the biodiesel production have been investigated (Leclercq et al., 2001). Nevertheless, some of these materials show low catalytic activity. In addition, they are complicated to generate, sensitive to moisture and easily leached in methanol.

Calcium oxide (CaO) is one of the best heterogeneous catalysts with good catalytic activity and low solubility in methanol. It is also cheap, environmentally friendly and easy to prepare. Many research articles have reported the study of natural materials such as egg shells (Wei et al., 2009) and sea shells (Lee et al., 2015; Nakatani et al., 2009) as starting materials for CaO preparation via calcination process. However, in some case, the catalyzed reactions still require at least 3 to 8 hours to finish (Lee et al., 2015; Wei et al., 2009; Boro et al., 2011). Reducing the reaction time would directly decrease the energy consumption and consequently reduce the production cost.

Co-solvent method is one way to improve the transesterification process. For example, tetrahydrofuran (THF), acetone, diethyl ether and chlorobenzene were used as a co-solvent with homogeneous catalyst in biodiesel production (Alhassan et al., 2014; Thanh et al., 2013; Soriano et al., 2009; Luu et al., 2014; Babaki et al., 2014). Some reports show that the co-solvent method can reduce the reaction time and reaction temperature and improve some fuel properties of the produced biodiesel.

A *river snail* is one kind of freshwater mussels in the family Viviparidae commonly found around muddy river area in Thailand. Fleshy part is consumed and the shells are always wasted. It is the focus of this work to use the river snail shells as a source for CaO catalyst preparation. The prepared catalyst was synthesized, characterized, and tested for catalytic activity in the transesterification of palm oil. In additions, reaction mechanism and the effects of co-solvent method were also

investigated. The purpose of this study is to produce biodiesel using CaO derived from river snail and to apply co-solvent method in the biodiesel production.

5.5 Methods

5.5.1 Materials

The palm oil (acid value = 0.30 mg KOH g^{-1}) and waste cooking oil (WCO, acid value = 1.54 mg KOH g^{-1}) in this work were purchased from commercial sources in Thai market. River snail shells were collected from local restaurants. Methanol (99.5%), acetone (99%), 1-propanol (99%), 2-propanol (99%), tetrahydrofuran (THF 99.5%), ethanol (99%), and ethylene glycol (99%) were obtained from Fluka. Hammett indicators namely phenolphthalein, indigo carmine, 2,4-dinitroaniline and 4-nitroaniline of AR grade purchased from Aldrich and Fluka were used in this work.

5.5.2 Catalyst preparation and characterization

The river snail shells were washed with water several times and air-dried overnight in an oven at 100 °C. The dried river snail shells were crushed, sieved and calcined at different temperatures (600-1000 °C) with a heating rate of 10 °C/min for 3 h.

The elemental compositions of river snail shells and the obtained catalysts were analyzed by a PHILIPS MagiX diffuse wavelength X-ray Fluorescence (XRF) spectrophotometer with 1 kW Rh Kα radiation. Thermal decomposition of the shells was analyzed by a Rigaku TG/DTA 8120 thermal analyzer under air flow with a heating rate of 10 °C/min. X-ray diffraction (XRD) patterns of both river snail shells and the resulting calcined materials was determined by a PHILIPS X'Pert-MDP X-ray

diffractometer using Cu Kα radiation (λ = 1.5418 Å) at 1600W, 40 kV and 40 mA. JEOL JSM 6010LV Scanning Microscope was used to investigate the samples. The samples were also analyzed by Fourier transforms infrared (FT-IR) spectroscopy using a Perkin–Elmer FTIR spectroscopy spectrum RXI spectrometer.

Brunauer Emmett Teller (BET) was used to investigate surface area, means pore diameter and pore volumes based on adsorption and desorption isotherm of N_2 gas on the Bel-sorp-mini II (Bel-Japan). Basic strength and basic site properties of calcined river snail shells were evaluated by Hammett indicator method and temperature programmed desorption method (TPD) on the Chemisorption Analyzer (Belcat B) with CO_2 as the probe molecule (Chen et al., 2014). Scanning electron microscopy (SEM) was operated using JEOL JSM 6010LV scanning electron microscope at an accelerated voltage of 10 kV.

5.5.3 Transesterification reaction

The transesterification of palm oil and WCO were carried out in a three-neck round bottom flask connected with a condenser and equipped with a thermocouple. The mixture of river snail shells-derived CaO catalysts and methanol was heated at 65 °C and added to palm oil. The reaction conditions were designed as follows: methanol to oil molar ratio of 6:1 to 18:1, amount of catalyst to oil is 1 wt.% to 7 wt.%, and magnetic stirring speed of 300 rpm. Both the type and the amount of the co-solvent were varied. The ratio of co-solvent to methanol (%v/v) was set at 5% and 10%.

To monitor the reaction, 0.5-1 mL of the reaction mixture was collected and analyzed every 30 min for 10 hours. Excess methanol and co-solvent in the sampled

mixture were evaporated in an oven before the analysis of biodiesel yield in term of the fatty acid methyl ester yield (%FAME) was performed. Proton nuclear magnetic resonance (^{1}H NMR) on a Brüker Ascend^{TM} 500 MHz spectrometer was employed to evaluate %FAME. Tetramethylsilane (TMS) and CDCl$_3$ were used as the internal reference and a solvent, respectively (Monteiro et al., 2009; Roschat et al., 2012 et al., Roschat et al., 2016). A representative example of ^{1}H NMR spectra for reaction conversion quantification is presented as Figure 5.1.
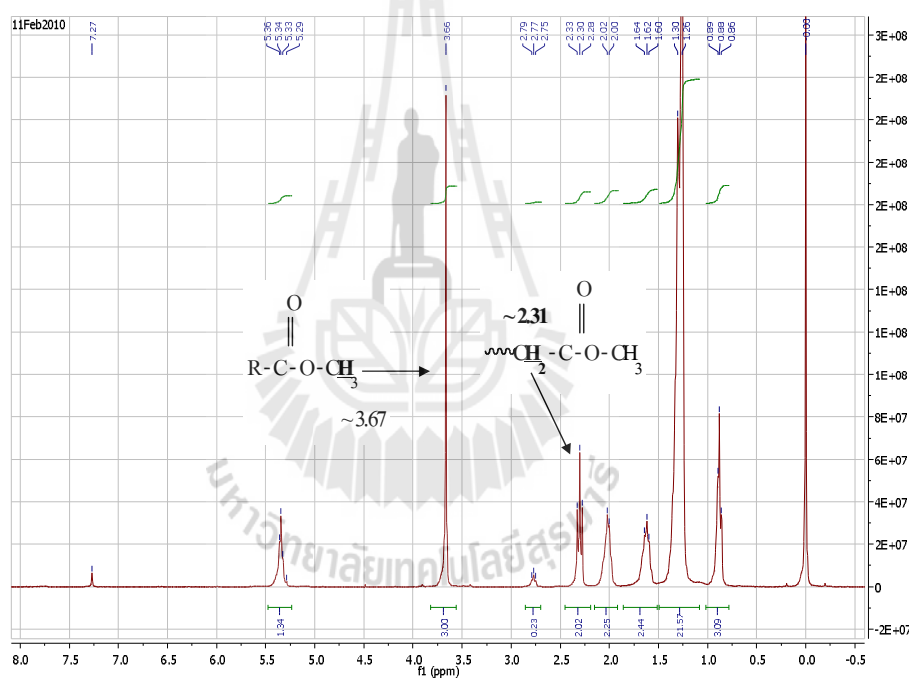
Figure 5.1 Analysis of biodiesel produced from the transesterification of palm oil and methanol using ^{1}H NMR.

5.5.4 Study of reaction kinetics

In a typical biodiesel production, 3 mol of alcohol react with 1 mol of triglyceride. Methanol is most often used in this reaction because of its suitable physical and chemical properties (Mahesh et al., 2015). According to Vujicic et al.

and Birla et al. (Vujicic et al., 2010; Birla et al., 2012), this transesterification can be assumed to be a single step reaction. The rate law of the reaction can be presented by Eq. 5.1:

$$r_a = \frac{-d[TG]}{dt} = k' \cdot [TG] \cdot [MeOH]^3 \tag{5.1}$$

where $[TG], [MeOH]$ and k' are concentration of triglyceride, concentration of methanol, and the equilibrium rate constant, respectively. During the reaction, excess amount of methanol was used to shift the equilibrium toward the product thus methanol concentration was considered constant. Therefore, the reaction behaves as a pseudo-first order reaction (Singh and Fernando, 2007; Roschat et al., 2016) and Eq. 5.1 can be rearranged to:

$$r_a = \frac{-d[TG]}{dt} = k \cdot [TG] \tag{5.2}$$

where k is modified rate constant ($k = k' \cdot [MeOH]^3$). Assuming the initial triglyceride concentration at initial time ($t = 0$), $[TG]_0$ is 1 mol and $[TG]_t$ is triglyceride concentration at time t, the integration of Eq. 5.2 gives Eq. 5.3:

$$-\ln[TG]_t = k \cdot t \tag{5.3}$$

$[TG]_t$ is related to %FAME yield by Eq. 5.4:

$$[TG]_t = 1 - x_{ME} \tag{5.4}$$

where x_{ME} is ($\frac{\%FAME}{100}$). Substituting $[TG]_t$ in Eq. 5.3 gives Eq. 5.5:

$$-\ln[1 - x_{ME}] = k \cdot t \tag{5.5}$$

Therefore, a plot of $-\ln[1 - x_{ME}]$ versus t will be linear and its slope is equal to k. On the other hand, activation energy (E_a) and the frequency factor (A) can be obtained from a slop and an intercept of lnk versus 1/T plot, respectively (Birla et al., 2012; Singh and Fernando, 2007; Zhang et al., 2010; Roschat et al., 2016).

5.5.5 Study of transesterification mechanism

Mechanism of transesterification reaction was studied on a reaction between 2 g of CaO catalyst obtained from river snail shells mixed with 20 mL of methanol at 65 °C for 30 min. In this case, both the liquid mixture and the solid catalyst were analyzed. 0.5 mL of the reaction mixture was sampled and analyzed with ^{1}H NMR and ^{13}C NMR. The solid catalysts were separated from reaction mixture by filtration (denoted as wet CaO-methanol sample). Some parts of the wet CaO-methanol sample were dried in vacuum for 10 min and in an oven at 65 °C for another 20 min to give dried CaO-methanol sample. Then, both of the resulting solid materials (wet CaO-methanol and dried CaO-methanol) were analyzed by FT-IR and TG-DTA method. In addition, effects of the mixing sequence of the reactants (palm oil and methanol) and CaO catalysts on the reaction kinetics were also investigated.

5.6 Results and discussion

5.6.1 Catalyst preparation and characterizations

As expected, XRF results indicated that river snail shells and the obtained catalysts were composed of more than 98.5% of CaO compound. Figure 5.2(a) shows TG/DTA analysis of river snail shells. The small weight loss due to the loss of water molecules and organic compounds was observed at 50-400 °C. The significant weight change was observed at temperature around 600-800 °C. After 800 °C, weigh of the sample remained constant at 53 wt.% which was in agreement with the theoretical weight change (loss 44 wt.%) in the decomposition of $CaCO_3$ to CaO (Wei et al., 2009).
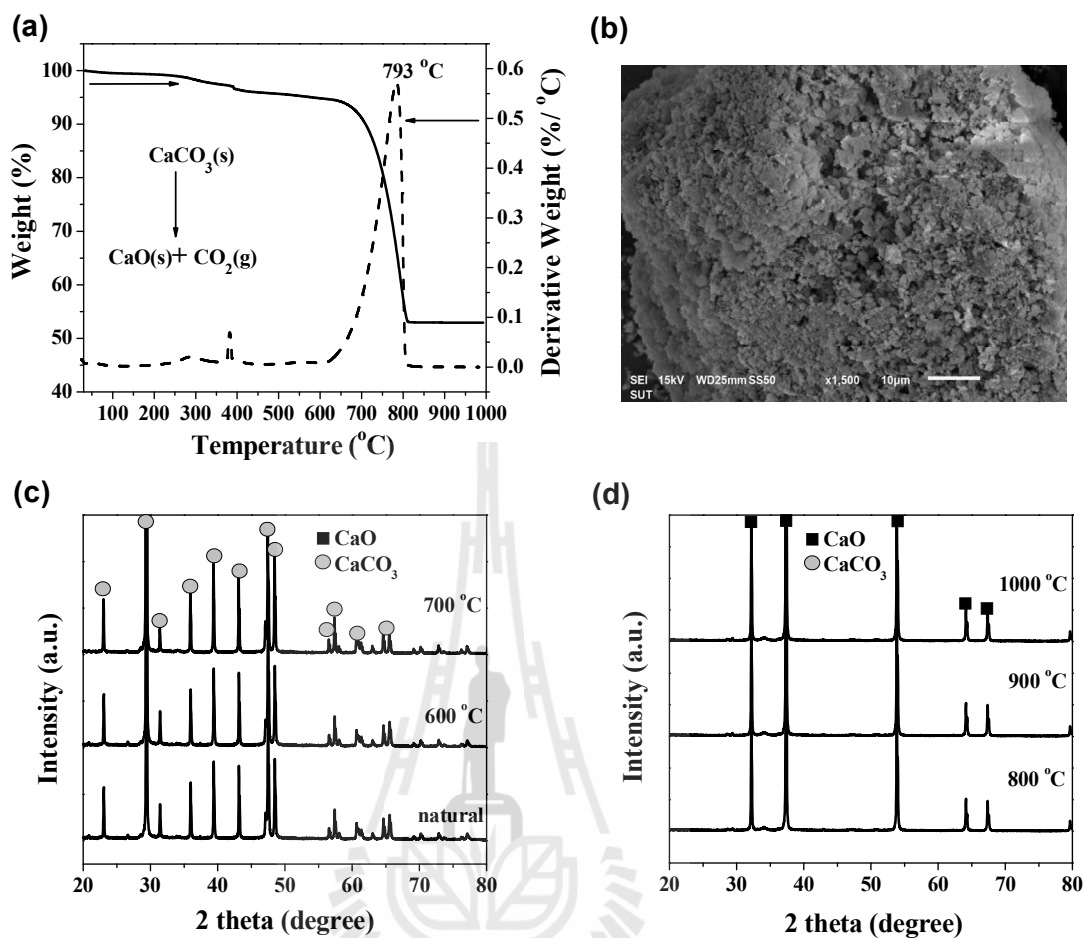
Figure 5.2 (a) TG/DTA profile of the river snail shells. (b) SEM image of river snail shells calcined at 800 °C for 3 h. (c) and (d) XRD patterns of river snail shells at different calcination temperatures for 3 h.

XRD patterns of river snail shells calcined at different temperatures are depicted in Figure 5.2(c) and (d). The results indicated that calcination the shells at temperature lower than 800 °C (600 and 700 °C) did not lead to the formation of CaO species and the sample contained only $CaCO_3$. The samples calcined at 800, 900 and 1000 °C for 3 h were consisted of CaO as a major phase with no indication of $CaCO_3$ remained. Results from TGA and XRD were in agreement, as both suggest that a temperature of

at least 800 °C was required to transform $CaCO_3$ to CaO. This conclusion is also in agreement with those reported by Lee et.al. (Lee et al., 2015).

The BET surface area, total pore volume and mean pore diameter directly impact the active sites on the catalysts. As shown in Table 5.1, calcining river snail shells at more than 800 °C significantly reduces BET surface area, total pore volume, and mean pore diameter of the sample because of the severe sintering of the particles. CO_2-TPD of river snail shells calcined at 800 °C showed higher total basic sites and basic site density (Basic site density = total basic site/BET surface area) than those of the shells calcined at 900 °C and 1000 °C. These results suggested that BET surface area correlates with the basic site of CaO catalysts. The total basic sites are strongly correlated to the catalytic activity of catalysts as catalysts with higher basic sites usually give higher biodiesel yield. It is therefore concluded that the optimum calcination temperature to prepare CaO catalysts from river snail shells is 800 °C. Similar results were also obtained in reports of Viriya-empikul et al. and Lee et al. (Viriya-empikul et al., 2012; Lee et al., 2014).

The basic strengths (H_ value) of all calcined river snail shells measured by Hammett indicator method were in the range of 15.0–18.4 as evidenced by their ability to change a color of 2,4-dinitroaniline (pKa = 15) but not 4-nitroaniline (pKa = 18.4). In contrast, The H_ value of uncalcined river snail shells was less than 8.0–10.0. SEM image of river snail shells-derived CaO catalysts calcined at 800 °C for 3 h as displayed in Figure 5.2(b), shows that the sample contained large particles with high porosity.

Table 5.1 Physicochemical properties of river snail shells-derived CaO catalyst calcined at different temperatures for 3 h.

Calcination temperature (°C)	BET surface area (m^2g^{-1})	total pore volume (cm^3g^{-1})	mean pore diameter (nm)	Basic sites (mmol/g)				Basic sites density ($\mu mol/m^2$)	basic strengths ($H\_$)
				Weak (<300 °C)	Medium (300-550 °C)	Strong (>550 °C)	Total		
800	3.5	1.87×10^{-2}	21.43	0.006	4.080	4.790	8.876	393.76	$15 < H\_ < 18.4$
900	2.7	6.61×10^{-3}	9.93	0.066	2.614	5.378	8.058	330.60	$15 < H\_ < 18.4$
1000	0.7	1.52×10^{-3}	8.94	0.114	2.926	4.786	7.826	86.63	$15 < H\_ < 18.4$

5.6.2 Optimization of reaction conditions on the transesterification palm oil

5.6.2.1 Effects of calcination temperatures of river snail shells

Figure 5.3(a) shows the influence of the calcination temperature on the activity of river snail shells-derived CaO catalysts. Catalytic activities of the shells calcined at different temperatures were investigated using palm oil and WCO. The results showed that %FAME yield significantly increased when the calcination temperature of the shells increased from 600 to 800 °C. On the other hand, increasing the calcination temperature to 900 and 1000 °C resulted in the samples with lower catalytic activity which gave lower %FAME yield under the same reaction condition. These results were expected as the sample calcined at 600 and 700 °C only contained $CaCO_3$ while calcining river snail shells at 900 and 1000 °C resulted in CaO with lower BET surface area and total basic site (Lee et al., 2015; Viriya-empikul et al., 2012). Hence, the optimum calcination temperature to synthesize CaO catalysts from river snail shells was 800 °C.

5.6.2.2 Effects of catalyst loading amount

The effects of catalyst loading amount on the transesterification of palm oil were tested by varying the amount of river snail shells-derived CaO catalysts from 1 wt.% to 7 wt.%. %FAME yield increased with increasing catalyst loading amount from 1 wt.% to 5 wt.% (Figure 5.3(b)) because more CaO catalysts could produce methoxide anion as a nucleophile which would then attack with electrophilic carbonyl carbon of triglycerides to give biodiesel. Therefore, increasing amount of catalysts generally enhance biodiesel production (Lee et al., 2015; Chen et al., 2014). However, the biodiesel yield did not increase when the catalyst loading amount was further

increased of 7 wt.%. This may be the problem of phase mixing between palm oil, methanol and solid catalyst as high viscosity of slurry limited mass transfer of reactants to catalysts (Liu et al., 2007; Mahesh et al., 2015). Therefore, the optimum catalyst loading was found to be 5 wt.% in this system.

5.6.2.3 Effects of methanol to oil ratio

Figure 5.3(c) illustrates variation of %FAME yield with different methanol to oil molar ratios using river snail shells-derived CaO as a catalyst. Yield of biodiesel increased when methanol to oil molar ratio was increased from 9:1 to 12:1. In general, increasing methanol to oil molar ratio will shift the reaction equilibrium toward the formation of biodiesel (Viriya-empikul et al., 2012; Obadiah et al., 2012). However, increasing the ratio to 15:1 did not change biodiesel yield and further increase methanol to oil ratio to 18:1 resulted in decreasing %FAME yield. In this case, glycerol by-product may dissolve in the excessive methanol and thereby inhibit the mixing between methanol with the catalysts and oil. Nevertheless, the optimum methanol to oil molar ratio in this work was 12:1 which could result in over 95% yield of FAME yield in 180 min at 65 °C.
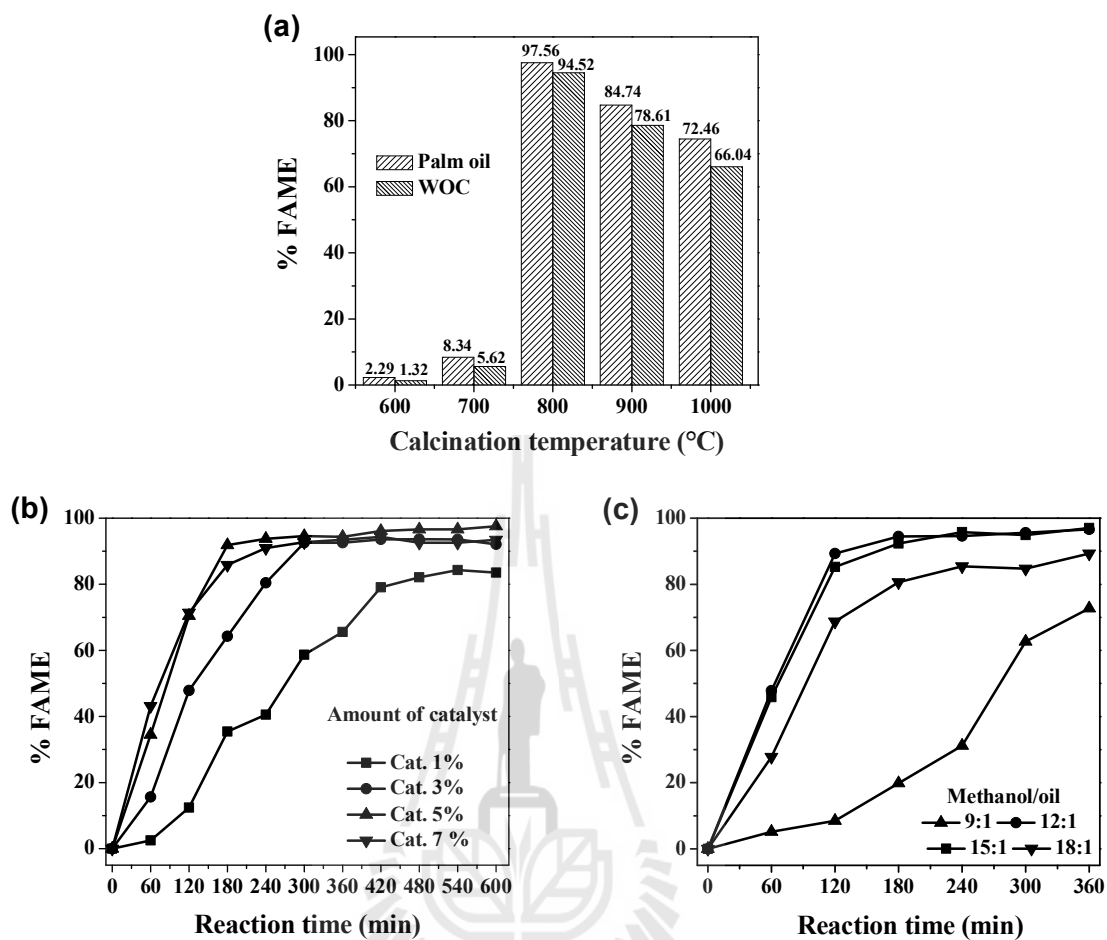
Figure 5.3 (a) %FAME yield obtained in transesterification using river snail shells-derived CaO catalysts calcined at designated temperatures for 3 h (reaction conditions: temperature = 65 °C, methanol/oil molar ratio = 12:1, catalyst amount of 5 wt.% for 180 min. (b) Effects of catalyst loading amount on %FAME yield (reaction conditions: temperature = 65 °C and methanol/oil molar ratio = 12:1). (c) Effects of methanol to oil molar ratio on %FAME yield (reaction conditions: temperature = 65 °C and catalyst loading amount of 5 wt.%).

5.6.3 Study of transesterification mechanism

Transesterification mechanism is very important for designing the reactor, controlling reaction and improving the biodiesel production process. Several articles reported the possible transesterification reaction mechanism via a typical nucleophilic substitution reaction (Zhang et al., 2010; Fan et al., 2013). In the basic catalyzed conditions, the reaction starts by removing a proton (H^+) from the methanol making methoxide anion (CH_3O^-) as a high reactive nucleophilic specie. The nucleophilic CH_3O^- attacks electrophilic carbonyl carbon in triglyceride to give biodiesel product and glycerol by-product as depicted in Figure 5.4. Hence, the key step in this mechanism is the generation of methoxide anion (Lee et al., 2015; Liu et al., 2007). In the present work, such reaction mechanism was carefully studied and verified.
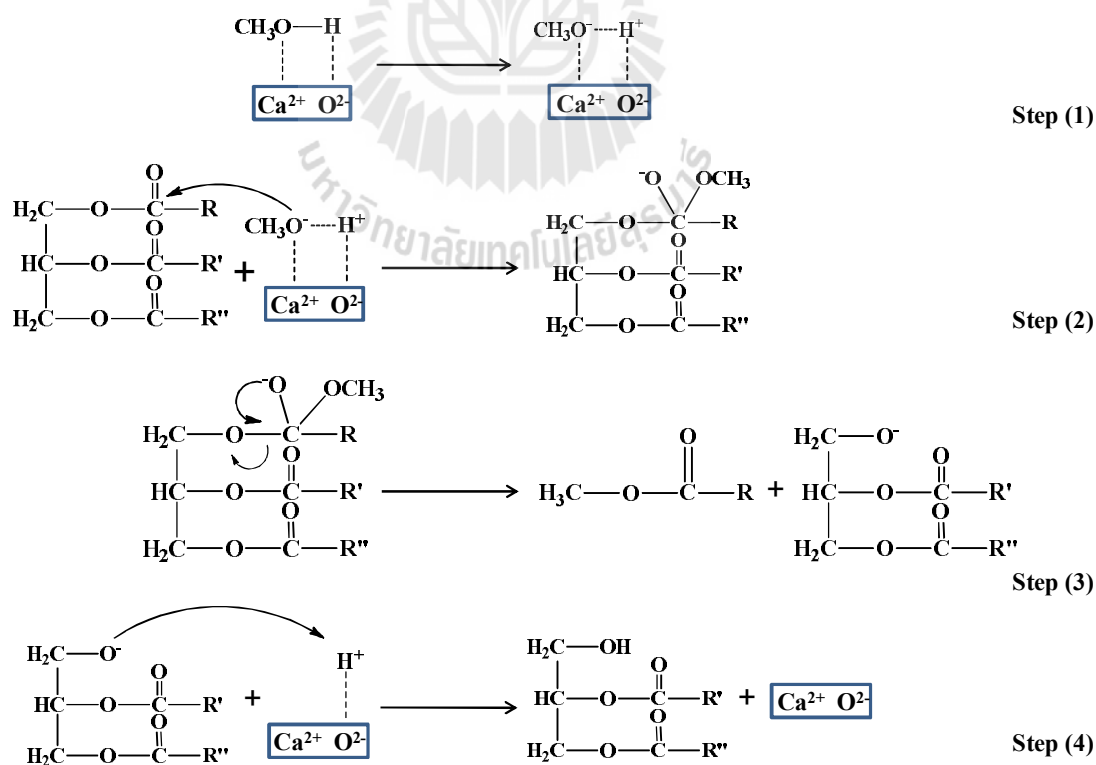
Figure 5.4 The possible CaO catalyzed transesterification reaction mechanism.

The overall of transesterification reaction

| Triglyceride | Methanol | | Biodiesel | Glycerol |
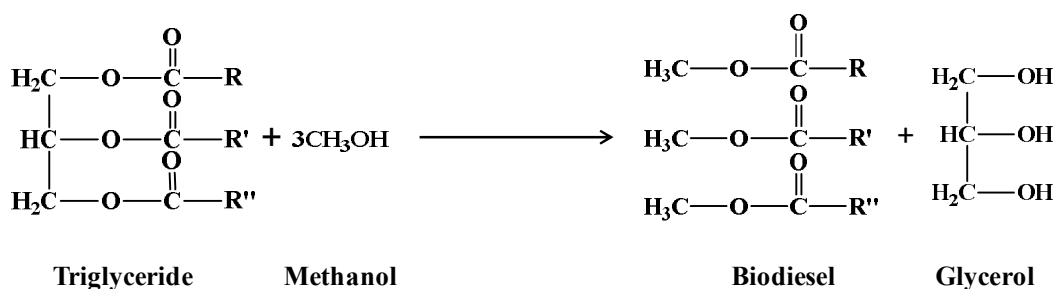
Figure 5.4 The possible CaO catalyzed transesterification reaction mechanism (Continued).

5.6.3.1 FT-IR analysis

Figure 5.5(a) shows FT-IR spectra of fresh CaO, dried CaO-methanol, wet CaO-methanol and liquid methanol as the assignments of each major IR peaks were listed in Table 5.2. The wet CaO-methanol sample displays similarly spectrum to liquid methanol because most of the methanol molecules overwhelm on surface CaO as a physical adsorption, as well as the peak at ~3660 cm^{-1} associated with CaO–H stretching vibration due to hydration process with moisture in the air changed CaO to Ca(OH)$_2$ (Esipovicha et al., 2014).

The dried CaO-methanol sample shows band peak at 1050-1100 cm^{-1} associated with stretching of C–O and band peak at 2700-2900 cm^{-1} assigned to C–H stretching vibration. These peaks were observed that there were significant to shift wave number compared with liquid methanol spectrum. Moreover, the peak at 1350-1500 cm^{-1} assigned to bending mode of CH$_3$ as showed a medium vibration and sharper peak. In contrast, O–H stretching band peak at 3000-3600 cm^{-1} illustrates very weak peak. Hence, from these FT-IR results, it can be confirmed that basic site on CaO surface transforms methanol into reactive CH$_3$O$^-$ and H$^+$ species as explained in

Figure 5.4 (Fan et al., 2013; Esipovicha et al., 2014). These species electrostatically

bind on the surface of the CaO catalyst.

Table 5.2 Shown band assignments of each FT-IR spectra.

Sample	Wave number (cm^{-1})	Assignment
Fresh CaO	500-550	Ca–O stretching
	~3660	CaO–H stretching from $Ca(OH)_2$
Dried CaO-methanol	1050-1100	C–O stretching
	2700-2900	O–H stretching
	1350-1500	CH_3 bending
	~3660	CaO–H stretching from $Ca(OH)_2$
Wet CaO-methanol	3000-3600	O–H stretching
	2800-3000	C–H stretching
	1350-1500	CH_3 bending
	1000-1100	C–OH stretching
	~3660	CaO–H stretching from $Ca(OH)_2$
Liquid methanol	3000-3600	O–H stretching
	2800-3000	C–H stretching
	1350-1500	CH_3 bending
	1000-1100	C–OH stretching
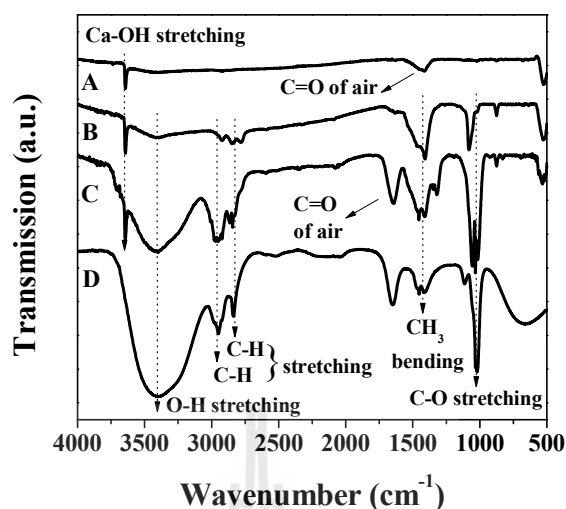
Figure 5.5 FT-IR spectra of (A) fresh CaO, (B) dried CaO-methanol, (C) wet CaO-methanol and (D) liquid methanol.

5.6.3.2 TG/DTA analysis

Figure 5.6(a) and (b) show TG/DTA curves of fresh CaO and dried CaO-methanol, and wet CaO-methanol, respectively. The results show that weight of the fresh CaO catalyst remained constant at 99.95% when being analyzed with TG/DTA from 35 to 900 °C. Dried CaO-methanol sample displayed 6% weight loss in the range of 180-280 °C which can be assigned to the loss of CH_3O^- and H^+ species binding on the CaO surface. This confirms that the formed CH_3O^- and H^+ species bind strongly on the surface of CaO more than methanol molecules. DTA curve shows endothermic peak maximum at 200 °C and 250 °C corresponding to the leaving of those species, respectively.

In addition, TG/DTA curves of the dried CaO-methanol sample also shows peak in range of 350-470 °C which corresponds to the thermal decomposition of $Ca(OH)_2$ into CaO (Roschat et al., 2016; Yoosuk et al., 2010). This indicates that

during the activation of the methanol by CaO catalyst some parts of the catalytic surface of CaO also undergoes hydrolysis to the inactive $Ca(OH)_2$. Thus, TG/DTA data strongly supports the possibility of CaO catalyzed transesterification mechanism of palm oil and methanol via the formation of methoxide anion on the surface CaO catalyst, and agrees with the FT-IR data.
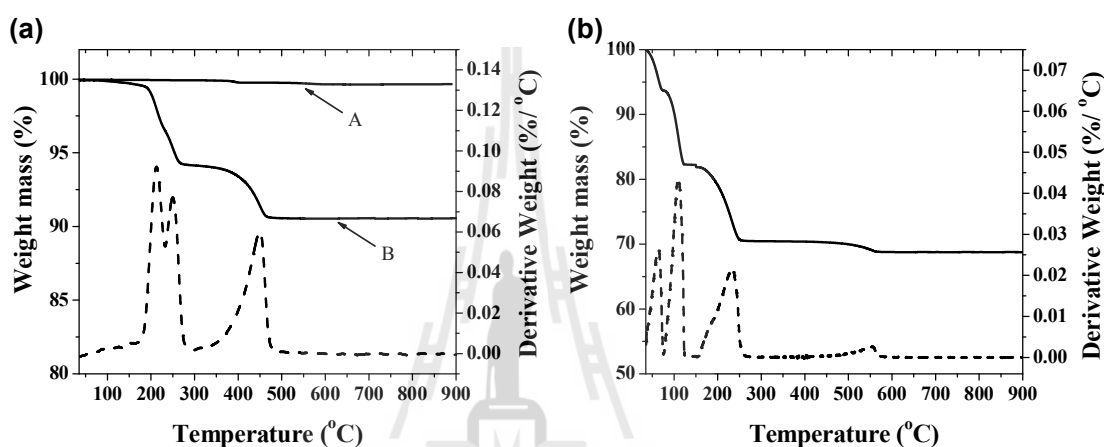
Figure 5.6 (a) TG/DTA curves of fresh CaO (A) and dried CaO-methanol (B). (b) TG/DTA curves of wet CaO-methanol.

5.6.3.3 NMR analysis

Figure 5.7(a) shows the expend ^1H NMR spectra of liquid methanol (spectrum 1) and dried CaO-methanol in $CDCl_3$ as a solvent (spectrum 2). As can be seen from Figure 5.7(a), O–H proton of methanol was strongly deshielded when methanol was reacted with CaO catalyst because its electron density was reduced by the two neighboring oxygen atom, and shifted from chemical shift of 3.33 ppm to 3.59 ppm. On the other hand, high electron density on oxygen atom of CH_3O^- specie formed shielded the CH_3 protons and shifted their peak upfield from chemical shift 3.46 ppm to 3.35 ppm. Similarly, such high electron on CH_3O^- species also shield the

carbon atom of the methoxide (CH_3O-) resulting in an upfiled shift of the ^{13}C NMR peak in dried CaO-methanol as illustrated in Figure 5.7(b). The chemical shift of the methoxide carbon (CH_3O-) shifted from 50.11 ppm to 49.98 ppm. These results confirm that methanol molecules are transformed into the reactive methoxide spices during the activation process by CaO catalyst.
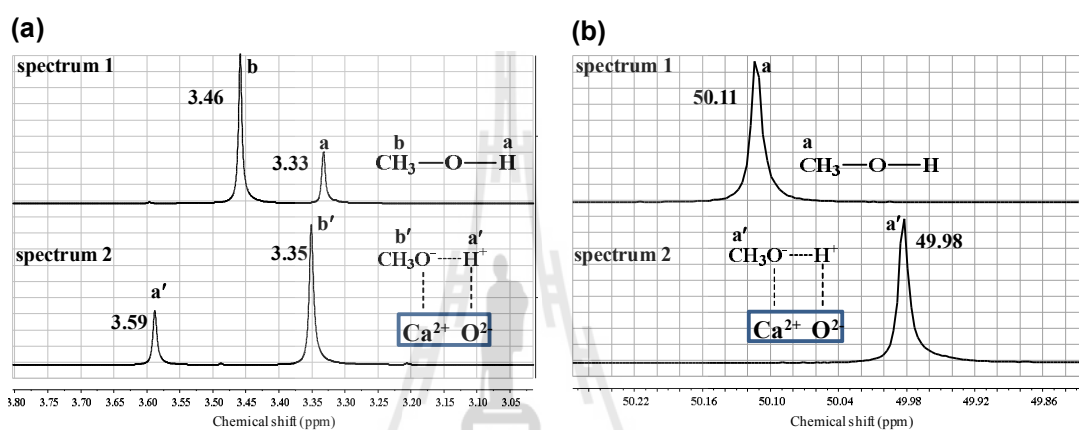
Figure 5.7 (a) the expand 500 MHz ^1H NMR and (b) 175 MHz ^{13}C NMR spectra of liquid methanol (spectrum 1) and dried CaO-methanol (spectrum 2) in CDCl$_3$.

5.6.3.4 Effect of mixing sequence on the reaction kinetics

According to Figure 5.4, the first step in the mechanism is methoxide anion formation. To further emphasize the importance of this step, the effects of mixing sequence of the reaction mixture on %FAME yield were investigated. When methanol was mixed with CaO catalyst before adding palm oil, %FAME yield of 94.34% was achieved after 180 min. Such %FAME yield was significantly higher than that obtained from a reaction prepared by first mixing CaO with palm oil (66.67%) as depicted in Figure 5.8(a). This difference clearly shows the significance of methoxide formation. When CaO catalyst was first mixed with palm oil, its surface

including active sites was cover by the oil hindering methoxide formation once methanol was added and consequently slowed the transesterification reaction.

The effect of mixing sequence is also reflected in the rate constants (k) obtained from $-\ln[1 - x_{ME}]$ versus reaction time plot as shown in Figure 5.8(b). When methanol was first mixed with CaO catalyst before adding palm oil, k constant was 1.28×10^{-2} min^{-1}. While mixed palm oil with CaO catalyst previously added methanol, k constant was 8.26×10^{-3} min^{-1}.
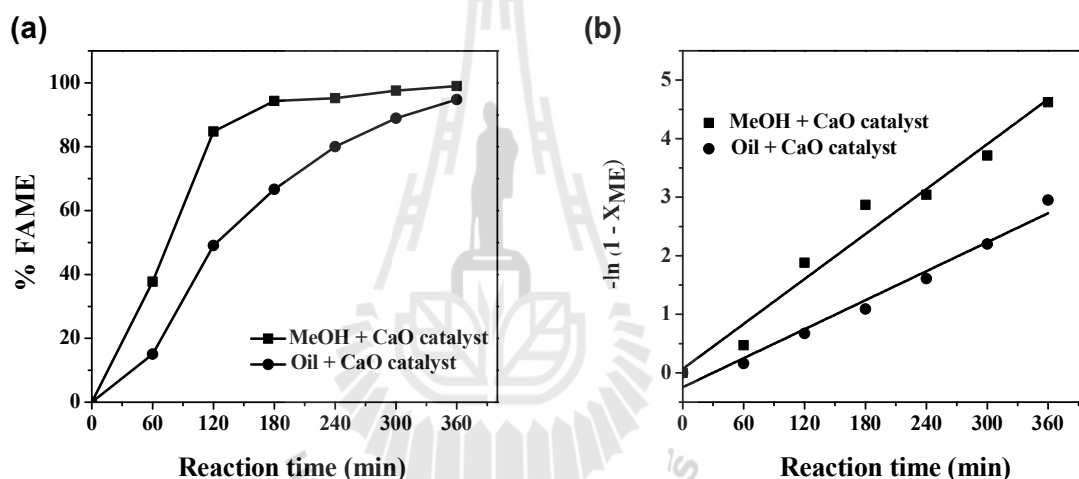
Figure 5.8 (a) the effect of mixing sequence of reaction mixture on %FAME yield and (b) kinetics study (reaction condition: methanol/oil molar ratio of 12:1, catalyst loading amount of 5 wt.% and temperature of 65 °C).
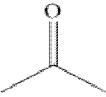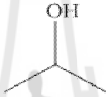
5.6.4 Effect of co-solvent on transesterification process

Phase separation between hydrophilic methanol, hydrophobic oil and solid catalyst is generally known to be the major problem in heterogeneous catalyzed reaction. Addition of another solvent into methanol can improve biodiesel production

as the mixing between methanol and palm oil will be improved (Soriano et al., 2009; Alhassan et al., 2014; Luu et al., 2014; Dianursanti et al., 2015).

Types and properties of co-solvent used in this study namely acetone, 1-propanol, 2-propanol, THF, ethanol and ethylene glycol are shown in Table 5.3. According to the obtained results shown in Table 5.4, %FAME yield was increased when co-solvents were used in the order: THF > 1-propanol > 2-propanol > acetone > ethanol > ethylene glycol. The results suggested that physicochemical properties especially polarity and boiling point of THF were suitable to increase the dissolution of palm oil in methanol. Increased polarity of co-solvents led to a decreased biodiesel yield as the high polar co-solvents can dissolve well in methanol but not in palm oil. These results agree with the report of Mohammer-Dado et al. (Mohammed-Dabo et al., 2012) who used THF as a co-solvent on homogeneous transesterification of *Jatropha curcas* seed oil catalyzed by sodium hydroxide.

Table 5.3 Some physicochemical properties of co-solvents used in this study [sourced from Mcgraw-Hill. 2004].

Properties	Co-solvents [a]					
	THF	acetone	2-propanol	1-propanol	ethanol	ethylene glycol
chemical structure						
Chemical formula	C_4H_8O	C_3H_6O	C_3H_8O	C_3H_8O	C_2H_6O	$C_2H_6O_2$
Molar mass (g/mo)	71.11	58.08	60.10	60.10	46.07	62.07
Appearance	colorless liquid	colorless liquid	colorless liquid	colorless liquid	colorless liquid	colorless liquid
Density at 20 °C (g/cm^3)	0.889	0.791	0.786	0.803	0.789	1.1132
Melting point (°C)	-108.4	-95	-89	-126	-114	-12.9
Boiling point (°C)	66	56	82.6	97	78.37	197.3

[a]Polarity order of co-solvents as THF < acetone < 2-propanol < 1-propanol < ethanol < ethylene glycol.

Table 5.4 The effect of co-solvent on the transesterification reaction of palm oil and methanol.

Type of co-solvent (v/v [a])	%FAME		k constant[b] ($\times 10^{-2}$ min^{-1})
	reaction time 90 min	reaction time 120 min	
non co-solvent system	63.93	80.01	1.836
THF 5%	93.53	97.27	4.002
THF 10%	95.03	96.68	4.087
acetone 5%	70.17	86.89	1.978
acetone 10%	90.23	95.28	2.765
2-propanol 5%	81.63	95.81	2.320
2-propanol 10%	88.44	94.59	2.183
1-propanol 5%	93.46	94.79	2.159
1-propanol 10%	94.44	95.69	2.067
ethanol 5%	62.50	89.69	1.960
ethanol 10%	75.47	93.45	2.09
ethylene glycol 5%	83.33	84.39	1.310
ethylene glycol 10%	80.60	85.84	1.340

[a]%v/v relative to amount of methanol, [b]Reaction conditions: methanol/oil molar ratio of 12:1, catalyst loading amount of 5 wt.% and 65 °C.

As shown in Figure 5.9(a), addition of 10% v/v of THF improved %FAME yield to 95.90% at the reaction time 90 min while non co-solvent system gives only 63.49% FAME yield. The obtained k value of 10% v/v THF co-solvent system was 4.09×10^{-2} min^{-1} which was twice larger than that of non co-solvent system (1.84×10^{-2} min^{-1}). The effects of THF on reaction kinetics were also observed in the decrease of activation energy (57.79 KJ/mol) and increase in frequency factor (1.17×10^{-7} min^{-1}) comparing to those of non co-solvent reaction (67.60 KJ/mol and 9.87×10^{8} min^{-1}) as shown in Figure 5.9(b).
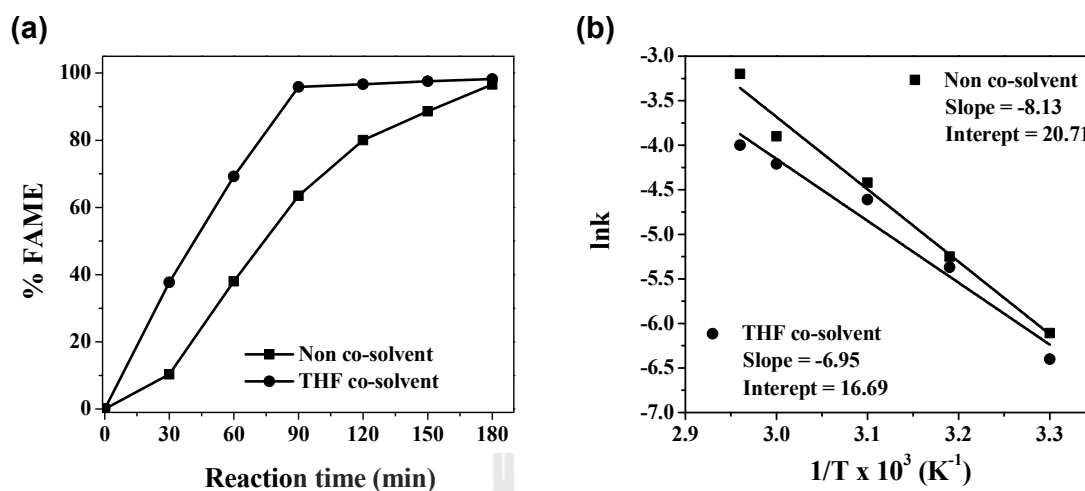
Figure 5.9 (a) %FAME of with and without 10 %v/v of THF systems. (b) Arrhenius plots of lnk versus 1/T for transesterification of palm oil with and without 10 %v/v THF systems (Reaction conditions: methanol/oil molar ratio of 12:1, catalyst loading amount of 5 wt.% and 65 °C).

5.7 Conclusion

Transesterification of palm oil to biodiesel product was catalyzed by river snail shells-derived CaO catalysts. The reaction time of transesterification was decreased from 180 min in non co-solvent reaction to 90 min in a co-solvent reaction with 10% v/v THF. Additionally, the possible transesterification mechanism was experimentally investigated. The results indicate that river snail shells-derived CaO catalysts and THF co-solvent are both capable of improving transesterification of palm oil in biodiesel production.

5.8 References

Alhassan, Y., Kumar, N., Bugaje, I. M., Pali, H. S. and Kathkar, P. (2014). Co-solvents transesterification of cotton seed oil into biodiesel: Effects of reaction conditions on quality of fatty acids methyl esters. **Energy Conversion and Management**. 84: 640-648.

Babaki, M., Yousefi, M., Habibi, Z., Mohammadi, M. and Brask, J. (2015). Effect of water, organic solvent and adsorbent contents on production of biodiesel fuel from canola oil catalyzed by various lipases immobilized on epoxy-functionalized silica as low cost biocatalyst. **Journal of Molecular Catalysis B: Enzymatic**. 120: 93-99.

Birla, A., Singh, B., Upadhyay, S. N. and Sharma, Y. C. (2012). Kinetics studies of synthesis of biodiesel from waste frying oil using a heterogeneous catalyst derived from snail shell. **Bioresource Technology**. 106: 95-100.

Boro, J., Thakur, A. J. and Deka, D. (2011). Solid oxide derived from waste shells of Turbonilla striatula as a renewable catalyst for biodiesel production. **Fuel Processing Technology**. 92: 2061-2067.

Chen, G., Shan, R., Shi, J. and Yan, B. (2014). Ultrasonic-assisted production of biodiesel from transesterification of palm oil over ostrich eggshell-derived CaO catalysts. **Bioresource Technology**. 171: 428-432.

Dianursanti. Religia, P. and Wijanarko, A. (2015). Utilization of n-hexane as co-solvent to increase biodiesel yield on direct transesterification reaction from marine microalgae. **Procedia Environmental Sciences**. 23: 412-420.

Esipovicha, A., Danova, S., Belousova, A. and Rogozhin, A. (2014). Improving methods of CaO transesterification activity. **Journal of Molecular Catalysis A: Chemical**. 395: 225-233.

Fan, M. M., Huang, J. L., Yang J. and Zhang, P. B. (2013). Biodiesel production by transesterification catalyzed be an efficient choline ionic liquid catalyst. **Applied Energy**. 108: 333-339.

Farooq, M., Ramli, A. and Subbarao, D. (2013). Biodiesel production from waste oil using bifunctional heterogeneous solid catalysts. **Journal of Cleaner Production**. 59: 131-140.

Kim, H. J., Kang, B. S., Kim, M. J., Park, Y. M., Kim, D. K., Lee, J. S. and Lee, K. Y. (2004). Transesterification of vegetable oil to biodiesel using heterogeneous base catalyst. **Catalysis Today**. 93-95: 315-320.

Leclercq, E., Finiels, A. and Moreau, C. (2001). Transesterification of rapeseed oil in the presence of basic zeolites and related solid catalysts. **Journal of the American Oil Chemists' Society**. 78: 1161-1165.

Lee, H. V., Juan, J. C., Abdullah, N. F. B. and Taufiq-Yap, Y. H. (2014). Heterogeneous base catalysts for edible palm and non-edible Jatropha-based biodiesel production. **Chemistry Central Journal**. 8: 1-9.

Lee, S. L., Wong, Y. C., Tan Y. P. and Yew, S. Y. (2015). Transesterification of palm oil to biodiesel by using waste obtuse horn shell-derived CaO catalyst. **Energy Conversion and Management**. 93: 282-288.

Leung, D. Y. C., Wu, X. and Leung, M. K. H. (2010). A review on biodiesel production using catalyzed transesterification. **Applied Energy**. 87: 1083-1095.

Liu, X. J., He, H. Y., Wang, Y. J. and Zhu, S. L. (2007). Transesterification of soybean oil to biodiesel using SrO as a solid base catalyst. **Catalysis Communications**. 8: 1107-1111.

Luu, P. D., Takenaka, N., Luu, B. V., Pham, L. N., Imamura, K. and Maeda, Y. (2014). Co-solvent method produce biodiesel from waste cooking oil with small pilot plant. **Energy Procedia**. 61: 2822-2832.

Luu, P. D., Troung, H. T., Luu, B. V., Pham, L. N., Imamura, K., Takenaka, N. and Maeda, Y. (2014). Production of biodiesel from Vietnamese *Jatropha cuecas* oil by a co-solvent method. **Bioresource Technology**. 173: 309-316.

Mahesh, S. E., Ramanathan, A., Meera, K. M. S. B. and Narayanan, A. (2015). Biodiesel production from waste cooking oil using KBr impregnated CaO as catalyst. **Energy Conversion and Management**. 91: 442-450.

Mcgraw-Hill. (2004). **Perry's Chemical Engineering Handbook**, Seventh Edition, 732-2293.

Mohammed-Dabo, I. A., Ahmad, M. S., Hamza, A., Muazu, K. and Aliyu, A. (2012). Co-solvent transesterification of jatropha curcas seed oil. **Journal of Petroleum Technology and Alternative Fuels**. 3(4): 42-51.

Monteiro, M. R., Ambrozin, A. R. P., Liao, L. M. and Ferreira, A. G. (2009). Determination of biodiesel blend levels in different diesel samples by ^{1}H NMR. **Fuel**. 88: 691-696.

Nakatani, N., Takamori, H., Takeda, K. and Sakugawa, H. (2009). Transesterification of soybean oil using combusted oyster shell waste as a catalyst. **Bioresource Technology**. 100: 1510-1513.

Obadiah, A., Swaroopa, G. A., Kumar, S. V., Jeganathan, K. R. and Ramasubbu, A. (2012). Biodiesel production from Palm oil using calcined waste animal bone as catalyst. **Bioresource Technology**. 116: 512-516.

Reyero, I., Arzamendi, G. and Gandía, L. M. (2014). Heterogenization of the biodiesel synthesis catalysis: CaO and novel calcium compounds as transesterification catalysts. **Chemical Engineering Research and Design**. 92: 1519-1530.

Roschat, W., Kacha, M., Yoosuk, B., Sudyoadsuk, T. and Promarak, V. (2012). Biodiesel production based on heterogeneous process catalyzed by solid waste coral fragment. **Fuel**. 98: 194-202.

Roschat, W., Siritanon, T., Yoosuk, B. and Promarak, V. (2016). Biodiesel production from palm oil using hydrated lime-derived CaO as a low-cost basic heterogeneous catalyst. **Energy Conversion and Management**. 108: 459-467.

Singh, A. K. and Fernando, S. D. (2007). Reaction kinetics of soybean oil transesterification using heterogeneous metal oxide catalysts. **Chemical Engineering & Technology**. 30: 1716-1720.

Soriano, U. N., Venditti, R. and Argyropoulos, S. D. (2009). Biodiesel synthesis via homogenous Lewis-acid-catalyzed transesterification. **Fuel**. 88: 560-565.

Thanh, T. L., Okitsu, K., Sadanga, Y., Takenaka, N., Maeda, Y. and Bandow, H. (2013). A new co-solvent method for the green production of biodiesel fuel-optimization and practical application. **Fuel**. 103: 742-748.

Viriya-empikul, N., Krasae, P., Nualpaeng, W., Yoosuk, B. and Faungnawakij, K. (2012). Biodiesel production over Ca-based solid catalysts derived from industrial wastes. **Fuel**. 92: 239-244.

Vujicic, Dj., Comic, D., Zarubica, A., Micic, R. and Boskovi, G. (2010). Kinetics of biodiesel synthesis from sunflower oil over CaO heterogeneous catalyst. **Fuel**. 89: 2054-2061.

Wang, Y. T., Fang, Z., Zhang, F. and Xue, B. J. (2015). One-step production of biodiesel from oils with high acid value by activated Mg–Al hydrotalcite nanoparticles. **Bioresource Technology**. 193: 84-89.

Wei, Z., Xu, C. and Li, B. (2009). Application of waste eggshell as low-cost solid catalyst for biodiesel production. **Bioresource Technology**. 101: 2883-2885.

Yoosuk, B., Udomsap, P., Puttasawat, B. and Krasae, P. (2010). Modification of calcite by hydration–dehydration method for heterogeneous biodiesel production process: The effects of water on properties and activity. **Chemical Engineering Journal**. 162: 135-41.

Zhang, L., Sheng, B., Xin, Z., Liu, Q. and Sun, S. (2010). Kinetics of transesterification of palm oil and dimethyl carbonate for biodiesel production at the catalysis of heterogeneous base catalyst. **Bioresource Technology**. 101: 8144-8150.

CHAPTER VI

RICE HUSK-DERIVED SODIUM SILICATE AS A HIGHLY EFFICIENT AND LOW-COST BASIC HETEROGENEOUS CATALYST FOR BIODIESEL PRODUCTION

6.1 Graphical abstract
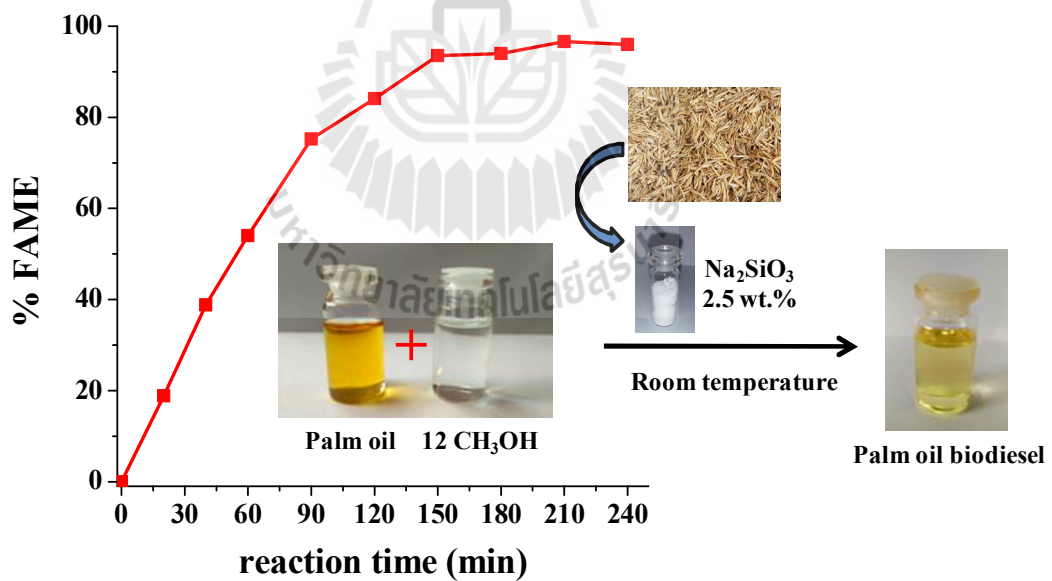
Rice husk-derived sodium silicate exhibits high potential as a low-cost solid catalyst for industrial biodiesel production.

6.2 Highlights

- Rice husk-derived sodium silicate was employed as high performance catalyst for transesterification of many kinds of oils to biodiesel.

- 97% yield of FAME was achieved in 30 min under heating at 65 °C.

- The room-temperature transesterification gave 94% yield of FAME after only 150 min.

- The kinetic of transesterification reaction of palm oil was investigated.

6.3 Abstract

In the present work, rice husk-derived sodium silicate (Na_2SiO_3) was prepared and employed as a solid catalyst for simple conversion of oils to biodiesel via the transesterification reaction. The catalyst was characterized by TG-DTA, XRD, XRF FT-IR, SEM, BET and Hammett indicator method. Under the optimal reaction conditions of catalyst loading amount of 2.5 wt.%, methanol/oil molar ratio of 12:1, the prepared catalysts gave 97% FAME yield in 30 min at 65 °C, and 94% FAME yield in 150 min at room temperature. The transesterification was proved to be pseudo-first order reaction with the activation energy (*Ea*) and the frequency factor (*A*) of 48.30 kJ/mol and 2.775×10^6 min^{-1} respectively. Purification with a cation-exchange resin efficiently removed all soluble ions providing high-quality biodiesel product that meets all the ASTM and EN standard specifications. Rice husk-derived sodium silicate showed high potential to be used as a low-cost, easy to prepare and high performance solid catalyst for synthesis of biodiesel.

6.4 Introduction

As issues relating to energy and environment are of main concern in the past decades, researches on alternative and sustainable energy have gained considerable interest. Biodiesel (fatty acid methyl ester, FAME) is one of good candidate for replacing petrol-diesel fuel because it can be used in any diesel-engine without modification (Onoji et al., 2016; Roschat et al., 2012; Lee et al., 2015). It is also clean, renewable, biodegradable, environmentally friendly and inexpensive (Huang et al., 2015; Chen et al., 2014). Generally, biodiesel can be produced via a direct transesterification reaction of vegetable oils or animal fats and alcohols in the presence of a catalyst (Chen 2014; Xie and Zhao, 2014; Sirisomboonchai et al., 2015). Commonly, KOH, NaOH and CH_3ONa are widely used as a homogeneous basic catalyst because they have high catalytic activity which can complete the reaction in 1 hour under mild condition at 40-60 °C (Tubino; 2016). Nevertheless, the use of these catalysts still involves many problems such as difficult catalyst separation, soap formation and reactor corrosion. In addition, large amount of water is usually required to wash the biodiesel product to eliminate the catalyst which leads to the increases in the overall production cost and the environment problems (Lee et al., 2015).

On the other hand, heterogeneous catalysts can be easily separated through filtration, reused and recycled several times and require no neutralization or washing process. In addition they can also produce a high purity glycerol by-product. Hence, heterogeneous-catalyst is an efficient and more cost-effective tool to produce biodiesel (Xie and Zhao, 2014; Taufiq-Yap et al., 2014; Sanchez et al., 2015). There are several reports on biodiesel production using heterogeneous catalysts such as Mo-Mn/γ-Al_2O_3-MgO (Farooq et al., 2013), KOH/bentonite (Soetaredjo et al., 2011),

Li_4SiO_4 (Dai et al., 2014; Wang et al., 2012), $LiAlO_2$ (Dai et al., 2015) and CaO-La_2O_3 (Mahesh et al., 2015). However, some of these catalysts still have to be developed because they show low catalytic activity, complicate to generate and absorb CO_2 and H_2O in air easily.

Calcium oxide (CaO) is one of the most studied catalyst materials as it has lower price, non-toxicity, less solubility in methanol and high catalytic activity. They can be prepared from natural waste obtuse horn (Lee et al., 2015), waste coral fragment (Roschat et al., 2012), hydrated lime (Roschat et al., 2016), ostrich eggshells (Chen et al., 2014)], waste oyster shells (Nakatani et al., 2009), chicken bones (Farooq et al., 2005), waste shells of egg, golden apple snail shells, and meretrix venus shells (Viriya-empikul et al., 2012). Although CaO catalysts offer many advantages, in some case, the catalyzed reactions still require long reaction times (at least 3 to 8 hours) which increased the production cost.

Sodium silicate (Na_2SiO_3) with formula $Na_2O \cdot nSiO_2$ is a well-known water-glass or liquid glass which can be easily prepared from SiO_2 and NaOH (Halasz et al., 2007; Arantes et al., 2013). Sodium silicate was also used as a starting reactant to synthesize mesoporous silica material (Yun-ym et al., 2012), *n*-alkane/silica composite phase (He et al., 2015) and β-zeolite (Selvam et al., 2003). Recently, several articles report the use of calcined sodium silicate as a solid basic catalyst in the transesterification of vegetable oil (soybean oil, rapeseed oil and jatropha oil) with methanol. Sodium silicate is an effective catalyst for transesterification under mild reaction condition and short reaction time (60 min at 60 °C). Furthermore, the catalyst can be reused for at least 5 times without loss of activity (Guo et al., 2010; Long et al., 2011; Guo et al., 2012; Kouzu et al., 2009).

An important focus of this work is to present a simplified way to synthesize sodium silicate from rice husk which is scrap from agricultural and to use the obtained as a low-cost basic heterogeneous catalyst in biodiesel production. The rice husk-derived sodium silicate were characterized and tested in the production of biodiesel using oils and methanol. Several parameters, such as catalyst amount, methanol/oil molar ratio, reaction temperature, type of oil and free fatty acid (FFAs) quantity and reusability are investigated. Fuel properties of the obtained biodiesel after purification and treatment process are evaluated by American Society for Testing and Material (ASTM) methods and European Standard methods (EN14214) for bio-auto fuels. In addition, reaction kinetics of transesterification using sodium silicate obtained from rice husk was investigated and compared with CaO catalysts.

6.5 Materials and methods

6.5.1 Materials

Many kinds of oils containing various amounts of FFAs including palm oil (acid value of 0.32 mg KOH/g oil), lard oil (acid value of 0.42 mg KOH/g oil), coconut oil (acid value of 0.28 mg KOH/g oil), sunflower oil (acid value of 0.20 mg KOH/g oil), soybean oil (acid value of 0.27 mg KOH/g oil), rice bran oil (acid value of 0.18 mg KOH/g oil), jatropha oil (acid value of 1.31 mg KOH/g oil) and waste cooking oil (acid value of 2.31 mg KOH/g oil) were obtained from commercial sources in Thailand and were used without any purification. The analytical grade methanol, Hammett indicators (phenolphthalein, thymolphthalein, indigo carmine, 2,4-dinitroaniline and 4-nitroaniline) and sodium hydroxide (NaOH) were purchased from Fluka and Sigma-Aldrich Chemical. Calcium oxide (analytical grade CaO_AR) was

purchased from Acros Chemical Co.Ltd. Rice husk collected from a local rice mill was washed with deionized water and dried at 110 °C overnight before uses.

6.5.2 Catalyst preparation and characterization

Figure 1 shows a flow diagram of the sodium silicate preparation. The dried rice husk was digested by reflux method using 1 M HCl at 100 °C for 3 h and then washed with water several times and dried at 110 °C overnight. After that, white rice husk ash (RHA) was obtained by calcining the digested rice husk at 700 °C for 3 h to remove organic contains (Kongmanklang and Rangsriwatananon, 2015). Next, 10 g of the obtained RHA and 100 mL of 1 M NaOH were mixed and boiled in a covered 250 mL Erlenmeyer flask for 1 h with constant stirring. After that, the resulting solution was dried in an oven at 110 °C for 6 h. Finally, the resulting materials were calcined in a furnace at designated temperature in air for 1 h.

Both the uncalcined and calcined materials were analyzed by X-ray powder diffraction (XRD) using a Bruker D5005 X-ray diffractometer with Cu Kα radiation (k = 1.5418 Å). Elemental compositions of the sample were analyzed by a PHILIPS Magi X wavelength dispersive X-ray Fluorescence (XRF) spectrophotometer with 1 kW Rh Kα radiation. Scanning electron microscopy (SEM) was performed on JEOL JSM 5410LV scanning electron microscope at an accelerated voltage of 20 kV. Brunauer Emmett Teller (BET) was employed on a Bel-sorp-mini II (Bel-Japan) to investigate surface area and pore volume.

The samples were characterized by Fourier transform infrared (FT-IR) spectroscopy with Perkin-Elmer FT-IR spectroscopy spectrum RXI spectrometer in the range of 450-4000 cm^{-1} with resolution of 4 cm^{-1} and potassium bromide (KBr)

was used as a matrix. Hammett indicator method was applied to test the basic strength by the following indicators with different acidity functions ($H\_$); phenolphthaleine ($H\_ = 9.8$), indigo carmine ($H\_ = 12.2$), 2,4-dinitroaniline ($H\_ = 15.0$) and 4-nitroaniline ($H\_ = 18.4$).

Rice husk

Digest with 1 M HCl
at 100 °C for 3 h

Digested rice husk

Calcine

Rice husk ash (RHA)

Mix with 1 M NaOH
and boil for 1 h

Resulting solution

Dry and calcine at
designated temperature
for 1 h

Sodium silicate (Na₂SiO₃)
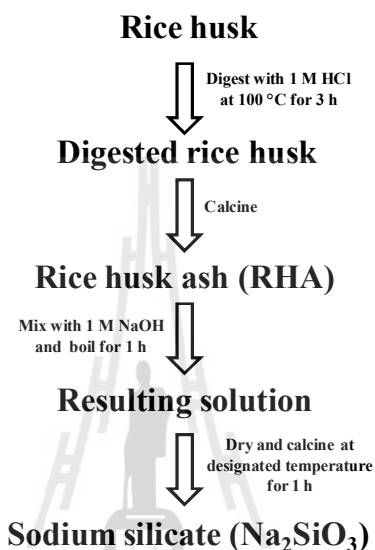
Figure 6.1 Flow diagram of the sodium silicate preparation.

6.5.3 Catalytic tests and product analysis

The transesterification was carried out in a three-neck round bottom batch reactor equipped with a reflux condenser, a magnetic stirrer (300 rpm) and a thermocouple. Palm oil was used as starting material to optimize reaction condition. A mixture of solid catalyst and methanol were preheated at designated temperature (55, 60, 65 and 70 °C) and added to 30 mL of oil. The transesterification reaction was performed with various catalysts loading amount (0-5.0 wt.% relative to oil weight)and methanol to oil molar ratios (3:1-11:1).

To follow the reaction progress, 0.5 mL of solution mixture was sampled and heated an oven at 80 °C for 3 h to remove excess methanol before biodiesel yield

analysis. Proton nuclear magnetic resonance (^{1}H NMR) on a Brüker Ascend^{TM} 500 MHz spectrometer was employed to evaluate biodiesel yield in term of the fatty acid methyl ester yield (%FAME). Tetramethylsilane (TMS) and CDCl$_3$ were used as the internal reference and a solvent, respectively (Roschat et al., 2012; Roschat et al., 2016). The amount of sodium ion leached from the catalyst in the obtained biodiesel was analyzed by atomic absorption spectrophotometry (AAS) (Roschat et al., 2012; Long et al., 2014).

The obtained biodiesel product was filtrated to separate catalyst, heated to remove excess methanol and treated with commercially available cation-exchange resins (Dowex® 50WX8) to eliminate sodium ion (Roschat et al., 2016). The treated biodiesel were tested by American Society for Testing and Material (ASTM D6751) methods and European Standard methods (EN14214) for bio-auto fuels (Yoosuk et al., 2010; Chen et al., 2014; Mathimani et al., 2015; Abedin et al., 2016).

6.6 Results and discussion

6.6.1 Catalyst characterization

Thermogravimetric analysis was used to determine the optimum calcination temperature of the digested rice husk to prepare RHA. As seen from Figure 6.2, the weight loss occurred in the range of 30-400 °C which indicated the removal of moisture and organic compounds such as cellulose, hemicelluloses and lignin. Based on TGA results, temperature at 700 °C was chosen for calcining the digested rice husk to produce RHA (Kongmanklang and Rangsriwatananon, 2015).

After boiled and dried, the mixture of RHA and NaOH was analyzed by TG-DTA as shown in Figure 6.3(a). There was only one major weight loss at below 200

°C which water molecules removal. Therefore, the temperature of 200, 300, 400, and 500 °C were selected to optimize the calcining temperature. As depicted in Figure 6.3(b), the XRD pattern of RHA shows amorphous phase with a broad curve. On the other hand, mixture of RHA and NaOH transformed to sodium silicate after calcination as their XRD patterns exhibit the characteristic peaks of Na_2SiO_3 crystalline phase (PDF 00-016-0818). Similar results were also reported by Guo et al. (Guo et al., 2010).
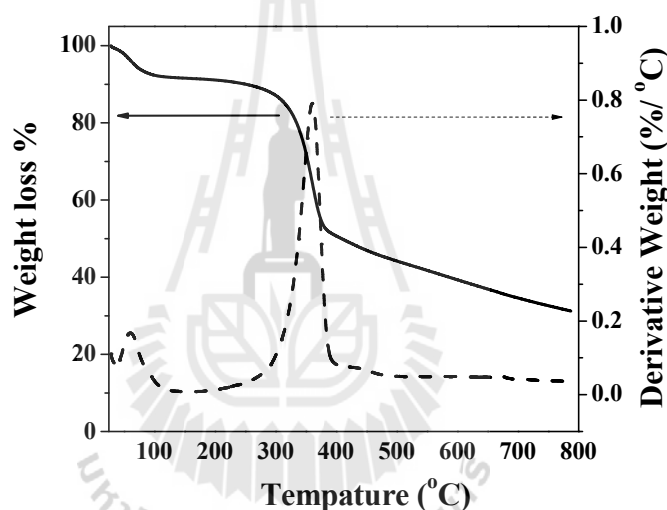
Figure 6.2 TG/DTA curve of the digested rice husk with 1 M HCl at 100 °C for 3 h.

The samples were analyzed by FT-IR spectroscopy as depicted in Figure 6.3(c). The spectra of all the calcined samples showed strong broad absorption bands at 999 cm^{-1} and 884 cm^{-1} corresponding to the stretching vibrations of Si–O and Si–O–Si, respectively. In addition, the absorption peaks at 510 cm^{-1}, 710 cm^{-1} and 1465 cm^{-1} were assigned to Si–O bending, Si–O–Si bending and Si=O stretching vibrations, respectively. These vibrations indicated the presence of Si-O-Si linking structure thus confirmed the formation of sodium silicate (Guo et al., 2010; Guo et al., 2012).

In addition, broad peaks at 3000-3600 cm^{-1} were attributed to Si–O–H stretching vibrations caused by the absorbed water molecules the surface. The surface morphology of sodium silicate calcined at 300 °C was studied by SEM as depicted in Figure 6.3(d) which illustrates agglomerated and large particles size of few microns.
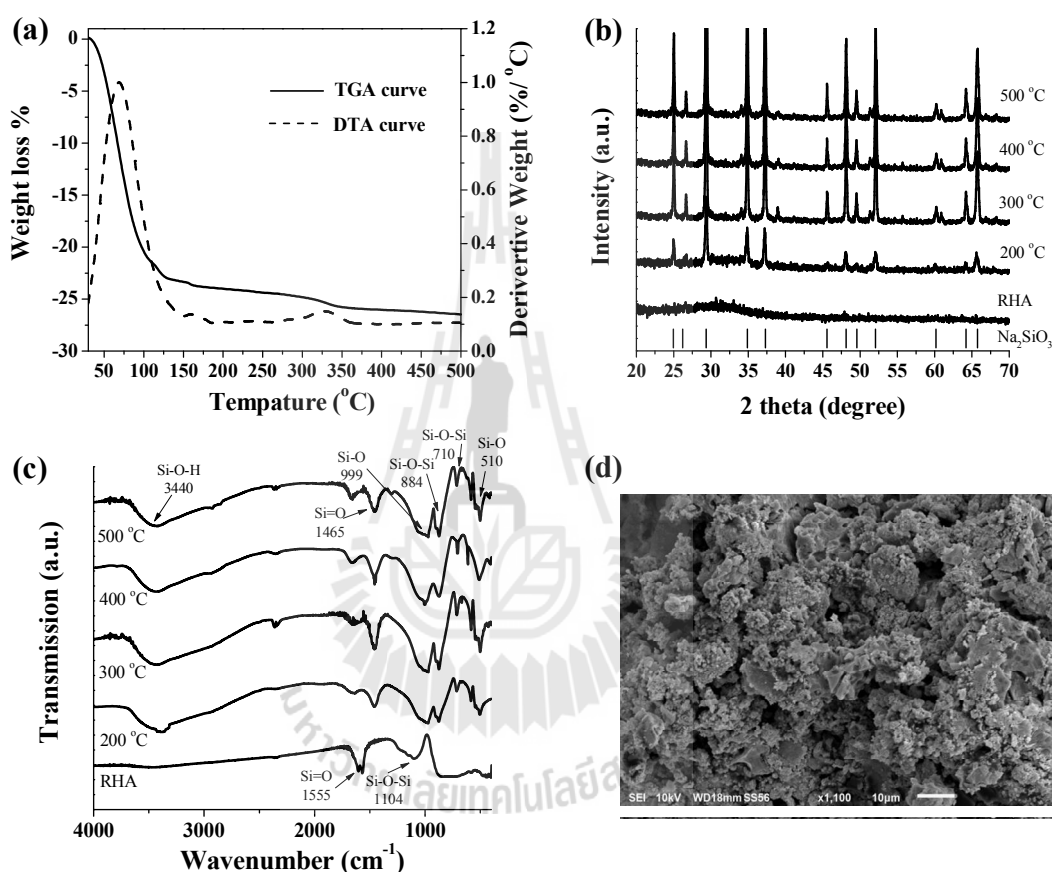
Figure 6.3 (a) TG/DTA curves of the resulting materials obtained from mixing and boiling the mixture of RHA and NaOH solution. (b) XRD patterns and (c) IR spectra of RHA and calcined the samples. (d) SEM image of the sodium silicate obtained from calcining the mixture of RHA and NaOH solution at 300 °C for 1 h.

The N$_2$ adsorption-desorption isotherm of all sodium silicate samples derived from rice husk are displayed in Figure 6.4(a-d). The adsorption-desorption of all

samples is a typical type II pattern which is a characteristic of a nonporous or macroporous material based on IUPAC's classification (Khemthong et al., 2012). The large particles of about few microns as seen from SEM image, the low BET surface area and the low pore volume (Table 1) are all consistent with this classification as well.
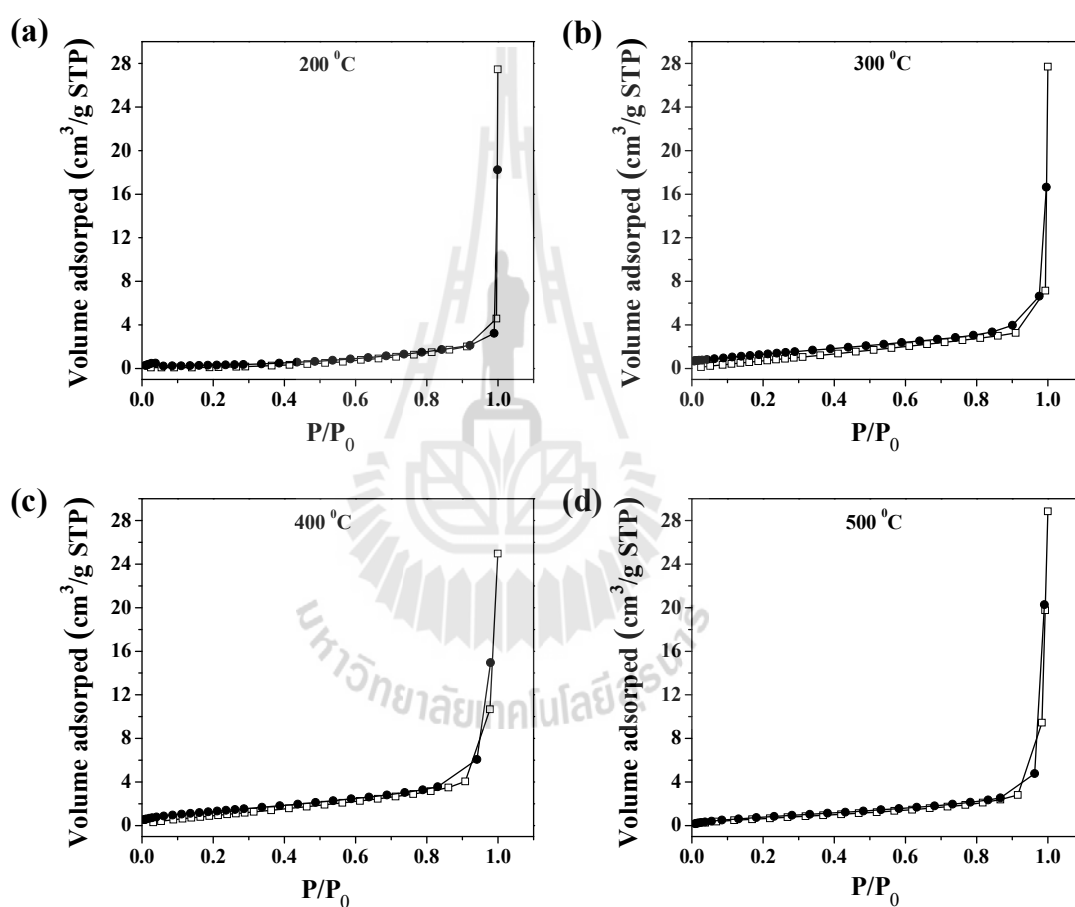
Figure 6.4 N_2 adsorption/desorption plots of sodium silicate derived from rice husk with different calcining temperatures of (a) 200 °C, (b) 300 °C, (c) 400 °C and (d) 500 °C.

Table 6.1 Physicochemical properties of sodium silicate derived from rice husk calcined at different temperatures.

Sample	BET surface area (m²/g)	Pore volume (cm³/g)	Basic strength ($H\_$)	Elemental composition (%)				
				SiO_2	Na_2O	Al_2O_3	MgO	other
Calcined at 200 °C	1.31	2.08	$15.0 < H\_ < 18.4$	68.98	30.07	0.21	0.11	0.63
Calcined at 300 °C	1.14	1.39	$15.0 < H\_ < 18.4$	68.96	30.10	0.22	0.12	0.60
Calcined at 400 °C	1.05	1.65	$15.0 < H\_ < 18.4$	69.04	29.97	0.19	0.09	0.71
Calcined at 500 °C	0.95	1.30	$15.0 < H\_ < 18.4$	69.05	30.01	0.19	0.09	0.66

The BET surface area of all samples was very similar. Nevertheless, the slight difference can be observed as higher calcining temperature resulted in a slightly lower surface area. Such difference is to be expected because at high temperature atoms in the small particles could diffuse to the boundary and fuse the particles together forming larger particles. Similar results were observed in report of Lee et al. (Lee et al., 2015). Although, all sodium silicate samples obtained from rice husk displayed low surface area, they show high basic strength as measured by Hammett indicator method which demonstrated $H\_$ values in the range of 15.0-18.4 as evidenced by its coloration with 2,4-dinitroaniline (pKa = 15) but not with 4-nitroaniline ($H\_$ = 18.4). In the basic catalyzed conditions, the reaction starts by active site removed a proton (H^+) from the methanol generating methoxide anion (CH_3O^-) as a highly reactive nucleophilic species and the nucleophilic CH_3O^- subsequently attacks electrophilic carbonyl carbon in triglyceride to give biodiesel product and glycerol by-product. Hence, the high basic strength is strongly correlated to the catalytic activity of catalysts as catalysts with higher basic strength usually give higher biodiesel yield (Huang et al., 2015). Elemental analysis of all calcined samples with XRF spectroscopy indicated that they were composed of mainly SiO_2 and Na_2O with approximately 1% of other elements as shown in Table 6.1.

6.6.2 Optimization of reaction conditions

6.6.2.1 Effects of calcining temperature of catalyst

The effects of calcination temperature of rice husk-derived sodium silicate on the catalytic activity was evaluated. As shown in Figure 6.5(a), FAME yield was only 84.39% when the sample was calcined at 200 °C. This may be due to

an incomplete conversion of the sample to sodium silicate crystalline phase as indicated by the low-intensity peaks in XRD pattern (Figure 6.1(b)). XRD patterns of the sample calcined at 300, 400 and 500 °C exhibit clear and sharp peaks, indicating more crystallinity. As a consequence, biodiesel yield was significantly increased to 98.04% when calcining temperature of the sample was increased from 200 to 300 °C. However, a further increase in calcining temperature resulted in a slightly decreased %FAME yield under the same reaction conditions. This reduction of %FAME yield was caused by the sintering effect during calcination which resulted in the lowering of surface area (Table 6.1). As a result, the optimal calcining temperature to synthesize sodium silicate catalysts from rice husk was 300 °C.

6.6.2.2 Effects of catalyst amount

The effects of catalyst loading amount on conversion of palm oil to biodiesel were studied and displayed in Figure 6.5(b). In transesterification mechanism, the basic sites of sodium silicate generate much more reactive nucleophile (methoxide anion) from methanol which will react with electrophilic carbonyl carbon of triglyceride to produce biodiesel. Therefore, as the amount of catalyst increases, active basic site will generally increase and the biodiesel product is enhanced (Lee et al., 2015; Farooq et al., 2005). As a result, the biodiesel yield increased from 49.37% to 97.80% when the catalyst content was increased from 0.5 wt.% to 2.5 wt.%. However, beyond 2.5 wt.% of catalyst loading amount, the biodiesel yield did not increase due to the limitation of mass transfer and the high viscosity of the reaction mixture, both of which, lead to the problem of mixing each

reactant component (Dai et al., 2015; Mahesh et al., 2015). Thus, 2.5 wt.% catalyst loading content was used to optimize transesterification condition in this study.

6.6.2.3 Effects of methanol to oil molar ratio

The effects of methanol to oil molar ratio on the biodiesel yield were investigated. As illustrated in Figure 6.5(c), the %FAME yield gradually increased as the molar ratio of methanol to palm oil increased from 6:1 to 12:1. Further increase in the methanol to oil molar ratio beyond 12:1, slightly decreased the conversion of palm oil to biodiesel. At high methanol to oil molar ratio, the glycerol by-product would dissolve in the excessive methanol and impede the reaction of methanol with oil and catalyst. Additionally, the polar hydroxyl group in methanol behaves as emulsifier which makes it more difficult to separation biodiesel product from the mixture resulting in the %FAME yield (Mahesh et al., 2015; Guo et al., 2010; Chen et al., 2015). In this case, the optimum methanol to oil molar ratio was, therefore, 12:1, which was 4 times more than the required stoichiometric molar ratio (3:1).

6.6.2.4 Effects of reaction temperature

Reaction temperature is one of the most important parameters which directly influence both the reaction rate and yield. In this work, effects of reaction temperature were examined by varying from 45 °C to 75 °C with constant reaction time (30 min). As presented in Figure 6.5(d), %FAME yield was increased from 42.32% to 96.15% when reaction temperature increased from 45°C to 65 °C. Further increase the temperature to over 65 °C which is above the boiling point of methanol (64.7 °C at 1 atm) resulted in the slightly decreased biodiesel yield as the evaporated

methanol inhibited the reaction on the three-phase interfaces namely liquid phase (palm oil), gas phase (methanol) and solid phase (catalysts) (Tan et al., 2015; Moushoul et al., 2016).
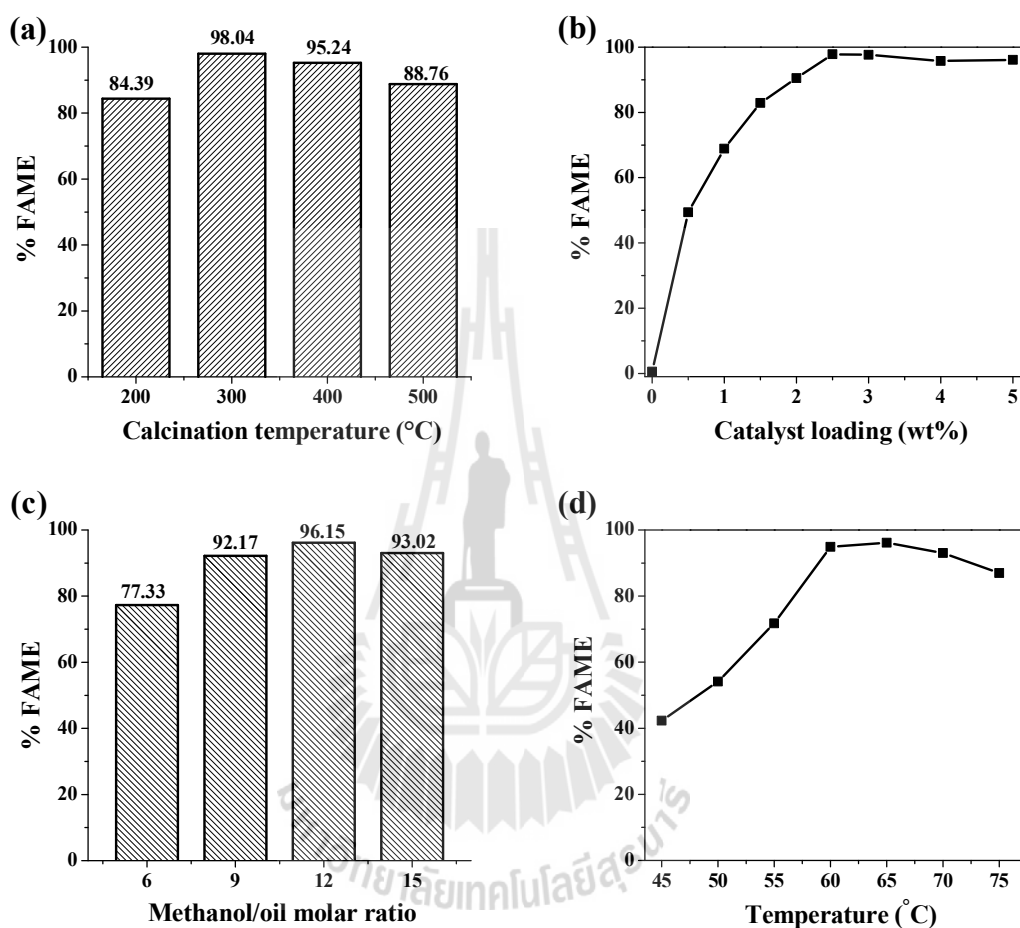
Figure 6.5 Effect of reaction conditions on %FAME yield. (a) Calcination temperature of catalyst (catalyst loading 2 wt.%, methanol/oil molar ratio of 9:1, 60 °C and reaction time of 30 min). (b) Catalyst loading amount (calcined the catalyst at 300 °C, methanol/oil molar ratio of 9:1, 60 °C and reaction time of 30 min). (c) Methanol to oil molar ratio (calcined the catalyst at 300 °C, catalyst loading 2.5 wt.%, 60 °C and reaction time of 30 min). (d) Reaction temperature (calcined the catalyst at 300 °C, catalyst loading 2.5 wt.%, methanol/oil molar ratio of 12:1 and reaction time of 30 min).

6.6.3 Effects of oil type

Free fatty acid (FFAs) value (mg KOH/g oil) in the oil has a significant effect on the biodiesel yield during transesterification reaction because high FFAs content causes soap formation which reduces catalyst activity (Guo et al., 2010; Chen et al., 2015; Fadhil et al., 2016). Many kinds of oils containing various amounts of FFAs namely palm oil, rice bran oil, coconut oil, lard oil, soybean oil, sunflower oil, jatropha oil and waste cooking oil were used to investigate the effects of FFAs on the biodiesel yield as seen in Figure 6.6. The results showed that type of oils did not have any effects on the FAME yield in this case as they all contain only small amount of FFAs content. In all cases, the FAME yields was maintained at over 93% even for jatropha and waste cooking oil which have the highest FFAs.

Type of oil	Acid value (mg KOH/g oil)
rice bran	0.18
sunflower	0.20
soybean	0.27
coconut	0.28
palm	0.32
lard	0.42
waste cooking	2.31
jatropha	1.31
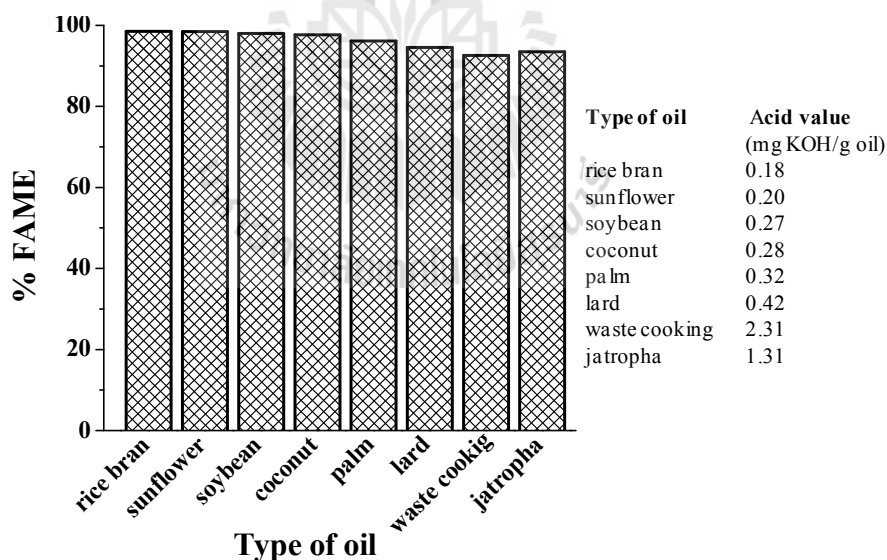
Figure 6.6 Effects of type of oils on the %FAME (calcined the catalyst at 300 °C, catalyst loading 2.5 wt.%, methanol/oil molar ratio of 12:1, 65 °C and 30 min).

6.6.4 Reusability of the catalysts

The reusability (without cleaning process) of rice husk-derived sodium silicate catalyst was investigated using the optimized condition. As illustrated in Figure 6.7, %FAME yield was still higher than 93% when the catalysts were reused for four times and the value decreased to 83% yield after the fifth time. The possible reason for the loss of catalytic activity was the leaching of active species (Shan et al., 2015; Syazwani et al., 2015).
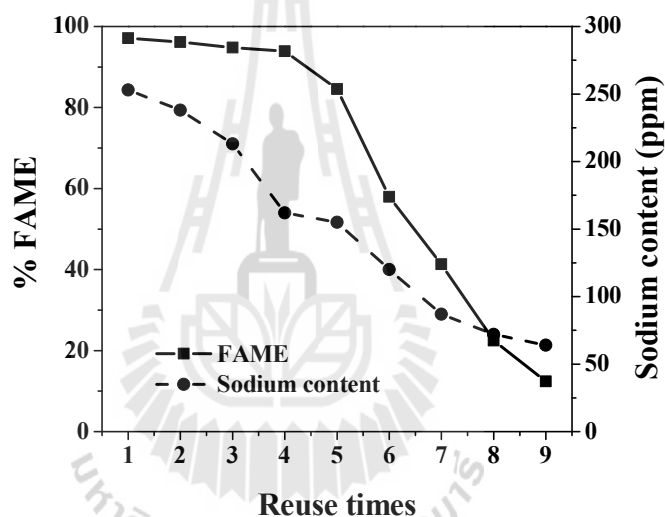
Figure 6.7 Effects of reuse of the catalyst on the %FAME and analysis amount of Na ion leaching content in biodiesel product (calcined the catalyst at 300 °C, catalyst loading 2.5 wt.%, methanol/oil molar ratio of 12:1, 65 °C and reaction time of 30 min).

In this case, the AAS analysis was used to evaluate the leached sodium (Na) ions (Figure 6.7). It is obvious from Figure 6.7 that Na ion was leached to the reaction mixture. The leaching decreased with reusing times but continue to occur. Although the catalysts remained active with some leaching in the first four runs, the activity

decreased after five times. It is believed that the catalysts were able to function with some degree of Na loss but when Na continued to leach, the catalysts will eventually deactivated.

Figure 6.8(a) compares XRD profiles of fresh catalysts and catalysts that have been used for 9 times. The sharpness of diffraction peaks is lower in the used catalysts indicating loss of crystalline phases during the reaction possibly due to Na leaching. In addition, FT-IR spectra in Figure 6.8(b) support the structure change of sodium silicate by showing absorption bands at 710 cm^{-1} and 884 cm^{-1} with lower intensity, relating to lower number of Si–O–Si bonds. In contrast, absorption bands at 999 cm^{-1} and 1465 cm^{-1} which correspond to Si–O bending and Si=O stretching vibrations have increased intensity, confirming that some Si–O–Si bonds were broken down during the reusing processes of the catalysts (Guo et al., 2010; Guo et al., 2012). Furthermore, the broader absorption band at 3440 cm^{-1} (Si–O–H stretching) in the used catalysts indicates that sodium silicate catalyst reacted with water molecules in the reactants (palm oil and methanol) which is to be expected as the reaction was carried out in an open air. In addition, liquid compounds in the reaction mixture namely palm oil, biodiesel, glycerol and methanol may cover the surface of the catalysts (Lee et al., 2015; Roschat et al., 2016).

Although leaching of Na ions from the catalysts seem to be the major cause of efficiency reduction of the catalysts in the transesterification reaction, the catalysts could be regenerated just by reaction with NaOH. Guo et al. (Guo et al., 2012) presented that the first, second and third time regenerated catalysts still performed excellently to give biodiesel yield over 96.5%. Hence, the possibility of using rice husk-derived sodium silicate as a high potential, low-cost and renewable catalysts.
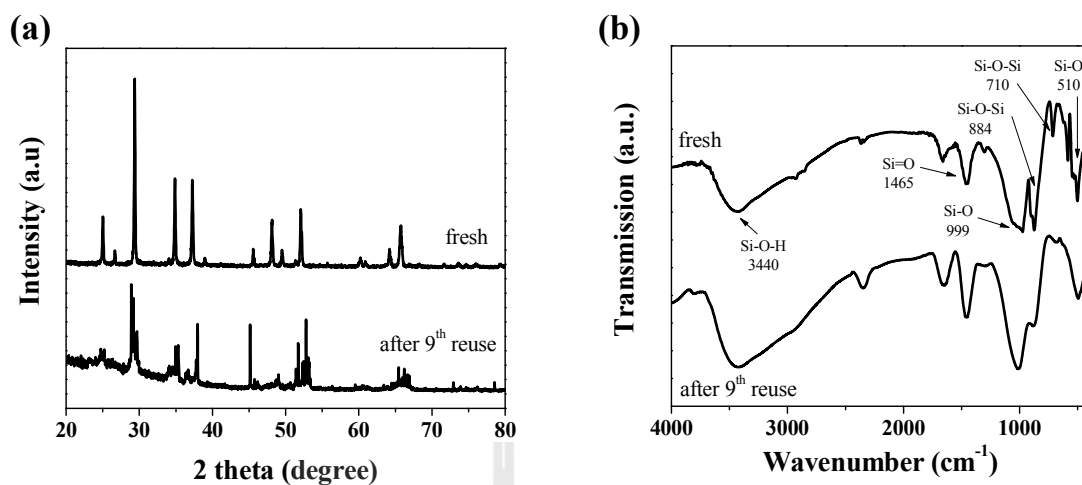
Figure 6.8 (a) XRD patterns and (b) IR spectra of rice husk-derived sodium silicate catalyst after 9th reuse compared with fresh the catalyst.

6.6.5 Catalytic activity comparison of rice husk-derived sodium silicate, CaO and NaOH

Figure 6.9 shows comparison of catalytic performance of rice husk-derived sodium silicate, CaO analytical grade (AR), CaO derived from eggshell (heterogeneous catalyst) and NaOH (homogeneous catalyst) under optimized reaction conditions. The results showed that FAME yield reached 96% within 15 min when NaOH catalyst was used, while the reaction catalyzed by rice husk-derived sodium silicate showed FAME yield of 97% after 30 min. For the reaction catalyzed by CaO both analytical grade (AR) and derived from eggshell, FAME yield reached about 96% after 180 min. In this research, it was found that the catalytic performance for conversion of palm oil to biodiesel was in the order of NaOH > sodium silicate > CaO. It is generally known that homogeneous basic catalysts especially NaOH and KOH exhibit higher catalytic activity than heterogeneous basic catalyst (Chen et al., 2015; Luu et al., 2014; Alhassan et al., 2014).
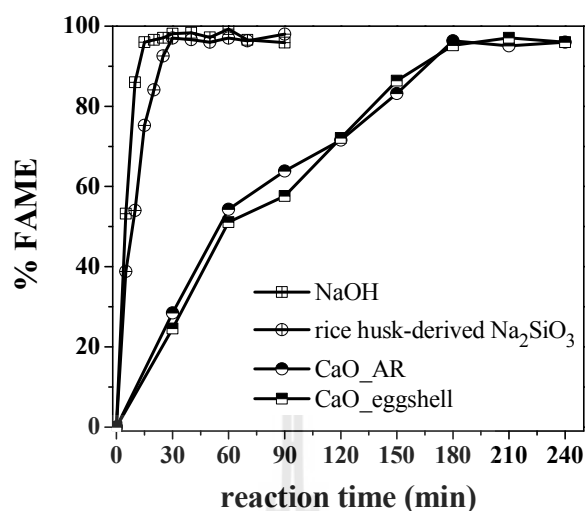
Figure 6.9 Comparison of catalytic efficiency of rice husk-derived sodium silicate against CaO and NaOH. Reaction condition of rice husk-derived sodium silicate: calcined the catalyst at 300 °C, catalyst loading 2.5 wt.%, methanol/oil molar ratio of 12:1 and 65 °C. Reaction condition of CaO_AR and CaO_eggshell as calcined the catalyst at 800 °C for 3 h (Viriya-empikul et al., 2012): catalyst loading 6 wt.%, methanol/oil molar ratio of 15:1 and 65 °C (Roschat et al., 2016). Reaction condition of NaOH: catalyst loading 0.75 wt.%, methanol/oil molar ratio of 6:1 and 60 °C (Alhassan et al., 2014).

Although both are heterogeneous catalyst, the catalytic activity of sodium silicate was significantly higher than that of CaO. Similar results were also reported by Guo et al. (Guo et al., 2010). In both sodium silicate and CaO case, the same active specie, CH_3O^-, is generated but the mechanism of the generation is different. Sodium silicate generates CH_3O^- by exchanging its Na^+ ion with H^+ of methanol while O^{2-} on CaO surface extracts H^+ from H_2O to form OH^- which then extracts H^+ from methanol to form CH_3O^-. The difference in mechanism is most likely the reason of the different

activity. In addition, Guo et al. (Guo et al., 2012) also reported that CaO may easily be packed by the glycerol by-product which inhibited $CH3O^-$ generation by interrupting the contact between methanol and basic sites of CaO.

In addition, the room-temperature transesterification reaction of palm oil catalyzed by rice husk-derived sodium silicate and NaOH catalysts were investigated as shown in Figure 6.10. It was clear that biodiesel yield reached 96% after 90 min (1.5 h) for reaction catalyzed by NaOH, while the reaction catalyzed by rice husk-derived sodium silicate gave 94 %FAME yield after 150 min (2.5 h).
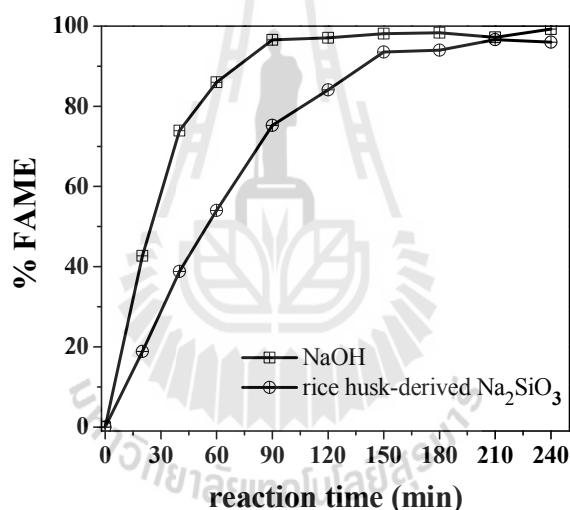
Figure 6.10 Comparison of catalytic performance between rice husk-derived sodium silicate and NaOH under room temperature conditions. Reaction condition of rice husk-derived sodium silicate: calcined the catalyst at 300 °C, catalyst loading 2.5 wt.%, methanol/oil molar ratio of 12:1. Reaction condition of NaOH: catalyst loading 0.75 wt.% and methanol/oil molar ratio of 6:1 (Alhassan et al., 2014).

Reducing production temperature and time means reducing the production cost. Generally, the use of heterogeneous catalyst such CaO (Roschat et al., 2012;

Sirisomboonchai et al., 2015; Viriya-empikul et al., 2012), KOH/bentonite (Soetaredjo et al., 2011), $LiAlO_2$ (Dai et al., 2015), CaO-based/Au (Moushoul et al., 2016), naturaldolomites (Nur et al., 2014) and $MgO–Li_2O$ (Lu et al., 2016) to produce biodiesel were performed at higher temperature (60-65 °C) and longer reaction time (2-6 h). Hence, it is also more cost-effective to apply rice husk-derived sodium silicate as a catalyst for biodiesel production at room temperature.

6.6.6 Kinetics of transesterification reaction catalyzed by rice husk-derived sodium silicate

To determine the kinetics of transesterification reaction, the effects of reaction temperature and time were investigated. To simplify the kinetic modeling, the reaction could be assumed pseudo-first order and the reaction rate can be explained by Eq. (6.1). In this case, excess methanol was used to shift the reaction equilibrium towards the product thus the reverse reduction is insignificant and will not be taken into account (Roschat et al., 2016; Birla et al., 2012; Maneerung et al., 2015).

$$r = -\frac{d[TG]}{dt} = k[TG] \tag{6.1}$$

r is the transesterification reaction rate and k is the rate constant ($k = k'[ROH]^3$). [TG] and t are triglyceride concentration and reaction time, respectively. Integrating and rearranging Eq. 6.1 from t = 0, [TG] = $[TG]_0$ till t = t, $[TG]_0 = [TG]_t$ gives Eq. 6.2:

$$\ln[TG]_0 - \ln[TG]_t = kt \tag{6.2}$$

$\ln[TG]_0$ is initial concentration of triglyceride which is assumed to be 1 M, thus $\ln[TG]_0 = 0$. While $[TG]_t$ is related to %FAME yield by $[TG]_t = 1 - x_{ME}$ where x_{ME} is $(\frac{\%FAME}{100})$. Substituting $[TG]_t$ in Eq. 6.2 gives Eq. 6.3:

$$-\ln[1 - x_{ME}] = k \cdot t \tag{6.3}$$

By fitting the experimental data to Eq. 6.3, the slope is equal to rate constant (k) which depends on reaction temperature. The Arrhenius plot of lnk versus 1/T in Eq. 6.4 can be used to calculate the activation energy (*Ea*) and frequency factor (*A*) for the transesterification reaction.

$$\ln k = -\frac{Ea}{R} \times \frac{1}{T} + \ln A \tag{6.4}$$

R is the gas constant (8.314 $Jmol^{-1}K^{-1}$) and T is the reaction temperature (K) (Maneerung et al., 2015).

Figure 6.11 compares rate constant (k) of reaction between using rice husk-derived sodium silicate with CaO_AR catalyst that obtained from under the optimized reaction condition. The rate constant of reaction catalyzed by rice husk-derived sodium silicate (7.49×10^{-2} min^{-1}) is 6 times higher than CaO_AR (1.28×10^{-2} min^{-1}).
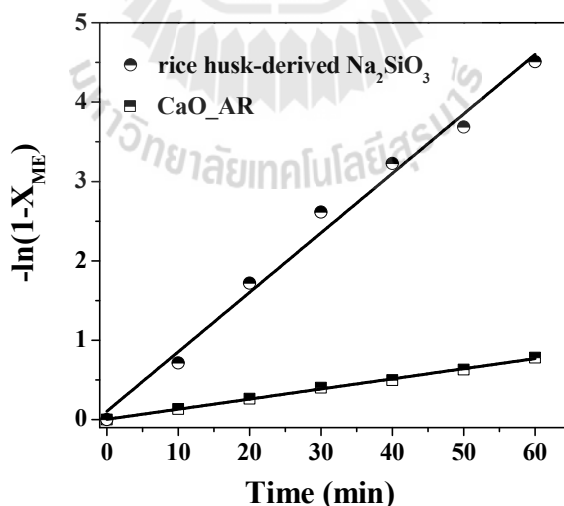
Figure 6.11 Comparison of kinetics study between using rice hush-derived sodium silicate and CaO_AR catalyst under the same reaction condition (reaction condition: catalyst loading 2.5 wt.%, methanol/oil molar ratio of 12:1 and 65 °C).

Figure 6.12(a) shows rate constant (k) of reaction catalyzed by rice husk-derived sodium silicate at various temperature. The obtained k is then used in Arrhenius plot (Figure 6.12(b)) which gives *Ea* and *A* of the reaction. The activation energy (*Ea*) obtained in this work is smaller than that using CaO catalyst as reported by Birla et al. (79 kJ/mol), Maneerung et al. (83.9 kJ/mol) and Kostic´ et al. (108.8 kJ/mol) (Birla et al., 2012; Maneerung et al., 2015; Kostic´ et al., 2016).
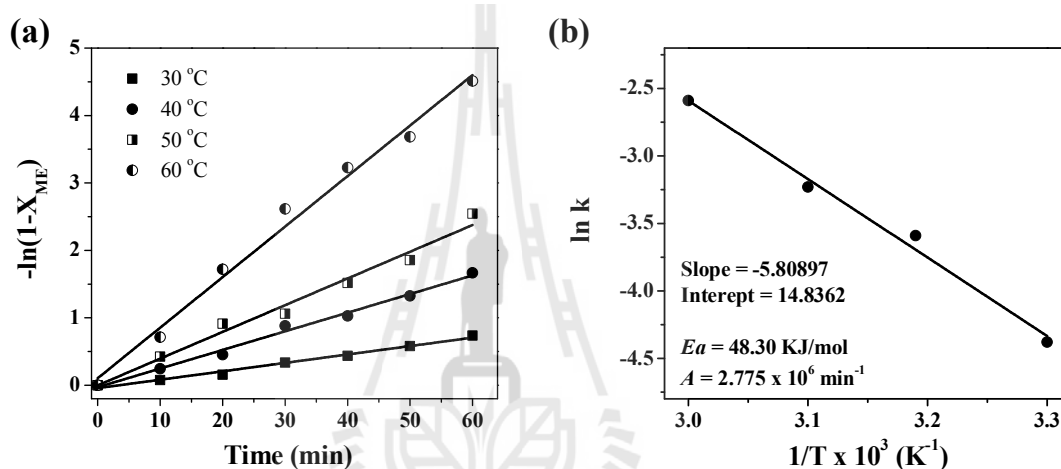
Figure 6.12 (a) $-\ln[1 - x_{ME}]$ versus reaction time plot at different temperatures; reaction condition: catalyst loading amount of 2.5 wt.%, methanol/oil molar ratio of 12:1. (b) Arrhenius plot lnk versus $1/T \times 10^{-3}$ (K^{-1}) for transesterification of palm oil using rice husk-derived sodium silicate.

6.6.7 Physicochemical properties of the palm oil biodiesel

The physicochemical properties of the palm oil biodiesel obtained from transesterification of palm oil catalyzed by rice husk-derived sodium silicate after purification with a cation-exchange resin to remove all soluble ions were measured by ASTM and EN14214 standard methods for bio-auto fuels and shown in Table 6.2.

Table 6.2 Fuel properties of palm oil biodiesel obtained from transesterification reaction under optimum condition catalyzed with rice husk-derived sodium silicate catalyst after purification treatment process.

Fuel properties	Unit	Standard	Palm oil biodiesel
Methyl ester content	%	96.5	98.6
Density @ 15 °C	Kg/m^3	860-900	871
Kinematic viscosity@ 40 °C	cSt	3.5-5.0	4.15
Flash point	°C	>120	183
Acid value	mg KOH/g oil	≤0.5	0.19
Water content	%w/w oil	≤0.050	0.012
Oxidation number	H	>6	16.16
Total contamination,	mg/kg (ppm)	≤24	18.9
Copper strip corrosion,	-	Number 1	Number 1
Cloud point	°C	(-3.0)-12.0	5.0
Pour point	°C	(-15.0)-10.0	2.0
Sulfated ash	%w/w oil	≤0.02	0.0137
Carbon residue	%w/w oil	≤0.05	0.0381
Sodium content	ppm	≤5	3.957

The produced biodiesel has high quality standard properties which are within the standard limits in terms of methyl ester content, density, viscosity, flash point, acid value, water content, oxidation number, total contamination, copper strip corrosion, cloud point, pour point, sulfated ash carbon residue and ion content. Consequently, all results in this work indicated that the low-cost rice husk-derived sodium silicate catalysts demonstrate good catalytic performance for biodiesel production and should be further promoted in industrial application.

6.7 Conclusion

An efficient sodium silicate solid base catalyst was synthesized by using rice husk and NaOH solution. The prepared catalysts were used in transesterification reaction of many kinds of oils to biodiesel. Under optimized reaction conditions, FAME yield reached 97% after only 30 min at 65 °C and 94% after 150 min (2.5 h) at room temperature reaction. This sodium silicate can be reused for four times with excellent activity without regeneration or treatment. The obtained biodiesel product after purification and treatment process by cation-exchange resin shows high quality fuel properties according to ASTM D6751 and EN 14214 standards indicating that the low-cost rice hush-derived sodium silicate catalysts has high catalytic performance and could be used for biodiesel production in industrial scale.

6.8 References

Abedin, M. J., Kalam, M. A., Masjuki, H. H., Sabri, M. F. M., Rahman, S. M. A., Sanjid, A. and Fattah, I. M. R. (2016). Production of biodiesel from a non-edible source and study of its combustion, and emission characteristics: A comparative study with B5, Renew. **Renewable Energy**. 88: 20-29.

Alhassan, Y., Kumar, N., Bugaje, I. M., Pali, H. S. and Kathkar, P. (2014). Co-solvents transesterification of cotton seed oil into biodiesel: Effects of reaction conditions on quality of fatty acids methyl esters. **Energy Conversion and Management**. 84: 640-648.

Arantes, R. S. and Lima, R. M. F. (2013). Influence of sodium silicate modulus on iron ore flotation with sodium oleate. **International Journal of Mineral Processing**. 125: 157-160.

Birla, A., Singh, B., Upadhyay, S. N. and Sharma, Y. C. (2012). Kinatics studies of synthesis of biodiesel from waste frying oil using a heterogeneous catalyst derived from snail shell. **Bioresource Technology**. 106: 95-100.

Chen, G., Rui, S., Jiafu, S. and Yan, B. (2014). Ultrasonic-assisted production of biodiesel from transesterification of palm oil over ostrich eggshell-derived CaO catalysts. **Bioresource Technology**. 171: 428-432.

Chen, G. Y., Shan, R., Shi, J. F. and Yan, B. B. (2015). Transesterification of palm oil to biodiesel using rice husk ash-based catalysts. **Fuel Processing Technology**. 133: 8-13.

Chen, S. Y., Lao-ubol, S., Mochizuki, T., Abe, Y., Toba, M. and Yoshimura, Y. (2014). Transformation of non-edible vegetable oils into biodiesel fuelscatalyzed by unconventional sulfonic acid-functionalized SBA-15. **Applied Catalysis B: Environmental**. 485: 28-39.

Chen, S. Y., Lao-ubol, S., Mochizuki, T., Abe, Y., Toba, M. and Yoshimura, Y. (2014). Production of Jatropha biodiesel fuel over sulfonic acid-based solid acids. **Bioresource Technology**. 157: 346-350.

Dai, Y. M., Chen, K. T. and Chen, C. C. (2014). Study of the microwave lipid extraction from microalgae for biodiesel production. **Chemical Engineering Journal**. 250: 267-273.

Dai, Y. M., Wu, J. S., Chen, C. C. and Chen, K. T. (2015). Evaluating the optimum operating parameters on transesterification reaction for biodiesel production over a LiAlO$_2$ catalyst. **Chemical Engineering Journal**. 280: 370-376.

Fadhil, A. B., Aziz A. M. and Al-Tamer, M. H. (2016). Biodiesel production from *Silybum marianum L*. seed oil with high FFA content using sulfonated carbon

catalyst for esterification and base catalyst for transesterification. **Energy Conversion and Management**. 108: 255-265.

Farooq, M., Ramli, A. and Naeem, A. (2005). Biodiesel production from low FFA waste cooking oil using heterogeneous catalyst derived from chicken bones. **Renewable Energy**. 76: 362-368.

Farooq, M., Ramli, A. and Subbarao, D. (2013). Biodiesel production from waste oil using bifunctional heterogeneous solid catalysts. **Journal of Cleaner Production**. 59: 131-140.

Guo, F., Peng, Z. G., Dai, J. Y. and Xiu, Z. L. (2010). Calcined sodium silicate as solid base catalyst for biodiesel production. **Fuel Processing Technology**. 91: 322-328.

Guo, F., Wei, N. N., Xiu, Z. L. and Fang, Z. (2012). Transesterification mechanism of soybean oil to biodiesel catalyzed by calcined sodium silicate. **Fuel**. 93: 468-472.

Halasz, I., Agarwal, M., Li, R. and Miller, N. (2007). Monitoring the structure of water soluble silicates. **Catalysis Today**. 126: 196-202.

He, F., Wang, X. and Wu, D. (2015). Phase-change characteristics and thermal performance of form-stable n-alkanes/silica composite phase change materials fabricated by sodium silicate precursor. **Renewable Energy**. 74: 689-698.

Huang, R., Cheng, J., Qiu, Y., Li, T., Zhou, J. and Cen, K. (2015). Using renewable ethanol and isopropanol for lipid transesterification in wet microalgae cells to produce biodiesel with low crystallization temperature. **Energy Conversion and Management**. 105: 791-797.

Khemthong, P., Luadthong, C., Nualpaeng, W., Changsuwan, P., Tongprem, P., Viriya-empikul, N. and Faungnawakij, K. (2012). Industrial eggshell wastes as the heterogeneous catalysts for microwave-assisted biodiesel production. **Catalysis Today**. 190:112-6.

Kongmanklang, C. and Rangsriwatananon, K. (2015). Hydrothermal synthesis of high crystalline silicalite from rice husk ash. **Hindawi Publishing Corporation Journal of Spectroscopy**. Volume 2015, Article ID 696513, 5 pages.

Kostic´, M. D., Bazargan, A., Stamenkovic´, O. S., Veljkovic´, V. B. and McKay, G. (2016). Optimization and kinetics of sunflower oil methanolysis catalyzed by calcium oxide-based catalyst derived from palm kernel shell biochar. **Fuel**. 163: 304-313.

Kouzu, M., Yamanaka, S., Hidaka, J. and Tsunomori, M. (2009). Heterogeneous catalysis of calciumoxide used for transesterification of soybean oil with refluxing methanol. **Applied Catalyst A: General**. 355: 94-99.

Lee, S. L.,Wong, Y. C., Tan, Y. P and Yew, S. Y. (2015). Transesterification of palm oil to biodiesel by using waste obtuse horn shell-derived CaO catalyst. **Energy Conversion and Management**. 93: 282-288.

Long, Y. D, Guo, F., Fang, Z., Tian, X. F., Jiang, L.Q. and Zhang, F. (2011). Production of biodiesel and lactic acid from rapeseed oil using sodium silicate as catalyst. **Bioresource Technology**. 102: 6884-6886.

Long, Y. D., Fang, Z., Su, T. C. and Yang, Q. (2014). Co-production of biodiesel and hydrogen from rapeseed and Jatropha oils with sodium silicate and Ni catalysts. **Applied Energy**. 113: 1819-1825.

Lu, H., Yu, X., Yang, S., Yang, H. and Tu, S. T. (2016). MgO–Li₂O catalysts templated by a PDMS–PEO comb-like copolymer for transesterification of vegetable oil to biodiesel. **Fuel**. 165: 215-223.

Luu, P. D., Troung, H. T., Luu, B. V., Pham, L. N., Imamura, K., Takenaka, N. and Maeda, Y. (2014). Production of biodiesel from Vietnamese *Jatropha cuecas* oil by a co-solvent method. **Bioresource Technology**. 73: 309-316.

Mahesh, S. E., Ramanathan, A., Begum, K. M. M. S. and Narayanan, A. (2015). Biodiesel production from waste cooking oil using KBr impregnated CaOas catalyst. **Energy Conversion and Management**. 91: 442-450.

Maneerung, T., Kawi, S. and Wang, C. H. (2015). Biomass gasification bottom ash as a source of CaO catalyst for biodiesel production via transesterification of palm oil. **Energy Conversion and Management**. 92: 234-243.

Mathimani, T., Uma, L. and Prabaharan, D. (2015). Homogeneous acid catalyzed transesterification ofmarine microalga *Chlorella* sp. BDUG 91771 lipid-An efficient biodiesel yield and its characterization, **Renewable Energy**. 81: 523-533.

Moushoul, E. B., Farhadi, K., Mansourpanah, Y., Nikbakht, A. M., Molaei, R. and Forough, M. (2016). Application of CaO-based/Au nanoparticles as heterogeneous nanocatalysts in biodiesel production. **Fuel**. 164: 119-127.

Nakatani, N., Takamori, H., Takeda, K. and Sakugawa, H. (2009). Transesterification of soybean oil using combusted oyster shell waste as a catalyst. **Bioresource Technology**. 100: 1510-1513

Nur, S. Z. A., Taufiq-Yap, Y. H., Nizah, R. M. F., Teo, S. H., Syazwani, O. N. and Islam, A. (2014). Production of biodiesel from palm oil using modified

Malaysian natural dolomites. **Energy Conversion and Management**. 78: 738-744.

Onoji, E. S., Iyuke, S. E., Igbafe, A. I. and Nkazi, D. B. (2016). Rubber seed oil: A potential renewable source of biodieselfor sustainable development in sub-Saharan Africa. **Energy Conversion and Management**. 110: 125-134.

Roschat, W., Kacha, M., Yoosuk, B., Sudyoadsuk, T. and Promarak, V. (2012). Biodiesel production based on heterogeneous process catalyzed by solid waste coral fragment. **Fuel**. 98:194-202.

Roschat, W., Siritanon, T., Yoosuk, B. and Promarak, V. (2016). Biodiesel production from palm oil using hydrated lime-derived CaO as a low-cost basic heterogeneous catalyst. Energy convers manage **Energy Conversion and Management**. 108: 459-467.

Sanchez, M., Marchetti, J. M., Boulifi, N. E., Aracil, J. and Martinez, M. (2015). Kinetics of Jojoba oil methanolysis using a waste from fish industryas catalyst. **Chemical Engineering Journal**. 262: 640-647.

Selvam, T., Bandarapu, B., Mabande, G. T. P., Toufar, H. and Schwieger, H. (2003). Hydrothermal transformation of a layered sodium silicate, kanemite, into zeolite Beta (BEAT). **Microporous and Mesoporous Materials**. 64: 41-50.

Shan. R., Chen, G., Yan, B., Shi, J. and Liu, C. (2015). Porous CaO-based catalyst derived from PSS-induced mineralization for biodiesel production enhancement. **Energy Conversion and Management**. 106: 405-413.

Sirisomboonchai, S., Abuduwayiti, M., Guan, G., Samart, C., Abliz, S., Hao, X., Kusakabe, K. and Abudula, A. (2015). Biodiesel production from waste cooking

oil using calcined scallop shellas catalyst. **Energy Conversion and Management**. 95: 242-247.

Soetaredjo, F. E., Ayucitra, A., Ismadji, S. and Maukar, A. L. (2011). KOH/bentonite catalysts for transesterification of palm oil to biodiesel. **Applied Clay Science**. 53: 341-346.

Syazwani, O. N., Rashid, U. and Yap, Y. H. T. (2015). Low-cost solid catalyst derived from waste *Cyrtopleura costata*(Angel Wing Shell) for biodiesel production using microalgae oil. **Energy Conversion and Management**. 101: 749-756.

Tan, Y. H., Abdullah, M. O., Hipolito, C. N. and Taufiq-Yap, Y. H. (2015). Waste ostrich- and chicken-eggshells as heterogeneous base catalyst for biodiesel production from used cooking oil: Catalyst characterization and biodiesel yield performance. **Applied Energy**. 60: 58-70.

Taufiq-Yap, Y. H., Teo, S. W., Rashid, U., Islam, A., Hussien, M. Z. and Lee, K. T. (2014). Transesterification of Jatropha curcas crude oil to biodiesel on calciumlanthanum mixed oxide catalyst: Effect of stoichiometric composition. **Energy Conversion and Management**. 88: 1290-1296.

Tubino, M., Junior, J. G. R. and Bauerfeldt, G. F. (2016). Biodiesel synthesis: A study of the triglyceride methanolysis reactionwith alkaline catalysts. **Catalysis Communications**. 75: 6-12.

Viriya-empikul, N., Krasae, P., Nualpaeng, W., Yoosuk, B. and Faungnawakij, K. (2012). Biodiesel production over Ca-based solid catalysts derived from industrial wastes. **Fuel**. 92: 239-244.

Vujicic, D., Comic, D., Zarubica, A., Micic, R. and Boskovi, G. (2010). Kinetics of biodiesel synthesis from sunflower oil over CaO heterogeneous catalyst. **Fuel** 89: 2054-2061.

Wang, J. X., Chen, K. T., Wu, J. S., Wang, P. H., Huang, S. T and Chen, C. C. (2012). Production of biodiesel through transesterification of soybean oil using lithiumorthosilicate solid catalyst. **Fuel Processing Technology**. 104: 167-173.

Xie, W. and Zhao, L. (2014). Heterogeneous CaO–MoO3–SBA-15 catalysts for biodiesel production from soybean oil. **Energy Conversion and Management**. 79: 34–42.

Yoosuk, B., Udomsap, P., Puttasawat, B. and Krasae, P. (2010). Modification of calcite byhydration–dehydration method for heterogeneous biodiesel productionprocess: the effects of water on properties and activity. **Chemical Engineering Journal**. 162: 135-141.

Yun-yu, Z., Xiao-xuan, L. and Zheng-xing, C. (2012). Rapid synthesis of well-ordered mesoporous silica from sodium silicate. **Powder Technology**. 226: 239-245.

CHAPTER VII

SYNTHESIS OF GLYCEROL CARBONATE FROM GLYCEROL AND DIMETHYL CARBONATE VIA TRANSESTERIFICATION REACTION CATALYZED BY CaO FROM NATURAL SOURCES AS GREEN AND ECONOMICAL CATALYSTS

7.1 Graphical abstract
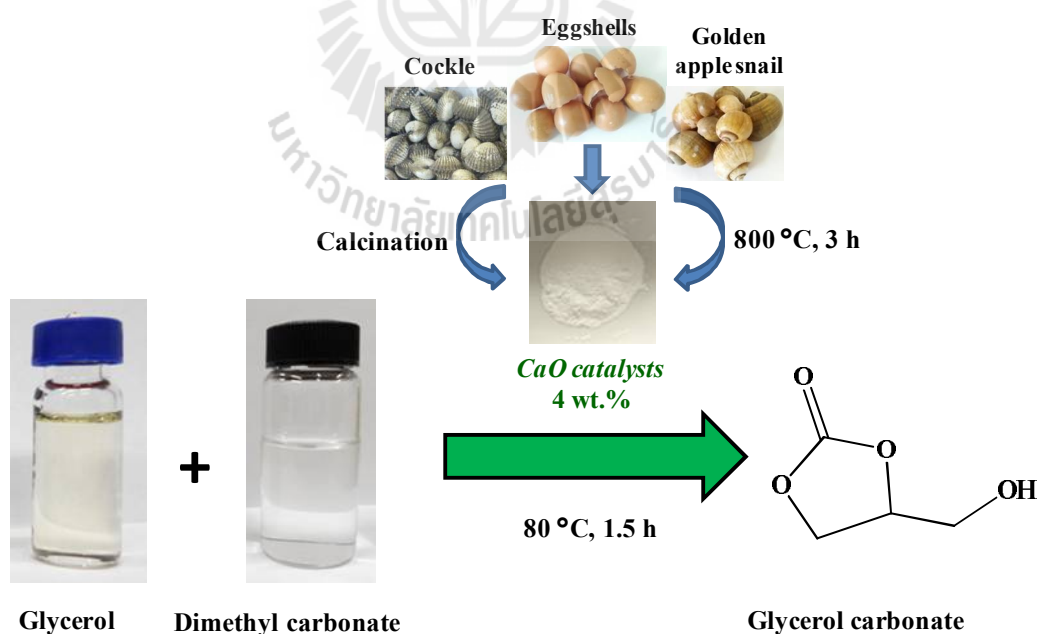
The shells are a high potential source of CaO preparation which is not only green and cheap but also highly efficient in glycerol carbonate production.

7.2 Highlights

- CaO derived from natural sources is green and economical solid base catalysts for glycerol carbonate production.

- Over 97% of glycerol carbonate yield is achieved from transesterification of dimethyl carbonate and glycerol within 1.5 h.

- ^{1}H NMR technique was used to determine glycerol carbonate yield (%) for the first time.

- The kinetics of the reaction was studied and compared the catalytic activity of each CaO catalysts.

7.3 Abstract

CaO catalysts derived from natural sources were investigated in the transesterification of dimethyl carbonate with glycerol to produce glycerol carbonate under various reaction conditions. The obtained CaO catalysts were characterized by several techniques namely TG-DTA, XRD, XRF, BET surface area, SEM, FT-IR, CO_2–TPD, and Hammett indicator test. Under the optimized reaction conditions of dimethyl carbonate/glycerol molar ratio of 4:1, catalyst loading amount of 4 wt.% and reaction temperature of 80 °C; over 97% yield of glycerol carbonate product could be achieved within 1.5 h. In addition, CaO could be easily recovered after the reaction and reused for at least four times without significant loss of activity. Comparison of the catalytic activity of all CaO catalysts was evaluated which indicated that CaO derived from natural materials showed excellent catalytic performance and could be a high potential, green and economical catalyst for application in glycerol carbonate production.

7.4 Introduction

Nowadays, biodiesel is being produced in great quantities because the increases of energy demand with continuous growth in human population and economic development has made the search for alternative and renewable sources of energy very important (Avhad and Marchetti, 2015). Biodiesel is a non-toxic fuel with high combustion efficiency, biodegradability, and better lubrication. It can be produced from plant or algal oils and animal fats (Witoon et al., 2014; Roschat et al., 2012). Typically, 1 mol of triglyceride including oils and fats react with 3 mol of alcohol especially methanol to give 3 mol of fatty acid methyl eater, which is called biodiesel, and 1 mol of glycerol by-product (Roschat et al., 2016). Hence, the production of every 1000 kg of biodiesel produces around 100 kg of glycerol by-product (Malyaadri et al., 2011). Biodiesel annual production is expected to reach 37 billion gallons in 2016 according to Oil World's estimate. Therefore, around 4 billion gallons of crude glycerol will be produced the same year (Rastegari and Ghaziaskar, 2015).

It is generally known that glycerol has a wide variety of uses and applications such as food, pharmaceutical, cosmetic, perfumery, coating and other industries (Roschat et al., 2012). The utilization of the glycerol by-product would significantly improve the economic aspect of overall biodiesel production. Nevertheless, the direct utilization of glycerol cannot accommodate such large volume obtained from biodiesel production. Moreover, glycerol itself is very cheap and most application requires additional purification process. Hence, the conversion of glycerol to other valuable chemicals such as propane diols, glycerol carbonate, acrolein, esters of glycerol and glyceric acid would not only generate added value for glycerol, but also

promote biodiesel production (Rastegari and Ghaziaskar, 2015; Zhou et al., 2015; Zheng et al., 2015).

Among different glycerol-related chemicals, glycerol carbonate (4-hydroxymethyl-1,3-dioxolan-2-one) is a very interesting glycerol derivatives because its high reactivity with alcohols, amines, carboxylic acids, ketones, and isocyanates, allow the uses as chemical intermediates in various reactions (Zheng et al., 2015; Dibenedetto et al., 2011). Glycerol carbonate itself can be employed as a solvent for NMR analysis and organic synthesis due to its high boiling point and polarity. In addition, the potential for applications of glycerol carbonate also included a membrane component for gas separation, reagent for coatings, detergents, polymers, lubricant, electrolyte, and the uses in cosmetics industry (Zheng et al., 2015; Jagadeeswaraiah et al., 2014; Teng et al., 2014).

To prepare glycerol carbonate from glycerol and dimethyl carbonate via transesterification reaction as depicted in Figure 7.1, heterogeneous catalyst is preferred over homogeneous ones because the reaction only involves milder and greener process conditions (Liu et al., 2013). Accordingly, various heterogeneous basic catalysts such as Mg/Al/Zr (Malyaadri et al., 2011), Ca-Al hydrocalumite (Zheng et al., 2015), KF/sepiolite (Algoufi et al., 2014), KNO_3/CaO (Hu et al., 2015) and $LiNO_3/Mg_4AlO_{5.5}$ (Liu et al., 2015) have been reported. One of the most interesting heterogeneous catalysts is CaO as it is less toxic, high active, cheap and easy to prepare form natural materials (e.g. limestone, dolomite and shells) (Lu et al., 2013; Wang et al., 2015).

In the present study, natural materials including eggshells, golden apple snail shells and cockle shells were used to generate CaO as a solid catalyst for glycerol

carbonate production. The simple modification process was used to enhance the catalytic performance of all samples. All shell-derived catalysts were characterized and their catalytic activities were investigated. Reusability of the catalysts and kinetic of reaction were investigated. The comparison of catalytic activity of the CaO catalysts obtained from the shells and a commercial CaO was also discussed.
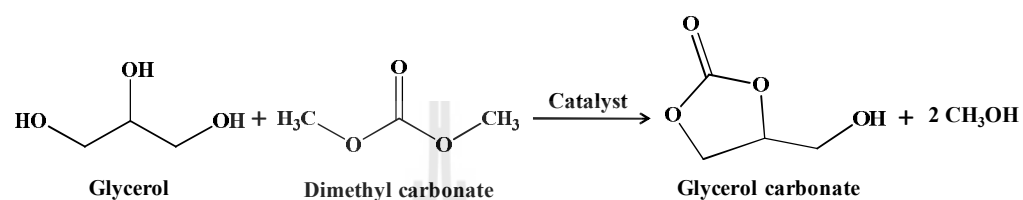
Figure 7.1 The schemes of glycerol carbonate synthesis from glycerol with dimethyl carbonate.

7.5 Experimental

7.5.1 Materials and catalysts preparation

Glycerol (commercial grade) was purchased from Chemipan Co.Ltd., Thailand. The analytical grade dimethyl carbonate and methanol were obtained from Chemical Express Co.Ltd. and Fluka. Calcium oxide analytical grade (CaO_AR) was purchased from Acros Chemical Co.Ltd. Hammett indicators namely, bromothymol blue, phenolphthalein, indigo carmine, 2,4-dinitroaniline, and 4-nitroaniline of analytical grade were purchased from Aldrich and Fluka. Eggshells, golden apple snail shells and cockle shells collected from local restaurants were cleaned with water several times and air-dried for 24 h before uses. The dried eggshells, golden apple snail shells and cockle shells were crushed, sieved and calcined at 800 °C (refer to TG/DTA results) for 3 h with a heating rate of 10 °C/min to obtain CaO_egg, CaO_gol and CaO_coc.

7.5.2 Material characterization

Thermal decomposition of all samples were analyzed by thermo-gravimetric/differential thermal analysis (TG-DTA) using a Rigaku TG-DTA 8120 thermal analyzer under air with a heating rate of 10 °C/min. The crystalline phases of all calcined samples were determined by X-ray diffraction (XRD) using a PHILIPS X′Pert-MDP X-ray diffractometer with Cu Kα radiation (k = 1.5418 Å) at 1600 W, 40 kV and 40 mA. The elemental compositions of all samples were analyzed by a PHILIPS Magi X diffuse wavelength X-ray Fluorescence (XRF) spectrophotometer with 1 kW Rh Kα radiation. The samples were also analyzed by Fourier transforms infrared (FT-IR) spectroscopy using a Perkin–Elmer FTIR spectroscopy spectrum RXI spectrometer in the range of 400–4000 cm^{-1} with resolution of 4 cm^{-1} and potassium bromide (KBr) was used as a matrix.

Brunauer Emmett Teller (BET) on the Bel-sorp-mini II (Bel-Japan) was applied to investigate surface area and pore volumes based on low temperature adsorption and desorption isotherm of N_2 gas. Scanning Electron Microscopy was done to study the morphology and size of the catalysts using JEOL JSM 6010LV scanning electron microscope at an accelerated voltage of 10 kV. Temperature programmed desorption using Chemisorption Analyzer (Belcat B) based on CO_2 as a probe molecule (CO_2-TPD) and He as a carrier gas was employed to study basic site properties of the catalysts. In addition, the basic strength ($H\_$) property was tested by Hammett indicator method using the following indicators with different acidity functions; bromothymol blue (pKa = 7.2), phenolphthalein (pKa = 9.8), indigo carmine (pKa = 12.2), 2,4-dinitroaniline (pKa = 15.0) and 4-nitroaniline (pKa = 18.4) (Roschat et al, 2016; Yoosuk et al., 2010).

7.5.3 Synthesis of glycerol carbonate from glycerol and dimethyl carbonate

The reaction was carried out on a three-neck round bottom flask batch reactor equipped with a reflux condenser, a magnetic stirrer (300 rpm), and a thermocouple. A mixture of solid catalyst and glycerol were preheated at designated temperature (60, 70, 75, 80 and 85 °C) for 30 min and then added to dimethyl carbonate. The transesterification reaction of dimethyl carbonate with glycerol was performed with various catalysts loading amount (1-5 wt.% relative to glycerol weight) and dimethyl carbonate to glycerol molar ratios (1:1-5:1). After the reaction, the mixture was taken out, and then the catalysts were separated by filtration, washed with methanol and dried at 100 °C for 1 h. The catalysts were collected and reused for the next run.

7.5.4 Product analysis

After catalysts separation, methanol by-product was evaporated from the reaction mixture by rotary evaporator before glycerol carbonate analysis. The obtained reaction mixture was analyzed by proton nuclear magnetic resonance (^{1}H NMR) using a Brüker Ascend^{TM} 500 MHz spectrometer as shown in Figure 7.2(a)-(d). Dimethyl Sulfoxide-d$_6$ (DMSO-d$_6$) was used as a solvent and the internal reference.

As an example, reaction mixtures from uncompleted transesterification of dimethyl carbonate with glycerol which contained unreacted glycerol and glycerol carbonate product was depicted in Figure 7.2(c). After reaction completed, ^{1}H NMR spectrum (Figure 7.2(b)) indicates that the final product is glycerol carbonate only one without side reaction to produce another product. This result can be confirmed by ^{13}C NMR analysis as displayed in Figure 7.3(a)-(c). As a reaction uncompleted, Figure

7.3(c) shows spectrum characteristic carbon atom of glycerol and glycerol carbonate but disappeared another compound and Figure 7.3(b) displays spectrum only characteristic carbon atom of glycerol carbonate as a final product after reaction completed.

Therefore, the conversion of the glycerol to glycerol carbonate (denoted as glycerol carbonate yield (%)) was calculated according to the ratio of the integration of the ^{1}H NMR signals of the methine proton ($-CH-$) in the glycerol at chemical shifts 3.41-3.46 ppm and that of methine proton ($-CH-$) of glycerol carbonate product at chemical shifts 4.81 ppm using Eq. 7.1:

$$\% \text{ glycerol carbonate yield} = \frac{b'_{CH}}{b_{CH} + b'_{CH}} \times 100 \qquad (7.1)$$

b'_{CH} and b_{CH} are the integration of the methine protons of glycerol carbonate and glycerol, respectively.

In addition, chemical structure and purity of the obtained glycerol carbonate product was confirmed and evaluated by gas chromatography–mass spectrometry (GC-MS) as presented in Figure 7.4(a) and (b).
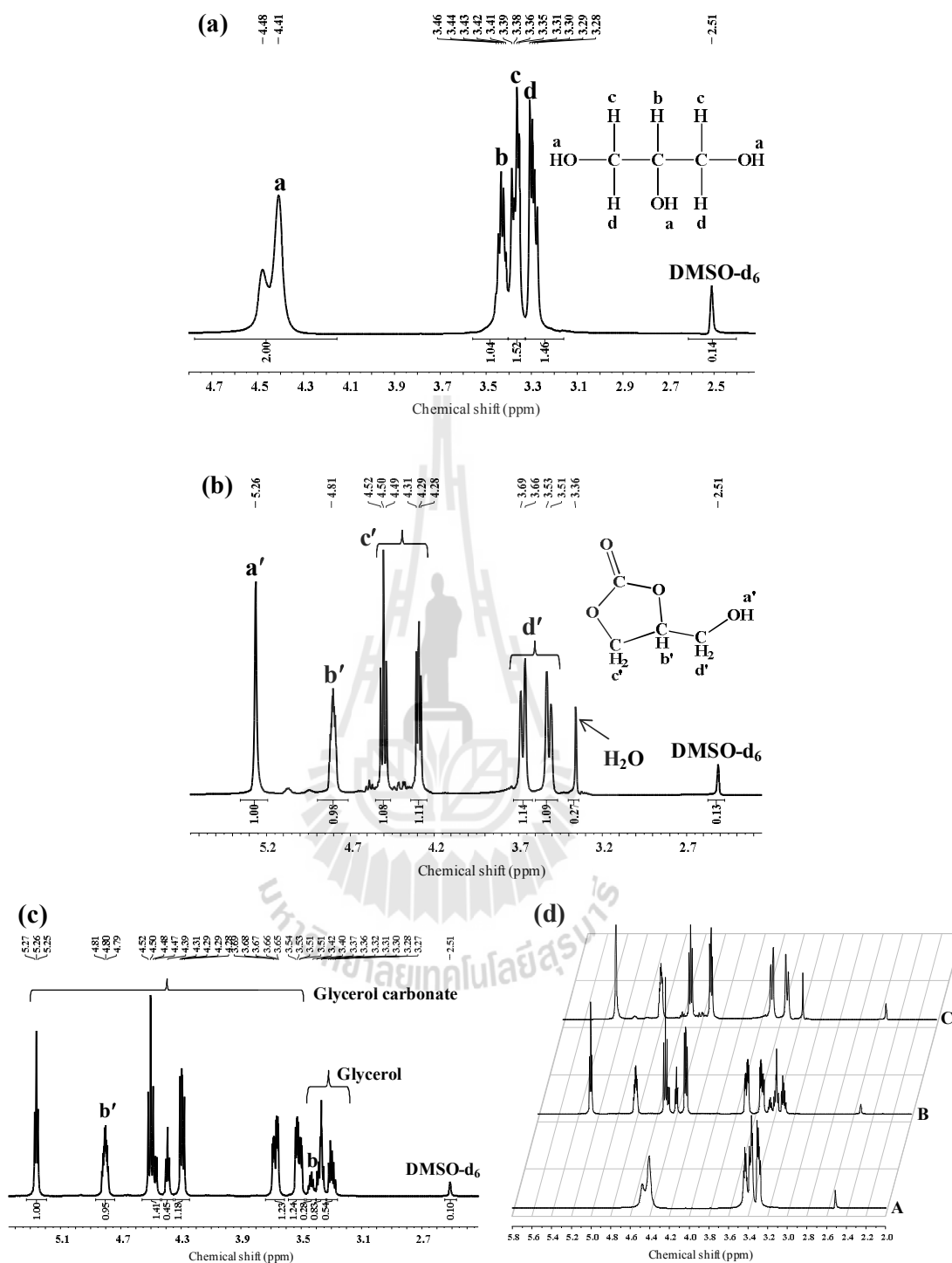
Figure 7.2 ^{1}H NMR spectrum of (a) glycerol, (b) glycerol carbonate, (c) uncompleted transesterification (glycerol + glycerol carbonate), and (d) plot stacked of glycerol (spectrum A), uncompleted transesterification (spectrum B) and completed reaction (spectrum C).

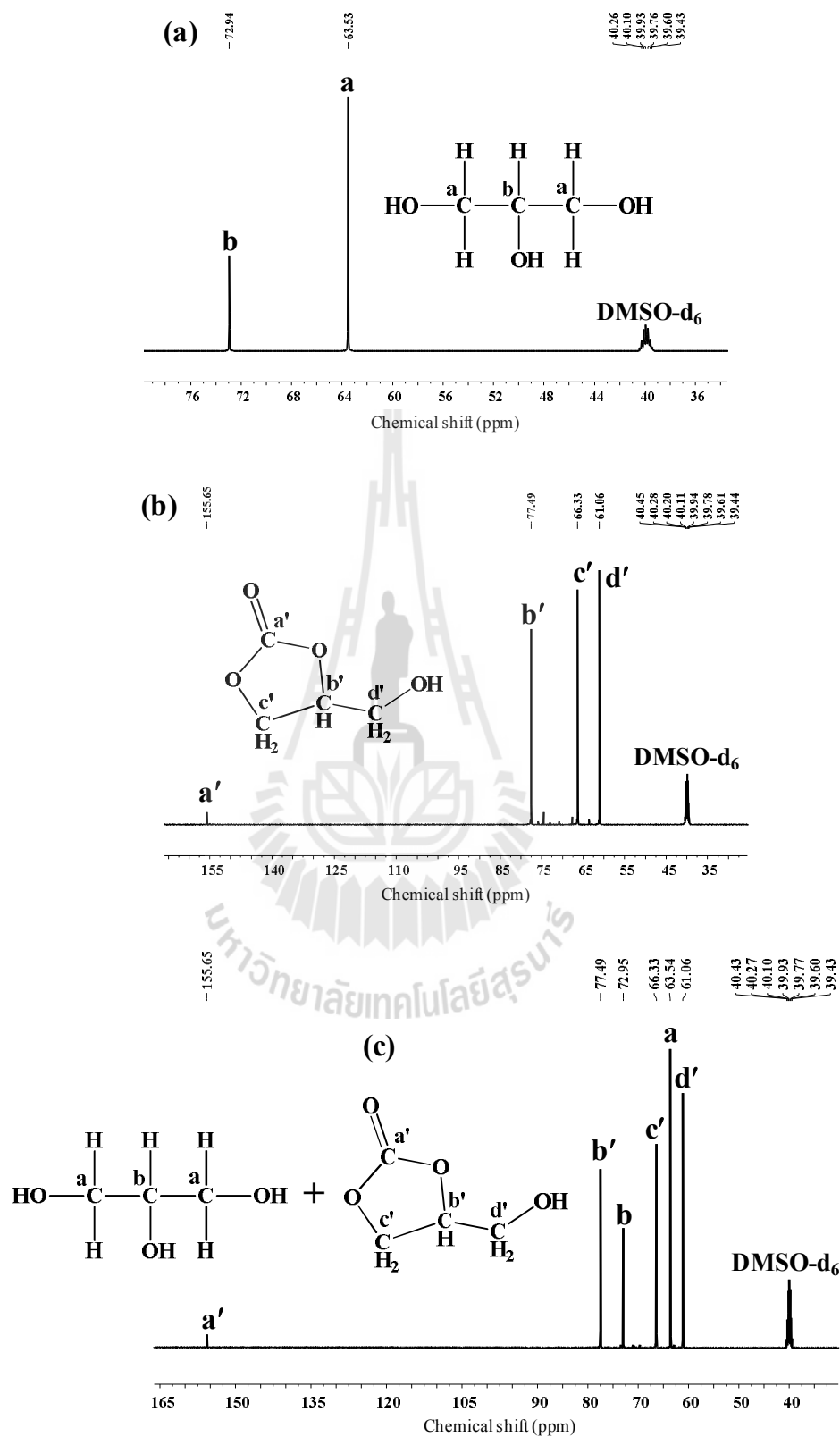**Figure 7.3** ^{13}C NMR spectrum of (a) glycerol, (b) glycerol carbonate and (c) uncompleted transesterification (glycerol + glycerol carbonate).
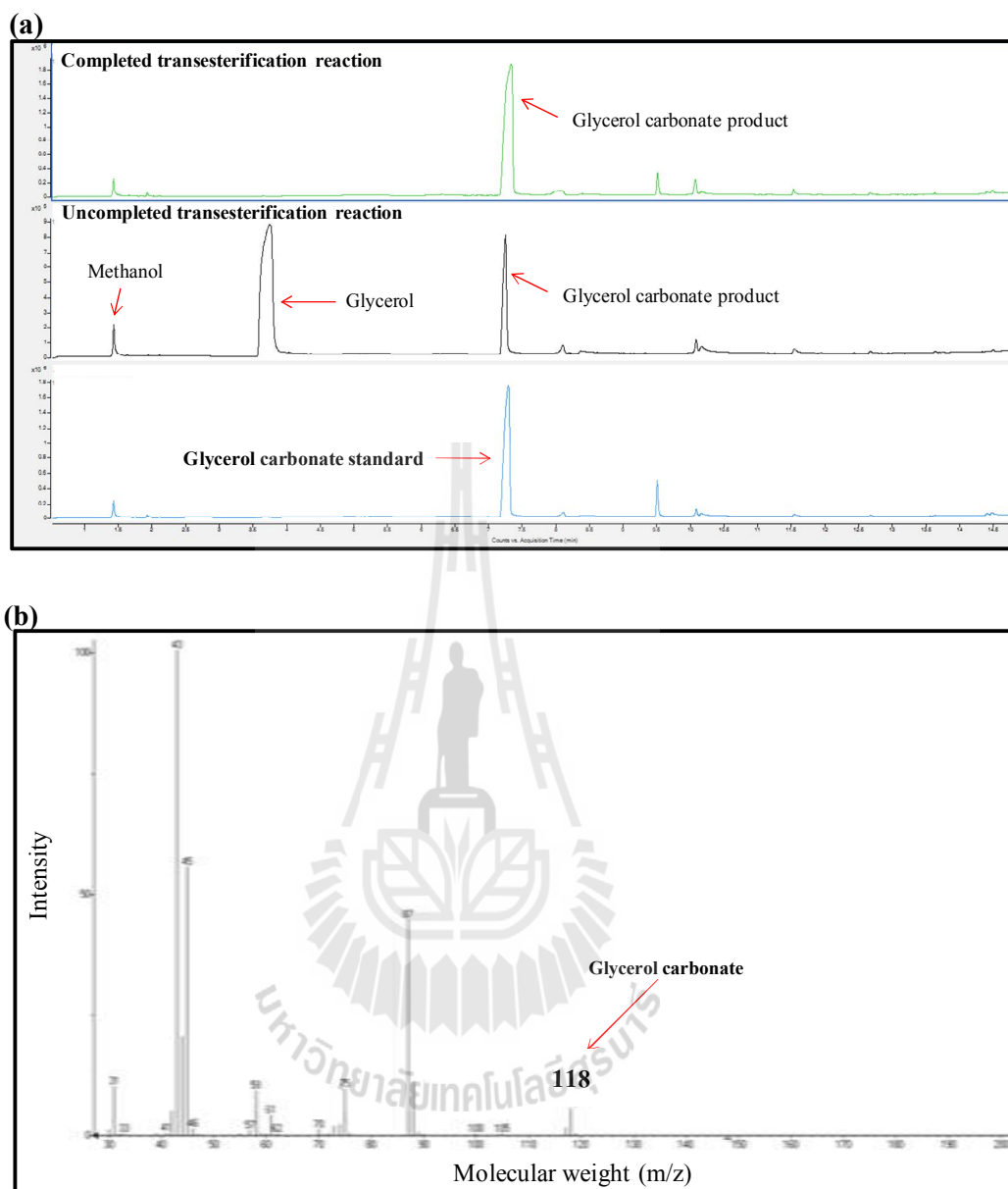
Figure 7.4 (a) GC profiles of glycerol carbonate standard, uncompleted transesterification reaction and completed transesterification reaction. (b) GC-MS spectrum of glycerol carbonate obtained from transesterification reaction catalyzed by cockle shells-derived CaO catalysts.

7.5.5 Study of reaction kinetics

Stoichiometrically, 1 mol of dimethyl carbonate reacts with 1 mol of glycerol to give 1 mol of glycerol carbonate as depicted in scheme 1. The transesterification is assumed to be a single step reaction whose rate law can be explained by Eq. 7.2:

$$r_a = \frac{-d[Gl]}{dt} = k'[Gl][DMC] \qquad (7.2)$$

where [Gl], [DMC] and k' are glycerol concentration, dimethyl carbonate concentration and the equilibrium rate constant, respectively. During the reaction, excess dimethyl carbonate was used to shift the equilibrium toward the product thus concentration of dimethyl carbonate was assumed to be constant. As a result, the reaction could be assumed as a pseudo-first order reaction and Eq. 7.2 can be rearranged to:

$$r_a = \frac{-d[Gl]}{dt} = k[Gl] \qquad (7.3)$$

k is modified rate constant (k = k'[DMC]). Integration and rearrangement of Eq. 7.3 gives Eq. 7.4:

$$\ln [Gl]_0 - \ln[Gl]_t = kt \qquad (7.4)$$

Assuming the initial glycerol at initial time (t = 0), $[Gl]_0$ is 1 mol and $[Gl]_t$ is glycerol concentration at time *t* rearranging Eq. 7.4 gives Eq. 7.5:

$$-\ln[Gl]_t = kt \qquad (7.5)$$

$[TG]_t$ is related to %yield of glycerol carbonate product

$$[Gl]_t = 1 - x_{GC} \qquad (7.6)$$

where x_{GC} is $\left(\frac{\text{Glycerol carbonate yield (\%)}}{100}\right)$ and substitute $[Gl]_t$ in Eq. 7.5 gives Eq. 7.7:

$$-\ln[1 - x_{GC}] = kt \qquad (7.7)$$

Therefore, plot of $-\ln[1 - x_{GC}]$ against t will be linear and its slope is equal to rate constant (k).

7.6 Results and discussion

7.6.1 Catalysts characterization

TG/DTA analysis of the eggshells, golden apple snail shells and cockle shells revealed about 44% weight loss at the temperature range of 600-800 °C which corresponded to carbon dioxide (CO_2) removal from calcium carbonate ($CaCO_3$) giving CaO (Figure 7.5(a)-(c)). Based on TG/DTA results, raw materials in this study were calcined at 800 °C in air for 3 h to produce CaO catalysts.

XRD patterns of all samples calcined at 800 °C for 3 h are illustrated in Figure 7.6(a). All samples demonstrated sharp peaks at $2\theta = 32.2°$, $37.3°$, $53.9°$, $64.2°$ and $67.4°$ matching with the standard XRD pattern of CaO (Lee et al., 2015; Chen et al., 2014). The chemical compositions of all calcined shell samples were also investigated by FT-IR as depicted in Figure 7.6(b). FT-IR spectra of calcined all the samples revealed a very small hydroxyl group stretching at approximately 3640 cm^{-1} caused by the absorbed water molecules on the surface but bands related to $CaCO_3$ were not observed. These results indicated that all shells were completely transformed to CaO after calcination at 800 °C for 3 h. Elemental compositions of all calcined shell samples determined with XRF spectroscopy, indicate over 98% of CaO summarized in Table 7.1.
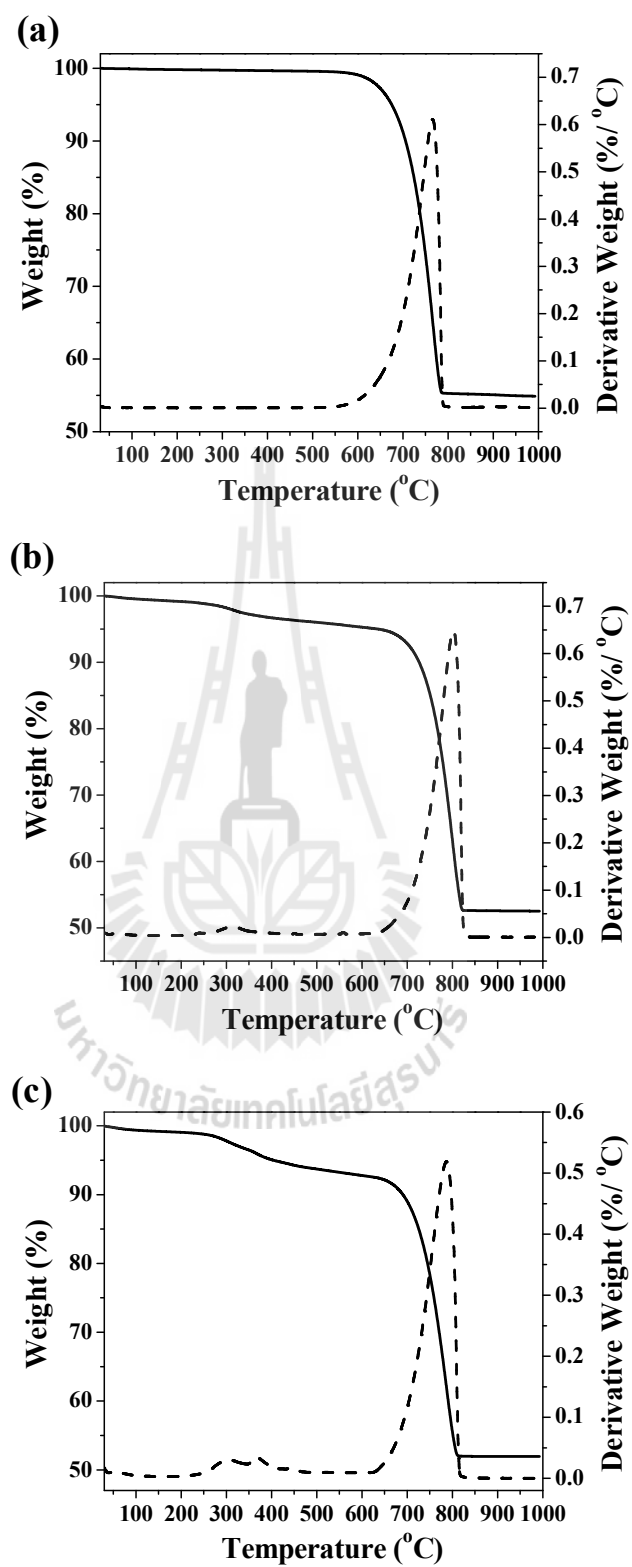
Figure 7.5 TG/DTA thermograms of (a) eggshells, (b) golden apple snail shells and

(c), cockle shells.
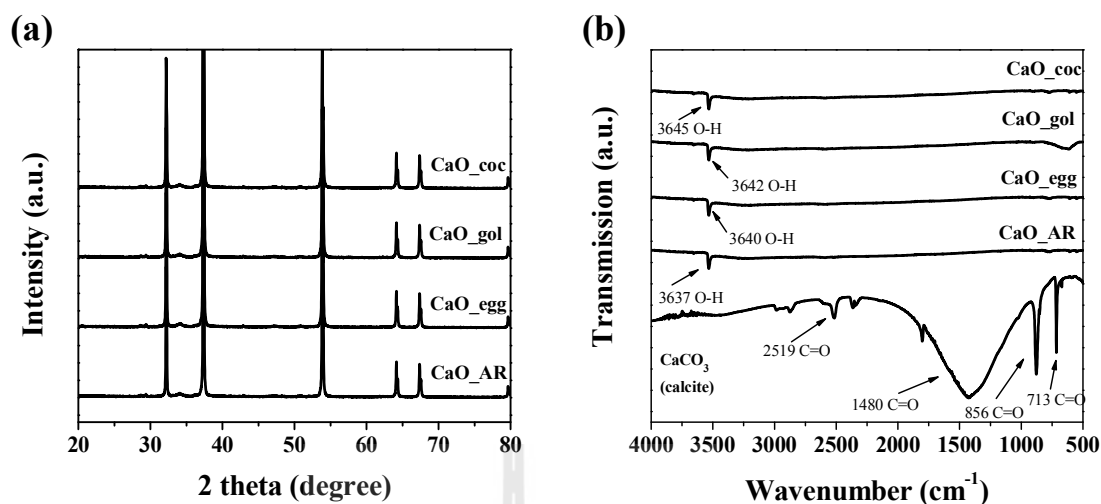
Figure 7.6 (a) XRD patterns and (b) FT-IR spectra of the calcined eggshells (CaO_egg), golden apple snail shells (CaO_gol) and cockle shells (CaO_coc) at 800 °C for 3 h, and CaO analytical grade (CaO_AR).

Table 7.1 Physicochemical properties of the shells-derived CaO catalyst calcined at 800 °C for 3 h.

Catalysts material	BET surface area (m^2g^{-1})	Pore volume (cm^3/g)	Basic strengths $H\_$	Total basic sites ($\mu mol/g$)	%Ca	Glycerol carbonate yield (%)[a]
CaO_AR	2.7	0.007	$15 < H\_ < 18.4$	207.3	99.6	78.1
CaO_egg	2.8	0.017	$15 < H\_ < 18.4$	211.5	98.7	84.5
CaO_gol	3.0	0.026	$15 < H\_ < 18.4$	218.0	98.5	85.9
CaO_coc	3.5	0.019	$15 < H\_ < 18.4$	247.5	99.1	92.1

[a]Reaction conditions: dimethyl carbonate/glycerol molar ratio = 3:1, catalyst amount = 3 wt.% at 80 °C for 2 h (Lu et al., 2013; Simanjuntak et al., 2011).

The Brunauer–Emmett–Teller surface area (S_{BET}) and the total pore volume of the calcined catalysts are shown in Table 7.1. From Table 7.1, S_{BET} of CaO obtained from cockle shells > golden apple snail shells > eggshells > CaO analytical grade,

respectively. The different value of S_{BET} of each catalyst could be related to its morphology as shown in Figure 7.7. According to SEM images in Figure 7.7(a), the calcined cockle shells show rod-like particles with some aggregation thus high agglomeration of small particles would be provided higher specific surface areas (Viriya-empikul et al., 2012). On the other hand, the calcined eggshells, golden apple snail shells and CaO analytical grade display similar morphology with plate-like particle as shown in Figure 7.7(b)-(d).
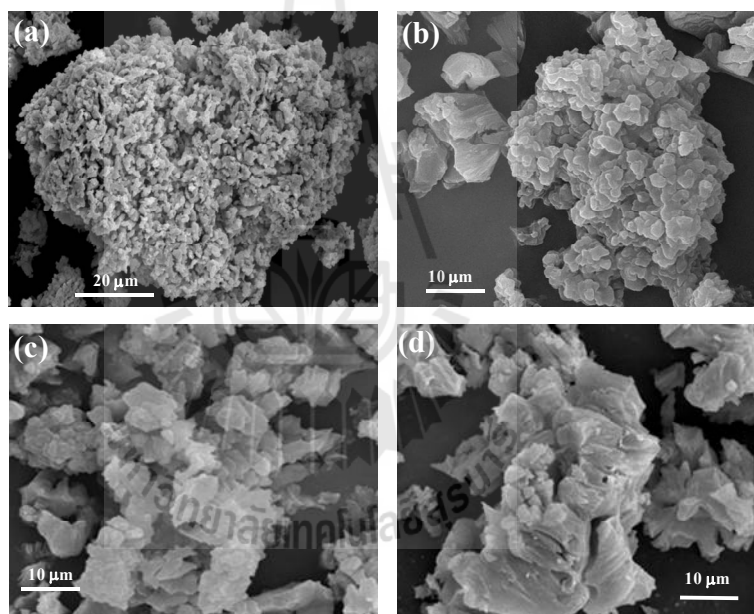
Figure 7.7 SEM images of the calcined cockle shells (a), eggshells (b) and golden apple snail shells (c) at 800 °C for 3 h, and (d) CaO analytical grade calcined.

Furthermore, the nitrogen adsorption/desorption isotherm of all the CaO samples are depicted in Figure 7.8(a)-(d). All of the samples display a type II isotherm based on IUPAC's classification which is produced with a low slope in the middle region of the isotherm and a desorption line almost overlapping with an adsorption

line. In particular, this isotherm is represented unrestricted monolayer–multilayer adsorption and attributed to a nonporous or macroporous material (Khemthong et al., 2012).
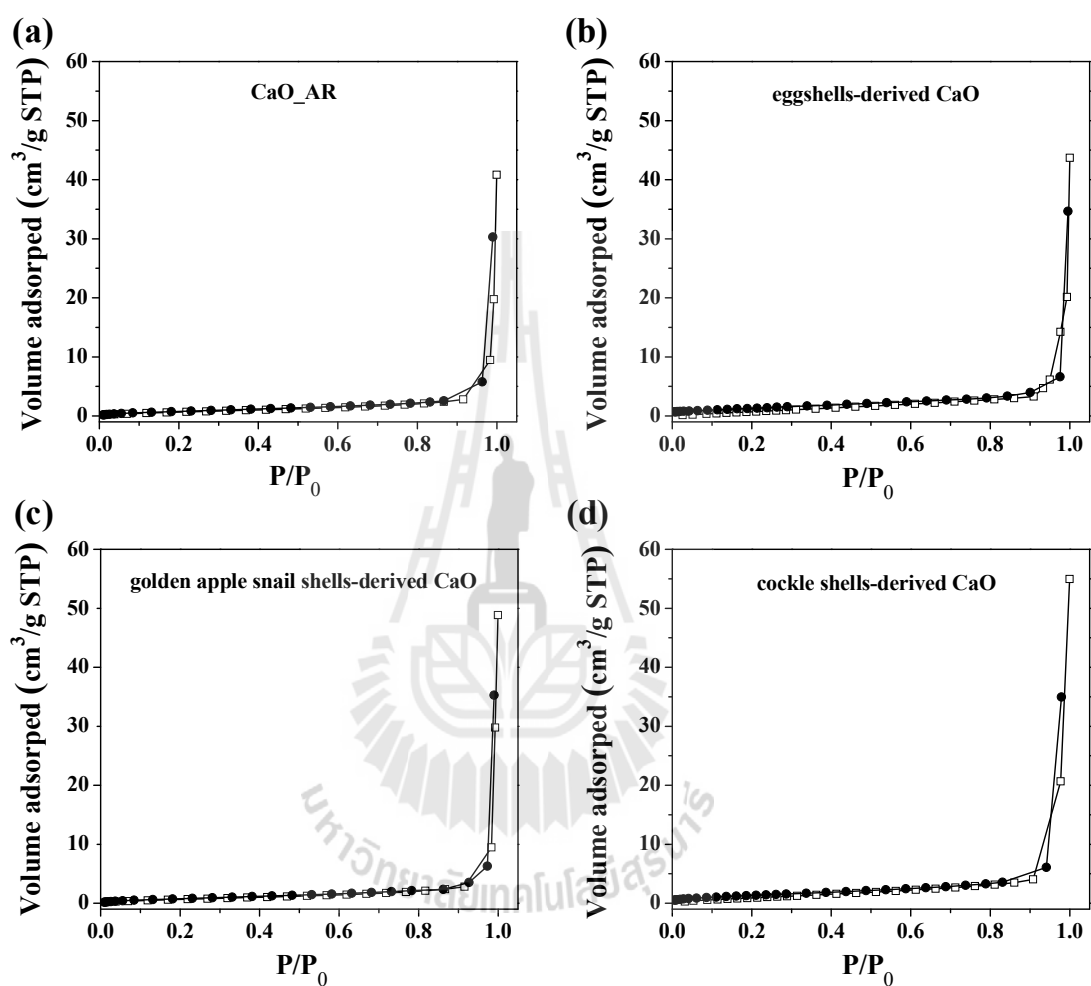
Figure 7.8 N_2 adsorption/desorption isotherms of (a) CaO analytical grade (CaO_AR), (b) eggshells-derived CaO, (c) golden apple snail shells-derived CaO and (d) cockle shells-derived CaO.

The basic strengths ($H\_$ value) of all calcined the shells and CaO_AR measured by Hammett indicator method were found to possess $H\_$ values in the range of 15.0–18.4, as evidenced by their ability to effect a color change with 2,4-dinitroaniline

(p*Ka* = 15) but not 4-nitroaniline (p*Ka* = 18.4). Furthermore, CO_2-TPD was used to determine the total basic site of all samples as summarized in Table 7.1. The total basic sites of CaO catalyst derived from the shells was the order of cockle shells > golden apple snail shells > eggshells > CaO analytical grade, respectively. These results suggest that basic sites of the catalysts are related to S_{BET}. The higher the S_{BET} usually result the higher basic sites. Both properties are required in heterogeneous catalysts for glycerol carbonate production (Roschat et al. 2016).

7.6.2 Catalyst screening

The aim of catalyst screening was to find the most efficient CaO derived from the shells for optimal reaction conditions of catalytic performance for transesterification of dimethyl carbonate with glycerol each shells derived-CaO catalyst was investigated under the same reaction conditions (dimethyl carbonate/glycerol molar ratio = 3:1, catalyst loading amount = 3 wt.%, 80 °C, 2 h). As summarized in Table 7.1, the order of glycerol carbonate yield from reactions catalyzed by CaO generating from cockle shells > golden apple snail shells > eggshells > CaO analytical grade, respectively. This result was expected as the S_{BET} and basic site of cockle shells-derived CaO catalyst were higher than those other of CaO catalysts. Therefore, cockle shells-derived CaO was selected use for reaction condition optimization.

7.6.3 Reaction optimizations

7.6.3.1 Effects of reaction temperature

The reaction temperature is obviously a critical parameter for the transesterification of dimethyl carbonate with glycerol as the operating temperature exert great influence on the reaction rate (Algoufi et al., 2014; Li and Wang, 2011). In this case, the effects of reaction temperature were investigated in the range of 65-85 °C by the use of cockle shells-derived CaO catalyst. As illustrated in Figure 7.9(a), the yield of glycerol carbonate increased with the temperature up to 80 °C due to the increases of mobility of the reacting molecules (Algoufi et al., 2014). At the reaction temperature of 85 °C, however, glycerol carbonate product was slightly decreased because dimethyl carbonate was vaporized (boiling point of dimethyl carbonate = 90 °C) which may cause a problem involving three phase system including glycerol as liquid phase, dimethyl carbonate as gas phase and CaO catalyst as solid phase. Therefore, the optimum reaction temperature in this study is 80 °C.

7.6.3.2 Effects of catalyst loading amount

The effects of catalyst loading on the glycerol carbonate yield were investigated using different mass ratio of CaO catalyst obtained by calcined cockle shells (1 wt.% to 6 wt.%). As seen in Figure 7.9(b), increasing the catalyst loading amount from 1 wt.% to 4 wt.% increased glycerol carbonate yield from 45.5% to 97.8%. In general, the basic sites of CaO generate calcium glyceroxide intermediate which then react with dimethyl carbonate to produce glycerol carbonate product and a methanol by-product (Jagadeeswaraiah et al., 2014; Teng et al., 2014). Hence, the increased catalyst content enhance glycerol carbonate yield. Although, further

increase of catalyst loading amount more did not give higher glycerol carbonate yield which may be caused from the limitations related to the mass transfer of reactants to the catalyst and increasing viscosity of the system. In the viewpoint of cost production, the optimal catalyst loading for transesterification of dimethyl carbonate with glycerol to glycerol carbonate in this work was 4 wt.%.
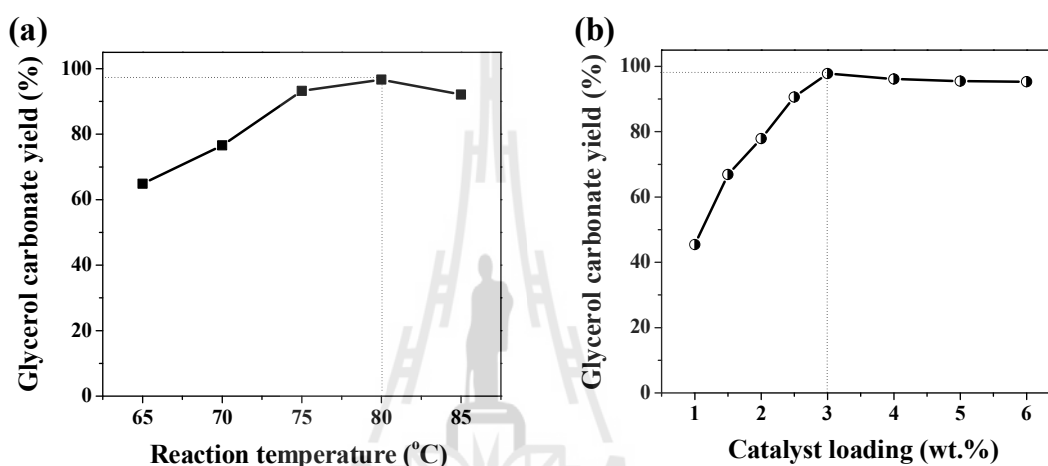
Figure 7.9 (a) Effect of the reaction temperature (reaction condition: CaO obtained from calcination cockle shells, dimethyl carbonate/glycerol molar ratio of 4:1, catalyst loading amount of 3 wt.% and 2 h). (b) Effect of catalyst loading amount (reaction conditions: CaO obtained from calcination cockle shells, catalyst dimethyl carbonate/glycerol molar ratio of 4:1, 80 °C and 2 h).

7.6.3.3 Effects of dimethyl carbonate to glycerol molar ratio

Theoretically, transesterification reaction requires only 1 mol of dimethyl carbonate and 1 mol of glycerol to produce 1 mol of glycerol carbonate and 2 mol of methanol by-product as shown in Figure 7.1 (Teng et al., 2014). Nevertheless, the transesterification requires an excess dimethyl carbonate to shift the equilibrium

toward the direction of the product. The effects of dimethyl carbonate to glycerol molar ratio on the glycerol carbonate yield were examined and the results are demonstrated in Figure 7.10. The yield of glycerol carbonate reached a maximum of 98.3% at the molar ratio of 4:1. Further increase of the dimethyl carbonate amount did not give higher yield of glycerol carbonate. The increase of dimethyl carbonate concentration in the reaction solution limits the interaction of CaO catalysts with glycerol and consequently decreased the reaction rate (Simanjuntak et al., 2013). Therefore, the optimal dimethyl carbonate to glycerol molar ratio in the present reaction was 4:1, which was more than that required by the stoichiometry.

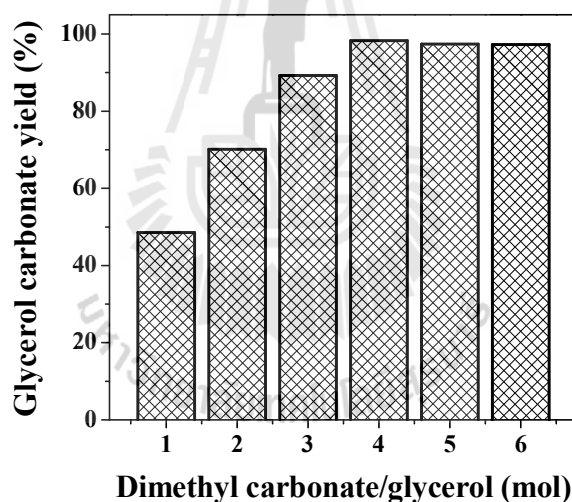**Figure 7.10** Effects of dimethyl carbonate to glycerol molar ratio on the yield of glycerol carbonate product. Reaction conditions: CaO obtained from calcination cockle shells, catalyst loading amount 4 wt.%, 80 °C and 2 h.

7.6.4 Catalyst reusability

The quality of a good solid catalyst is entrenched in its reusability potential. The reusability of cockle shells-derived CaO catalysts was under the optimized reaction

condition as presented in Figure 7.11. After each reaction was completed, the catalysts were separated by filtering and washed with methanol. The results showed that glycerol carbonate yield in the first four cycles was maintained at above 90%, but decreased to 55% in the 7th recycle. This decrease might be caused by the reaction of catalysts with moisture and CO_2 forming $Ca(OH)_2$ and $CaCO_3$ (Roschat et al., 2016; Zheng et al., 2014).
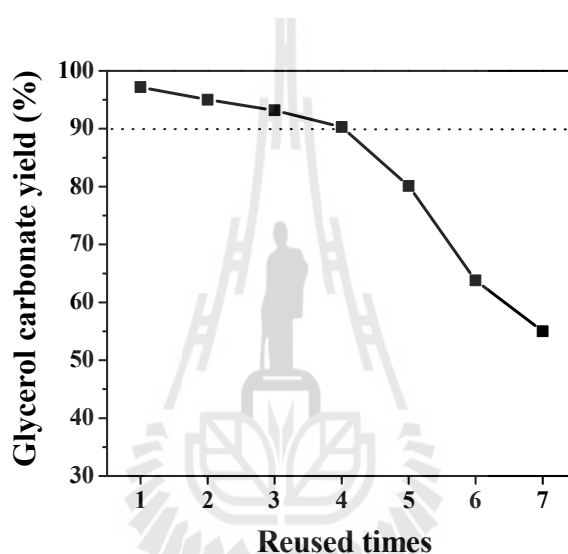
Figure 7.11 Reusability of cockle shells-derived CaO catalyst for synthesis of glycerol carbonate. Reaction conditions: dimethyl carbonate/glycerol molar ratio of 4:1, catalyst loading amount of 4 wt.%, 80 °C and 2 h.

In addition, liquid compound in the reaction mixture including dimethyl carbonate, glycerol, glycerol carbonate and methanol may overwhelm the surface of the catalysts (Figure 7.12(a)). Some agglomeration of the catalysts was also observed in SEM image (Figure 7.12(b)). Moreover, the basic strength of CaO catalysts ($H\_$) decreased to 7.2-9.8 which indicated the reduction of the catalyst active sites. Furthermore, the Ca content in the glycerol carbonate product from first reaction was

detected by atomic absorption spectroscopy (AAS) method to be 53.94 ppm. Thus, the leaching of calcium ion is one of the causes which have influence on reducing the catalytic activity of CaO catalysts (Bai et al., 2013).
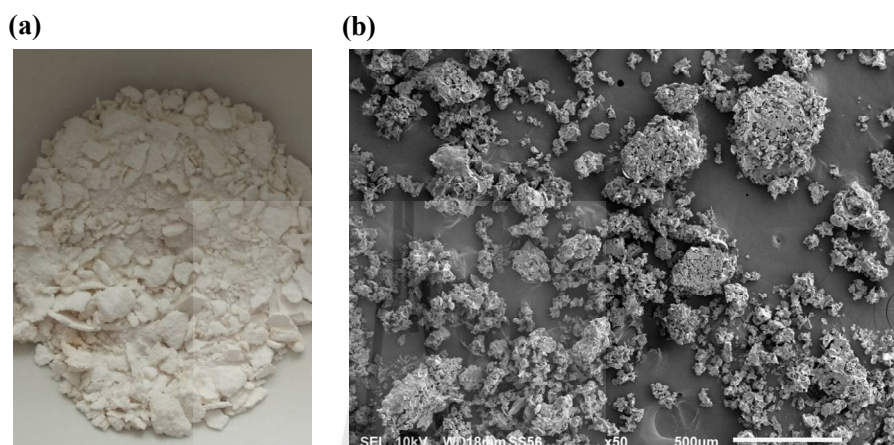
Figure 7.12 (a) Catalyst image and (b) SEM image of the CaO catalyst after being reused 7 times.

7.6.5 Comparison of the shells-derived CaO catalyst against CaO_AR

Figure 7.13(a) shows comparison of catalytic performance of each shells derived CaO catalyst and CaO analytical grade under optimal reaction conditions. The results indicated that all shells derived CaO catalysts had high catalytic activity and the order of catalytic activity of CaO samples was found to be CaO_coc > CaO_gol > CaO_egg > CaO_AR, respectively. The kinetics of reaction catalyzed by shells-derived CaO and CaO analytical grade were evaluated. As depicted in Figure 7.13(b), the obtained k value of CaO derived from cockle shells, golden apple snail shells, eggshells and CaO analytical grade were 2.47×10^{-2} min^{-1}, 2.26×10^{-2} min^{-1}, 2.24×10^{-2} min^{-1} and 2.00×10^{-2} min^{-1}, respectively. The obtained k corresponded with S$_{BET}$ and total basic site of each catalyst.

The best catalyst in this study was CaO catalyst derived from cockle shells which gave glycerol carbonate yield of over 97% such yield was higher than those obtained from the reactions catalyzed by commercial CaO (Ochoa-Go′mer et al., 2009), MgO (Ochoa-Go′mer et al., 2009) and Mg/Zr/Sr mixed oxide (Parameswaram et al., 2013). These results indicated that CaO obtained from natural sources is a promising candidate to replace homogeneous catalyst in the synthesis of glycerol carbonate from glycerol and dimethyl carbonate through transesterification reaction under mild conditions as they are very cheap, highly active, and easy to recover and recycle.
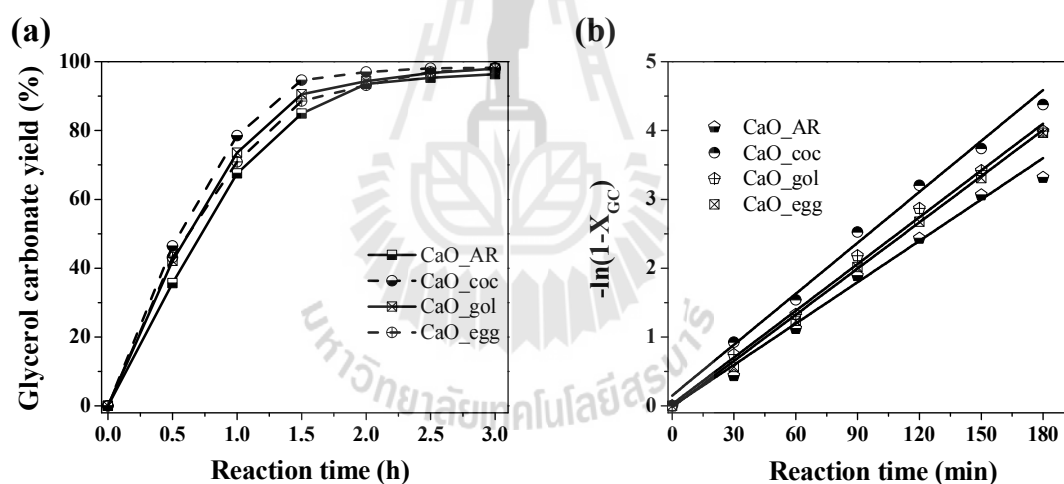

Figure 7.13 (a) Comparison of catalytic activity between CaO derived from the shells and CaO analytical grade, and (b) −ln(1-X_{GC}) versus reaction time plot of each CaO catalysts. Reaction conditions: dimethyl carbonate/glycerol molar ratio of 4:1, catalyst loading amount of 4 wt.% at 80 °C.

7.7 Conclusions

High yield of glycerol carbonate can be achieved by transesterification of dimethyl carbonate with glycerol using different types of natural material derived CaO catalysts including cockle shells, golden apple snail shells and eggshells. Physicochemical properties and catalytic performance of each shells-derived CaO catalyst were evaluated and compared with CaO analytical grade. The results indicated that all CaO catalysts showed very high catalytic activity especially CaO derived from calcination cockle shells which provided glycerol carbonate yield of over 97% within 1.5 h. This CaO catalyst can be easily recovered and recycled for at least 4 times without any treatment. Therefore, the shells are a high potential source of CaO preparation which is not only green and cheap but also highly efficient in glycerol carbonate production.

7.8 References

Algoufi, Y. T., Akpan, U. G., Asif, M. and Hameed, B. H. (2014). One-pot synthesis of glycidol from glycerol and dimethyl carbonate over KF/sepiolite catalyst. **Applied Catalysis A: General**. 487: 181-188.

Alhassan, Y., Kumar, N., Bugaje, I. M., Pali, H. S. and Kathkar, P. (2014). Co-solvent transesterification of cotton seed oil into biodiesel: Effects of reaction condition on quality of fatty acids methyl esters. **Energy Conversion and Management.** 84: 640-648.

Avhad, M. R. and Marchetti, J. M. (2015). A review on recent advancement in catalytic materials for biodiesel production. **Renewable & Sustainable Energy Reviews**. 50: 696-718.

Bai, R., Wang, Y., Wang, S., Mei, F., Li, T. and Li, G. (2013). Synthesis of glycerol carbonate from glycerol and dimethyl carbonate catalyzed by NaOH/γ-Al$_2$O$_3$. **Fuel Processing Technology**. 106: 209-214.

Chen, G., Shan, R., Shi, J. and Yan, B. (2014). Ultrasonic-assisted production of biodiesel from transesterification of palm oil over ostrich eggshell-derived CaO catalysts. **Bioresource Technology**. 171: 428-432.

Dibenedetto, A., Angelini, A., Aresta, M., Ethiraj, J., Fragale, C. and Nocito, F. (2011). Converting wastes into added value products: from glycerol to glycerol carbonate, glycidol and epichlorohydrin using environmentally friendly synthetic routes. **Tetrahedron**. 67: 1308-1313.

Hu, K., Wang, H., Liu, Y. and Yang, C. (2015). KNO$_3$/CaO as cost-effective heterogeneous catalyst for the synthesis of glycerol carbonate from glycerol and dimethyl carbonate. **Journal of Industrial and Engineering Chemistry**. 28: 334-343.

Jagadeeswaraiah, K., Ramesh-Kumar, Ch., Sai-Prasad, P. S., Loridant, S. and Lingaiah, N. (2014). Synthesis of glycerol carbonate from glycerol and urea over tin-tungsten mixed oxide catalysts. **Applied Catalysis A: General**. 469: 165-172.

Khemthong, P., Luadthong, C., Nualpaeng, W., Changsuwan, P., Tongprem, P, Viriya-empikul, N. and Faungnawakij, K. (2012). Industrial eggshell wastes as

the heterogeneous catalysts for microwave assisted biodiesel production. **Catalysis Today**. 190: 112-116.

Lee, S. L., Wong, Y. C., Tan, Y. P. and Yew, S. Y. (2015). Transesterification of palm oil to biodiesel by using waste obtuse horn shell-derived CaO catalyst. **Energy Conversion and Management**. 93: 282-288.

Li, J. and Wang, T. (2011). Chemical equilibrium of glycerol carbonate synthesis from glycerol. **The Journal of Chemical Thermodynamics**. 43: 731-726.

Liu, P., Derchi, M. and Hensen, E. J. M. (2013). Synthesis of glycerol carbonate by transesterification of glycerol with dimethyl carbonate over MgAl mixed oxide catalysts. **Applied Catalysis A: General**. 467: 124-131.

Liu, Z., Wang, J., Kang, M., Yin, N., Wang, Z., Tan, Y. and Zhu, Y. (2015). Structure-activity correlations of $LiNO_3/Mg4AlO_{5.5}$ catalysts for glycerol carbonate synthesis from glycerol and dimethyl carbonate. **Journal of Industrial and Engineering Chemistry**. 21: 394-399.

Lu, P., Wang, H. and Hu, K. (2013). Synthesis of glycerol carbonate from glycerol and dimethyl carbonate over the extruded CaO-based catalyst. **Chemical Engineering Journal**. 228: 147-154.

Malyaadri, M., Jagadeeswaraiah, K., Sai-Prasad, P. S. and N. Lingaiah. (2011). Synthesis of glycerol carbonate by transesterification of glycerol with dimethyl carbonate over Mg/Al/Zr catalysts. **Applied Catalysis A: General**. 401: 153-157.

Ochoa-Gómez, J. R., Gómez-Jiménez-Aberasturi, O., Maestro-Madurga, B., Pesquera-Rodríguez, A., Ramírez-López, C., Lorenzo-Ibarreta, L., Torrecilla-Soria, J. and Villarán-Velasco, M. C. (2009). Synthesis of glycerol carbonate

from glycerol and dimethyl carbonate by transesterification: catalyst screening and reaction optimization. **Applied Catalysis A: General**. 366: 315-324.

Parameswaram, G., Srinivas, M., Hari-Babu, B., Sai-Prasad, P. S. and Lingaiah, N. (2013). Transesterification of glycerol with dimethyl carbonate for the synthesis of glycerol carbonate over Mg/Zr/Sr mixed oxide base catalysts. **Catalysis Science & Technology**. 3: 3242-3249.

Rastegari, H. and Ghaziaskar, H. S. (2015). From glycerol as the by-product of biodiesel production to value-added monoacetin by continuous and selective esterification in acetic acid. **Journal of Industrial and Engineering Chemistry**. 21: 856-861.

Roschat, W., Kacha, M., Yoosuk, B., Sudyoadsuk, T. and Promarak, V. (2012). Biodiesel production based on heterogeneous process catalyzed by solid waste coral fragment. **Fuel**. 98:194-202.

Roschat, W., Siritanon, T., Yoosuk, B. and Promarak, V. (2016). Biodiesel production from palm oil using hydrated lime-derived CaO as a low-cost basic heterogeneous catalyst. **Energy Conversion and Management**. 108: 459-467.

Simanjuntak, F. S. H., Kim, T. K., Lee, S. D., Ahn, B. S., Kim, H. S. and Lee, H. (2011). CaO-catalyzed synthesis of glycerol carbonate from glycerol and dimethyl carbonate: Isolation and characterization of an active Ca species. **Applied Catalysis A: General**. 401: 220-225.

Simanjuntak, F. S. H., Widyaya, V. T., Kim, C. S., Ahn, B. S., Kim, Y. J. and Lee, H. (2013). Synthesis of glycerol carbonate from glycerol and dimethyl carbonate using magnesium–lanthanum mixed oxide catalyst. **Chemical Engineering Science.** 94: 265-270.

Teng, W. K., Ngoh, G. C., Yusoff, R. and Aroua, M. K. (2014). A review on the performance of glycerol carbonate production via catalytic transesterification: Effects of influencing parameters. **Energy Conversion and Management**. 88: 484-497.

Teng, W. K., Ngoh, G. C., Yusoff, R. and Aroua, M. K. (2014). A review on the performance of glycerol carbonate production via catalytic transesterification: Effects of influencing parameters. **Energy Conversion and Management**. 88: 484-497.

Viriya-empikul, N., Krasae, P., Nualpaeng, W., Yoosuk, B. and Faungnawakij, K. (2012). Biodiesel production over Ca-based solid catalysts derived from industrial wastes. **Fuel**. 92: 239-244.

Wang, H., Pang, L., Yang, C. and Liu, Y. (2015). Production of glycerol carbonate via reactive distillation and extractive distillation: An experimental study. **Chinese Journal of Chemical Engineering**. 23: 1469-1474.

Witoon, T., Bumrungsalee, S., Vathavanichku, P., Palitskun, S., Saisriyoot, M. and Faungnawakij, K. (2014). Biodiesel productionfrom transesterification of palm oil with methanol over CaO supported on bimodal meso-macroporous silica catalyst. **Bioresource Technology**. 156: 329-334.

Yoosuk, B., Udomsap, P., Puttasawat, B. and Krasae, P. (2010). Modification of calcite by hydration–dehydration method for heterogeneous biodiesel production process: the effects of water on properties and activity. **Chemical Engineering Journal**. 162: 135-141.

Zheng, L., Xia, S., Hou, Z., Zhang. M. and Hou, Z. (2014). Transesterification of glycerol with dimethyl carbonate over Mg-Al hydrotalcites. **Chinese Journal of Catalysis**. 35: 310-318.

Zheng, L., Xia, S., Lu, X. and Hou, Z. (2015). Transesterification of glycerol with dimethyl carbonate over calcined Ca-Al hydrocalumite. **Chinese Journal of Catalysis**. 36: 1759-1765.

Zhou, Y., Ouyang, F., Song, Z. B., Yang, Z. and Tao, D. J. (2015). Facile one-pot synthesis of glycidol from glycerol and dimethyl carbonate catalyzed by tetraethylammonium amino acid ionic liquids. **Catalysis Communications**. 66: 25-29.
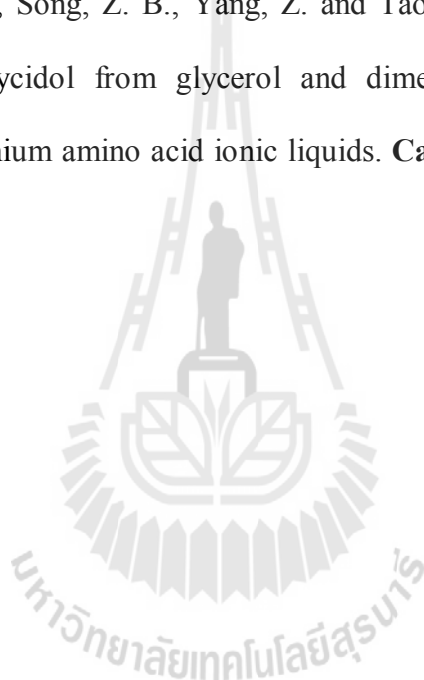
CHAPTER VIII

SUMMARY

The current research focuses on searching for an alternative green and simple ways to improve biodiesel production. The use of non-edible inexpensive rubber seed oil to produce biodiesel has been demonstrated. Three different catalysts prepared from natural sources have been studied as catalysts for transesterification. A novel simple quantitative method to probe biodiesel product has been investigated and proposed. Finally, a catalyst for glycerol carbonate preparation is prepared and studied.

In summary, the results have demonstrated that rubber seed, non-edible crops, collected from the Northeast province of Thailand can be used as a new raw material to produce oil for biodiesel production. The rubber seed oil was extracted using simple solvent extraction technique and its had lower FFAs contained than previously reported. Under optimum conditions of catalyst content of 9 wt.%, methanol/oil molar ratio of 9:1, reaction temperature of 65 ºC with a constant stirring of 200 rpm, sodium metasilicate granule can convert the rubber seed oil to yield biodiesel with a %FAME exceeding 97% in 40 min. The capability to use oil extracted from rubber seed as inexpensive feedstock in combination with utilization of these heterogeneous catalysts would additionally improve the economic aspect of overall biodiesel production, making cost-efficient biodiesel in Thailand.

TLC visualized by UV light can be utilized as a potential screening and monitoring technique in biodiesel production by transesterification process. This method has a small error of within ±2-4% FAME comparing to ^{1}H NMR and GC spectroscopy. Types of catalysts have no effects on the results obtained from the TLC analysis. Hence, TLC visualized by UV light is an efficient, low-cost and simple alternative method to evaluate %FAME in biodiesel product especially for those who have limit access to complicate instrument.

Hydrated lime-derived CaO can be utilized as high efficient heterogeneous solid catalyst for transesterification of palm oil to biodiesel product. The results indicated that calcination was an appropriate method to improve catalytic activity of hydrated lime. The hydrated lime-derived CaO catalyst showed very high activity and provides FAME yield of 97.2% after only 2 h. This CaO catalyst could be reused for at least 5 times and tolerated a maximum of 5 wt.% water content. After purification and treatments, high quality biodiesel could be obtained.

River snail shells-derived CaO catalyst was synthesized for the first time as a solid catalyst for transesterification of palm oil to biodiesel product. The reaction time of transesterification was decreased from 180 min in non co-solvent reaction to 90 min in a co-solvent reaction with 10% v/v THF. The co-solvent method of THF/methanol successfully decreases activation energy of reaction. Additionally, the possible transesterification mechanism was experimentally investigated.

Rice husk-derived sodium silicate was employed as a high performance catalyst for transesterification of many kinds of oils to biodiesel. Under optimized reaction conditions, FAME yield reached 97% after only 30 min at 65 °C and 94% after 150 min (2.5 h) at room temperature. The obtained biodiesel product after purification and

treatment process by cation-exchange resin shows high quality fuel properties according to American Society for Testing and Material (ASTM D6751) methods and European Standard methods (EN14214) for bio-auto fuels.

The transesterification of dimethyl carbonate with glycerol to produce glycerol carbonate was investigated in the presence of CaO catalyst derived from natural source materials under various reaction condition. The results indicated that all of the CaO catalysts showed very high catalytic activity to convert glycerol into glycerol carbonate product. Especially CaO derived from calcined cockle shells provides over 97% yield glycerol carbonate within 1.5 h. This CaO catalyst can be easily recovered and recycled for at least 4 times without any treatment process.

APPENDIX
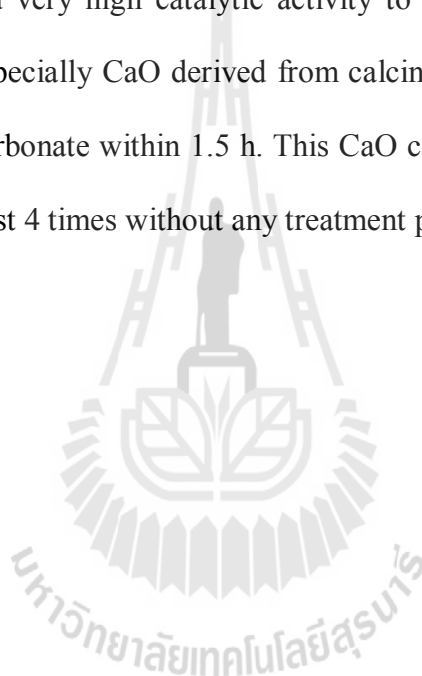
THESIS OUTPUT

A. Publication

1. Roschat, W., Siritanon, T., Yoosuk, B. and Promarak, V. (2016). Biodiesel production from palm oil using hydrated lime-derived CaO as a low-cost basic heterogeneous catalyst. **Energy Conversion and Management**, 108: 459-467. (Impact factor (2014): 4.380).

2. Roschat, W., Siritanon, T., Kaewpuang, T., Yoosuk, B. and Promarak, V. (2016). Economical and green biodiesel production process using river snail shells-derived heterogeneous catalyst and co-solvent method. **Bioresource Technology**, 209: 343-350. (Impact factor (2014): 4.494).

3. Roschat, W., Siritanon, T., Yoosuk, B. and Promarak, V. (2016). Rice husk-derived sodium silicate as a highly efficient and low-cost basic heterogeneous catalyst for biodiesel production. **Energy Conversion and Management**, 119: 453-462 (Impact factor (2014): 4.380).

B. Submitted manuscript

1. Roschat, W., Siritanon, T., Yoosuk, B., Sudyoadsuk, T. and Promarak, V. (2016). Rubber seed oil as potential non-edible feedstock for biodiesel production using heterogeneous catalyst in Thailand. Renewable Energy (Impact factor (2014): 3.476), *Submitted*.

C. Presentation

1. <u>Roschat, W.</u>, Keawpeung, T., Yoosuk, B., and Promarak, V. A Simple Analysis of Biodiesel by Thin Layer Chromatography (TLC), *The 7ᵗʰ Thailand Renewable Energy for Communication Conference: (TREC-7)* 12 – 14 November 2014, Rajamangala University Of Technology Rattanakosin, wang klai kangwon campus, Prachuapkhirikhan (Oral presentation).

2. <u>Roschat, W.</u>, Keawpeung, T., Yoosuk, B., and Promarak, V. Synthesis of glycerol carbonate from glycerol and dimethyl carbonate catalyzed by CaO as a heterogeneous catalyst, *40ᵗʰ Congress on Science and Technology of Thailand (STT40)* 2 - 4 December 2014 at Hotel Pullman Khon Kaen, Thailand (Oral presentation).

3. <u>Roschat, W.</u>, Siritanon, T., Keawpuang, T., Yoosuk, B., and Promarak, V. The green biodiesel production by using river sanil shell-derived CaO catalyst and co-solvent method, *41ˢᵗ Congress on Science and Technology of Thailand (STT41)* 6 - 8 November 2015 at Suranaree University of Technology, Nakhon Ratchasima, Thailand (Oral presentation).

CURRICULUM VITAE

Mr.WUTTICHAI ROSCHAT

Education

2009	B.Sc. Chemistry (First class honors), Ubon Ratchathani Rajabhat University, Thailand.
2011	M.Sc. Chemistry, Ubon Ratchathani University, Thailand.
2012-2015	Ph.D. Candidate (Chemistry) at Suranaree University of Technology, Thailand.

International Publications

Rohschat, W., Kacha, M., Yoosuk, B., Sudyoadsuk, T. and Promarak, V. (2012). Biodiesel production based on heterogeneous process catalyzed by solid waste coral fragment. Fuel, 98, 194-202. (Impact factor (2014): 3.520)

Roschat, W., Siritanon, T., Yoosuk, B. and Promarak, V. (2016). Biodiesel production from palm oil using hydrated lime-derived CaO as a low-cost basic heterogeneous catalyst. Energy Conversion and Management, 108, 459-467. (Impact factor (2014): 4.380)

Roschat, W., Siritanon, T., Kaewpuang, T., Yoosuk, B. and Promarak, V. (2016). Economical and green biodiesel production process using river snail shells-derived heterogeneous catalyst and co-solvent method. Bioresource Technology, 209: 343-350. (Impact factor (2014): 4.494).

Roschat, W., Siritanon, T., Yoosuk, B. and Promarak, V. (2016). Rice husk-derived sodium silicate as a highly efficient and low-cost basic heterogeneous catalyst for biodiesel production. Energy Conversion and Management, 119: 453-462 (Impact factor (2014): 4.380).